



## **URBAN DEVELOPMENT DIRECTORATE (UDD)**

Ministry of Housing and Public Works  
Government of the People's Republic of Bangladesh

***FINAL REPORT ON GEOTECHNICAL AND  
GEOPHYSICAL SURVEY  
Under  
ENGINEERING GEOLOGICAL AND GEOPHYSICAL  
SURVEYS UNDER PREPARATION OF  
DEVELOPMENT PLAN FOR MEHERPUR ZILLA***

**May 2025**

**Submitted by**



IN JOINT VENTURE WITH

**CREATIVE  
SOIL  
INVESTIGATION**

Address: Flat# D1, House # 64/1,  
Lake Circus, Kalabagan, Dhaka-1205.

## CONTENTS

<b>1. INTRODUCTION .....</b>	<b>4</b>
1.1. Background .....	4
<b>1.2. Client: About Urban Development Directorate (UDD) .....</b>	<b>4</b>
1.3. Location and Accessibility .....	5
1.4. Aims and Objectives .....	6
<b>2. METHODOLOGY .....</b>	<b>8</b>
<b>2.1. Strategic Methodology .....</b>	<b>8</b>
<b>3. SUB-SURFACE GEOLOGY OF THE STUDY AREA.....</b>	<b>14</b>
3.1. Subsurface 3D Model of Different Layers through Geotechnical Investigation.....	14
3.2. Subsurface Cross-section .....	15
<b>3.3. Bearing Capacity for Shallow Foundation.....</b>	<b>19</b>
<b>4. SEISMIC HAZARD ASSESSMENT.....</b>	<b>29</b>
4.1. Seismic Hazard Analysis in Bangladesh.....	29
4.2. Methodology .....	31
4.3. Results and Discussion.....	36
4.4. Engineering Geological Mapping .....	40
4.4.1 Shear Wave Velocity Estimation .....	41
4.4.2. Soil Type Determination Based on AVS30 .....	44
4.5. Site Response .....	46
<b>4.5.1 Site Response of Meherpur District.....</b>	<b>48</b>
<b>5. LIQUEFACTION POTENTIAL INDEX (LPI) ASSESSMENT.....</b>	<b>52</b>
5.1. Methodology .....	52
<b>Calculation of Cyclic Resistance Ratio (CRR) .....</b>	<b>53</b>
<b>Seismic Factors.....</b>	<b>54</b>
5.2. Discussions of Liquefaction Hazard Map .....	55
<b>6. GEOENGINEERING SUITABILITY .....</b>	<b>59</b>
6.1. Geoengineering Suitability of Meherpur District.....	61
<b>7. CONCLUSION .....</b>	<b>63</b>
<b>8. REFERENCES .....</b>	<b>65</b>

## LIST OF FIGURES

FIGURE 1 LOCATION MAP OF THE PROJECT AREA PRESENTING 3 UPAZILAS OF MEHERPUR ZILLA .....	6
FIGURE 2 BLOCK DIAGRAM OF METHODOLOGY. ....	8
FIGURE 3 TEST LOCATION MAP OF MEHERPUR DISTRICT WITH GEOMORPHOLOGICAL UNITS. ....	10
FIGURE 4 TEST LOCATION MAP OF MEHERPUR SADAR UPAZILA, MEHERPUR WITH GEOMORPHOLOGICAL UNITS.....	11
FIGURE 5 TEST LOCATION MAP OF MUJIBNAGAR UPAZILA, MEHERPUR WITH GEOMORPHOLOGICAL UNITS .....	12
FIGURE 6 TEST LOCATION MAP OF GANGNI UPAZILA, MEHERPUR WITH GEOMORPHOLOGICAL UNITS.....	13
FIGURE 7 (A) LEGEND AND LITHOLOGIC CHARACTERISTIC OF SUBSURFACE OF STUDY AREA; (B) SUBSURFACE 3-D MODEL SHOWING NE PART; (C) SUBSURFACE 3-D MODEL IN SW PART. ....	15
FIGURE 8 CROSS-SECTION LINE MAP OF MEHERPUR. ....	16
FIGURE 9 CROSS-SECTION A-A'. ....	17
FIGURE 10 CROSS-SECTION B-B'. ....	17
FIGURE 11 CROSS-SECTION C-C'. ....	17
FIGURE 12 CROSS-SECTION D-D'. ....	18
FIGURE 13 CROSS-SECTION E-E'. ....	18
FIGURE 14 CROSS-SECTION F-F'. ....	18
FIGURE 15 FOUNDATION LAYER DEPTH OF MEHERPUR DISTRICT. ....	28
FIGURE 16 SEISMOTECTONIC MAP OF BANGLADESH AND SURROUNDING REGIONS SHOWING EPICENTERS OF EARTHQUAKES (DECLUSTERED CATALOG) FROM 1762 TO 2016 ((RAHMAN ET AL., 2020). ....	31
FIGURE 17 SEISMOTECTONIC AREAL SOURCES FOR THE STUDY AREA. ....	34
FIGURE 18 PGA MAPS OF MEHERPUR DISTRICT AT 10% PROBABILITY OF EXCEEDANCE IN 50 YEARS AND AT 2% PROBABILITY OF EXCEEDANCE IN 50 YEARS. ....	37
FIGURE 19 SA MAPS OF SHORT PERIOD OF MEHERPUR DISTRICT AT 10% PROBABILITY OF EXCEEDANCE IN 50 YEARS AND AT 2% PROBABILITY OF EXCEEDANCE IN 50 YEARS. ....	38
FIGURE 20 SA MAPS OF LONG PERIOD OF MEHERPUR DISTRICT AT 10% PROBABILITY OF EXCEEDANCE IN 50 YEARS AND AT 2% PROBABILITY OF EXCEEDANCE IN 50 YEARS. ....	39
FIGURE 21 UNIFORM HAZARD SPECTRA FOR THE STUDY AREA. ....	40
FIGURE 22 COMPARISON BETWEEN PGA VALUES OF STUDY AREA AT 10% AND 2% PROBABILITY OF EXCEEDANCE IN 50 YEARS. ....	40
FIGURE 23 REGRESSION ANALYSIS BETWEEN MEASURED SPT-N VALUE AND SHEAR WAVE VELOCITY (Vs) OBTAINED FROM DOWN-HOLE SEISMIC TEST (PS-LOGGING). ....	42
FIGURE 24 SPT-N VALUE AND Vs EMPIRICAL RELATIONS FOR ALL SOILS IN THE STUDY AREA. ....	43
FIGURE 25 ENGINEERING GEOLOGICAL MAP OF MEHERPUR DISTRICT. ....	44
FIGURE 26 SOIL CLASSIFICATION MAP OF MEHERPUR DISTRICT- ACCORDING TO NEHRP PROVISIONS BASED ON THE AVERAGE SHEAR WAVE VELOCITY DISTRIBUTION DOWN TO 30 M. ....	46
FIGURE 27 PGA MAPS AT GROUND SURFACE OF MEHERPUR DISTRICT AT 10% PROBABILITY OF EXCEEDANCE IN 50 YEARS AND AT 2% PROBABILITY OF EXCEEDANCE IN 50 YEARS. ....	49
FIGURE 28 SA MAPS OF SHORT PERIOD AT GROUND SURFACE OF MEHERPUR DISTRICT AT 10% PROBABILITY OF EXCEEDANCE IN 50 YEARS AND AT 2% PROBABILITY OF EXCEEDANCE IN 50 YEARS. ....	50
FIGURE 29 SA MAPS OF LONG PERIOD AT GROUND SURFACE OF MEHERPUR DISTRICT AT 10% PROBABILITY OF EXCEEDANCE IN 50 YEARS AND AT 2% PROBABILITY OF EXCEEDANCE IN 50 YEARS. ....	51
FIGURE 30 SHOWING THE LIQUEFACTION HAZARD SCENARIO OF PIROJPUR SADAR UPAZILA AREA CONSIDERING MAGNITUDE =7.5 MW AND PGA 0.145G. ....	56
FIGURE 31 CRITERIA RASTER FILES FOR COMPOSITE HAZARD MAP. ....	59
FIGURE 32 CRITERIA RASTER FILES MULTIPLIED BY THE WEIGHTED AND SUMMED UP VALUE FOR COMPOSITE HAZARD MAP. ....	60
FIGURE 33 GEOENGINEERING SUITABILITY OF MEHERPUR DISTRICT. ....	61

### List of Table

TABLE 1 DISTRIBUTION OF DIFFERENT ENGINEERING GEOLOGICAL AND GEOPHYSICAL INVESTIGATIONS	9
TABLE 2 ALLOWABLE BEARING CAPACITY FOR SHALLOW FOUNDATION OF MEHERPUR DISTRICT.....	21
TABLE 3 PRESUMPTIVE VALUES OF BEARING CAPACITY FOR LIGHTLY LOADED STRUCTURES (BNBC 2020) .....	26
TABLE 4 COMPLETENESS OF DIFFERENT CATALOGS ESTIMATED WITH THE METHOD OF STEPP (1972) ..	33
TABLE 5 SEISMICITY PARAMETERS FOR THE AREAL SOURCES.....	35
TABLE 6 DEFINITION OF SITE CLASS BASED ON AVS30 — ACCORDING TO NEHRP (NATIONAL EARTHQUAKE HAZARD REDUCTION PROGRAM, USA) PROVISIONS.....	45
TABLE 7 SITE CLASSIFICATION BASED ON SOIL PROPERTIES (BNBC, 2020) .....	45
TABLE 8 SITE SOIL CLASSIFICATION ACCORDING TO NEHRP (BSSC, 2015) AND BNBC, 2020.....	47
TABLE 9 PEAK GROUND ACCELERATION SITE COEFFICIENTS ( $F_{PGA}$ ) (BSSC, 2015).....	48
TABLE 10 SHORT-PERIOD SITE COEFFICIENTS $F_A$ (BSSC, 2015) .....	48
TABLE 11 LONG-PERIOD SITE COEFFICIENTS $F_V$ (BSSC, 2015) .....	48
TABLE 12 CLASSIFICATION OF LIQUEFACTION POTENTIAL INDEX USED IN DIFFERENT STUDIES .....	55
TABLE 13 TABLE SHOWING THE LIQUEFACTION SCENARIO CONSIDERING MAGNITUDE =7.5 MW AND $PGA$ 0.146G FOR MEHERPUR DISTRICT.....	57
TABLE 14 RATING AND WEIGHT VALUE FOR GEOLOGICAL SUITABILITY.....	60
TABLE 15 LAND-USE RECOMMENDATION BASED ON GEOENGINEERING SUITABILITY.....	62



## 1. INTRODUCTION

### 1.1. Background

Bangladesh is situated in a region that is highly susceptible to natural disasters due to its geographical location, diverse land features, extensive river network, and monsoon climate. This highlights the importance of conducting a comprehensive ***Subsurface Geotechnical and Geophysical Study*** to support sustainable urban development. The success of such initiatives relies on the inclusion of subsurface geotechnical and geophysical information as essential resources.

Additionally, effective land use planning is crucial for modern urban development, yet Bangladesh currently lacks widespread implementation of comprehensive land use strategies. Therefore, it is vital to assess both the surface and subsurface geological conditions, along with the associated geological hazards and risks in the area, before initiating any land use planning efforts. A thorough geotechnical and geophysical site characterization, combined with potential risk analysis, is key to ensuring resilient urban development in the face of potential challenges.

To create a safe and resilient urban environment, it is essential to conduct a detailed analysis of the geological and geotechnical characteristics of the site. This process includes a comprehensive risk assessment to identify and understand potential hazards. The development plan must integrate detailed information about the subsurface geophysics and geotechnical properties to accurately evaluate the soil conditions in the project area. Furthermore, it is critical to assess natural geological risks such as earthquakes, liquefaction, and landslides, and to incorporate their potential impact into infrastructure design.

To achieve the objectives of the ***Subsurface Geotechnical and Geophysical Study***, part of the ***Preparation of Development Plan for Meherpur Zilla***, the following objectives need to be pursued: follows:

- GIS and RS-based geomorphological and/or geological map of the project area
- Sub-surface lithological 3D model development and relevant interpretation
- Soil classification map using geophysical and geotechnical investigations
- Engineering geological map based on Average Shear Wave (AVS30)
- Seismic Hazard Assessment (PGA/PGV, and SA) map of the project area
- Engineering properties and bearing capacity of subsoil
- Liquefaction susceptibility map construction of the study area
- Geological Suitability Map.

### 1.2. Client: About Urban Development Directorate (UDD)

In response to rapid urbanization, population growth and economic development in the early 1960s, there was a need to establish a regional and central office for physical planning. As a result, the **Urban Development Directorate (UDD)** was founded on July 17, 1965, under the administrative control of the Works, Power, and Irrigation Department. The main functions of UDD include:

- i. Advising the Government on urbanization, land use planning and land development policies.
- ii. Preparing and coordinating regional plans, master plans, and detailed layout and site plans for existing and new urban centers, excluding areas covered by town development authorities of Dhaka, Chittagong, Khulna, and Rajshahi.
- iii. Conducting socio-economic research and data collection to determine future urban development locations and patterns.
- iv. Developing urban development programs for execution by sectoral agencies and obtaining approval from the National Council. Assisting agencies in selecting implementation sites.
- v. Being the focal point in the Government for internationally aided physical planning and human settlement programs.
- vi. Organizing seminars and workshops to raise awareness about physical planning and disseminating information through regular publication of research and planning materials on urbanization and human settlement planning and development.
- vii. Providing in-service training for officers and staff of organizations involved in spatial planning and development.
- viii. Advising existing urban development authorities on their operations at their request.

### 1.3. Location and Accessibility

**Meherpur Sadar Upazila:** Meherpur Sadar Upazila covers an area of 276.15 square kilometers. It is situated between 23°40' and 23°52' north latitudes and 88°34' and 88°47' east longitudes. The upazila is bounded by Gangni upazila and west Bengal state of India on the north, damurhuda and mujibnagar upazilas on the south, Gangni and alamdanga upazilas on the east, West Bengal state of India on the west (Source: Banglapedia).

**Mujibnagar Upazila:** Mujibnagar Upazila is situated in an area spanning 111.51 square kilometers and located in between 23°36' and 23°45' north latitudes and in between 88°34' and 88°43' east longitudes. It is bounded by meherpur sadar upazila on the north, damurhuda and Meherpur Sadar upazilas on the east, West Bengal of India on the south and on the west.

**Gangni Upazila:** Gangni Upazila with an area of 363.95 sq km and located between 23°44' and 23°52' north latitudes and in between 88°34' and 88°47' east longitudes. It is bounded by daulatpur (kushtia) upazila on the north, alamdanga and meherpur sadar upazilas on the south, Daulatpur (Kushtia), mirpur (Kushtia) and Alamdanga upazilas on the east, Meherpur Sadar upazila and west bengal state of India on the west (Source: Banglapedia).

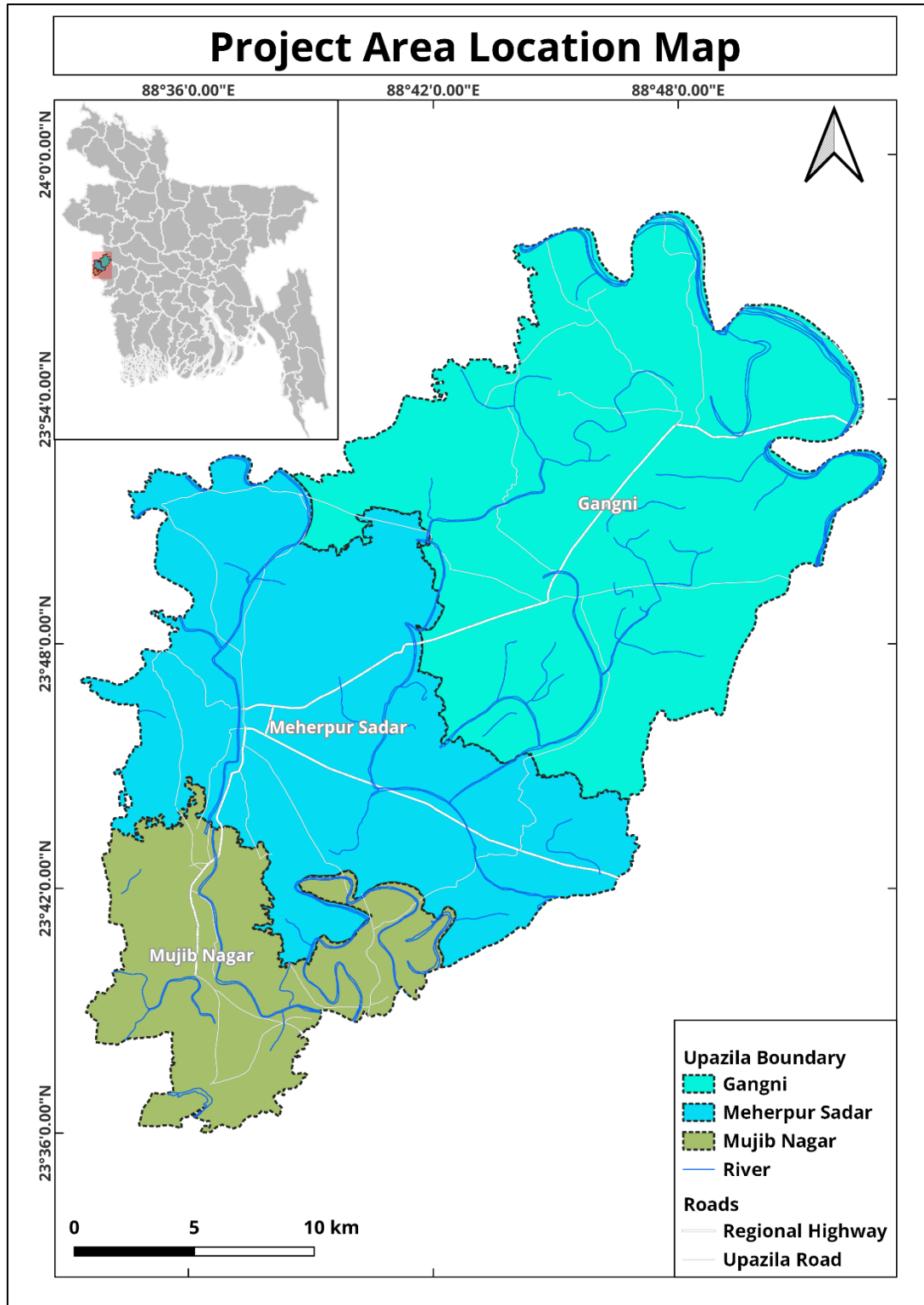


Figure 1 Location Map of the Project Area Presenting 3 Upazilas of Meherpur Zilla.

## 1.4. Aims and Objectives

The primary objective of this project is to carry out a comprehensive subsurface geotechnical and geophysical study in the Gangni, Mujibnagar, and Meherpur Sadar Upazilas located in Meherpur district. This study is an essential component of the development plan being formulated for these three Upazilas. The insights gained from this research will inform key

decision-making processes regarding land-use, infrastructure development and environmental management in the area. In order to achieve the objective, the following specific objectives need to be accomplished:

- GIS based geological/ geomorphological map of the project area
- Sub-surface lithological 3D model development and relevant interpretation
- Soil classification map using geophysical and geotechnical investigations
- Engineering geological map based on Average Shear Wave (AVS30)
- Seismic hazard assessment (PGA/PGV, and SA) map of the project area
- Foundation layers delineation and developing engineering properties of the sub-soil
- Liquefaction susceptibility map construction of the study area
- Formulation of Policies and plans for mitigation of different types of hazards, minimizing the adverse impacts of climate change and recommend possible adaptation strategies for the region.

## 2. METHODOLOGY

### 2.1. Strategic Methodology

The methodology consists of both field and laboratory investigations. To conduct this project work engineering geological and geophysical data of soil have been collected, analysed and interpreted. Engineering geological/Geotechnical data have been collected from field investigations i.e., boring, standard penetration test (SPT), and laboratory investigations i.e., soil physical properties test, direct shear test and triaxial test of soil sample. Geophysical data will be collected from down-hole seismic test (PS logging); multi-channel analysis of surface wave (MASW) and Singles Microtremor survey. The total works are conducted through the following methodology (flowchart) (Figure 2)-

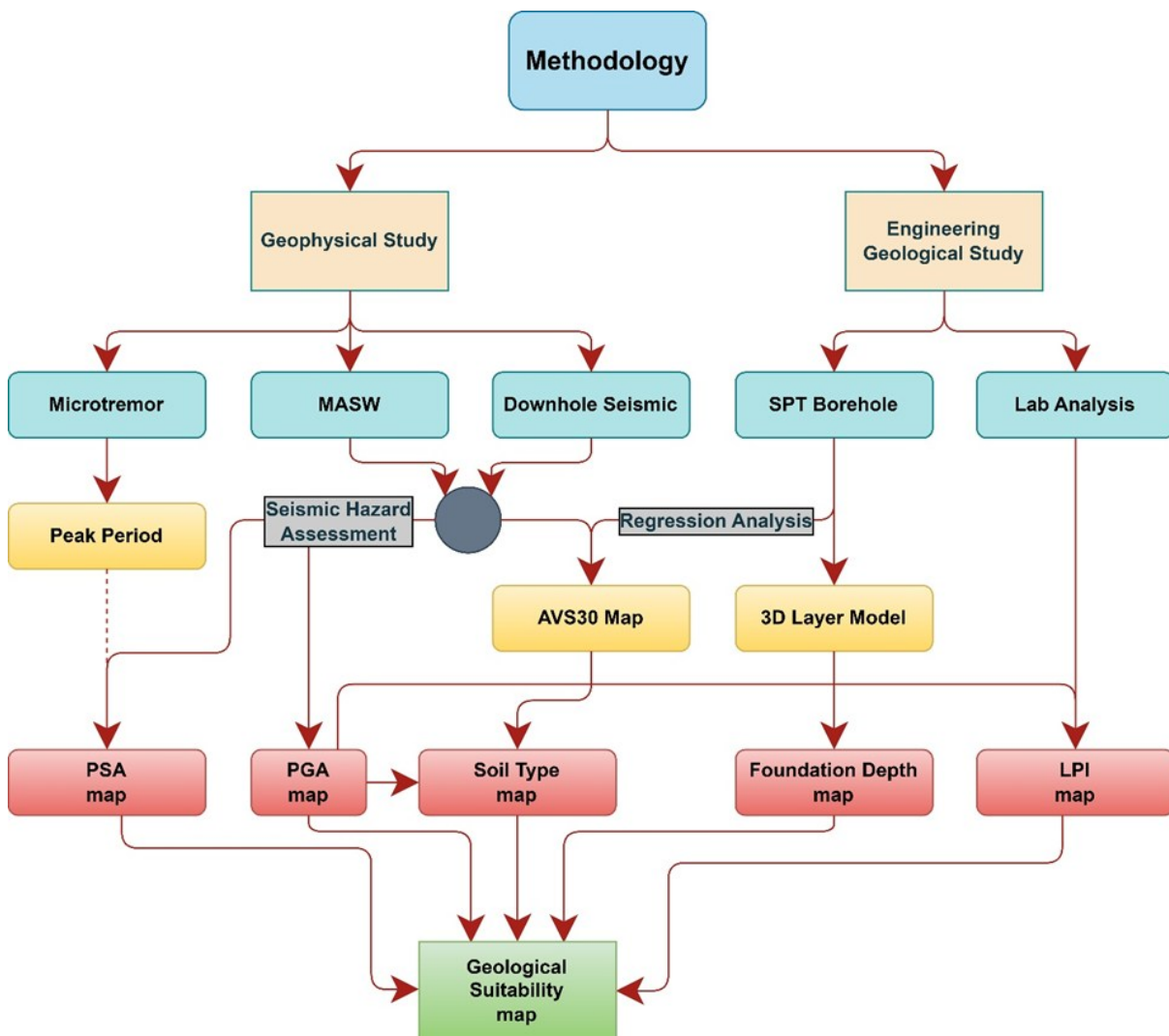


Figure 2 Block Diagram of Methodology.

*Table 1 Distribution of Different Engineering Geological and Geophysical Investigations*

Area (approx. 600 sq km)	Name of Investigation Methods			
	SPT	PS-logging	MASW	Microtremor
Meherpur Sadar Upazila	17	4	5	5
Mujibnagar Upazila	10	2	3	3
Gangni Upazila	03 (Secondary-28 nos.)	1 (Secondary=6 nos.)	3 (Secondary=5 nos.)	7
<b>Total</b>	<b>30</b>	<b>7</b>	<b>11</b>	<b>15</b>

Test locations of the project area are shown in following figure 3 to 6.

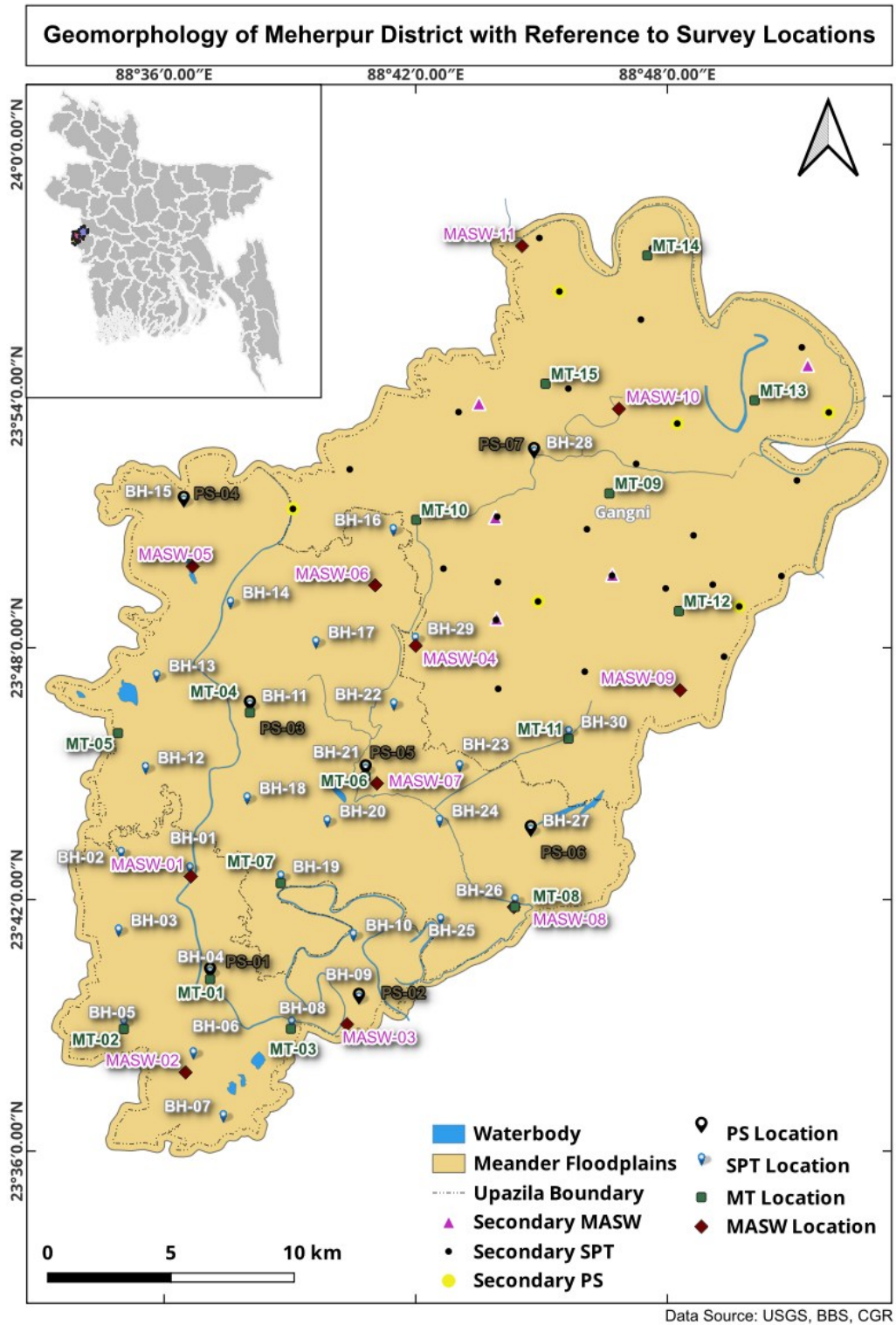


Figure 3 Test Location Map of Meherpur District with Geomorphological units.



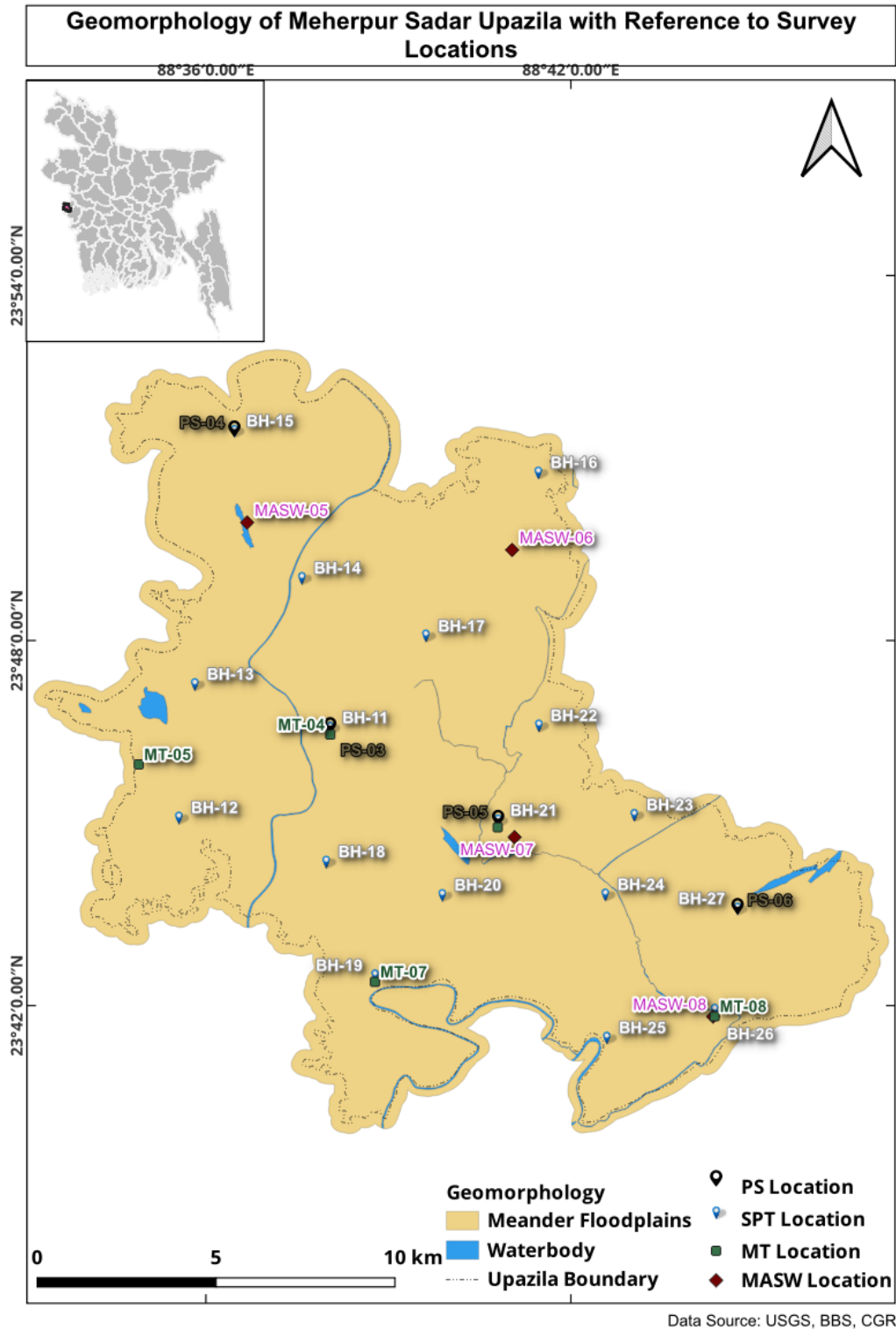


Figure 4 Test Location Map of Meherpur Sadar Upazila, Meherpur with Geomorphological units



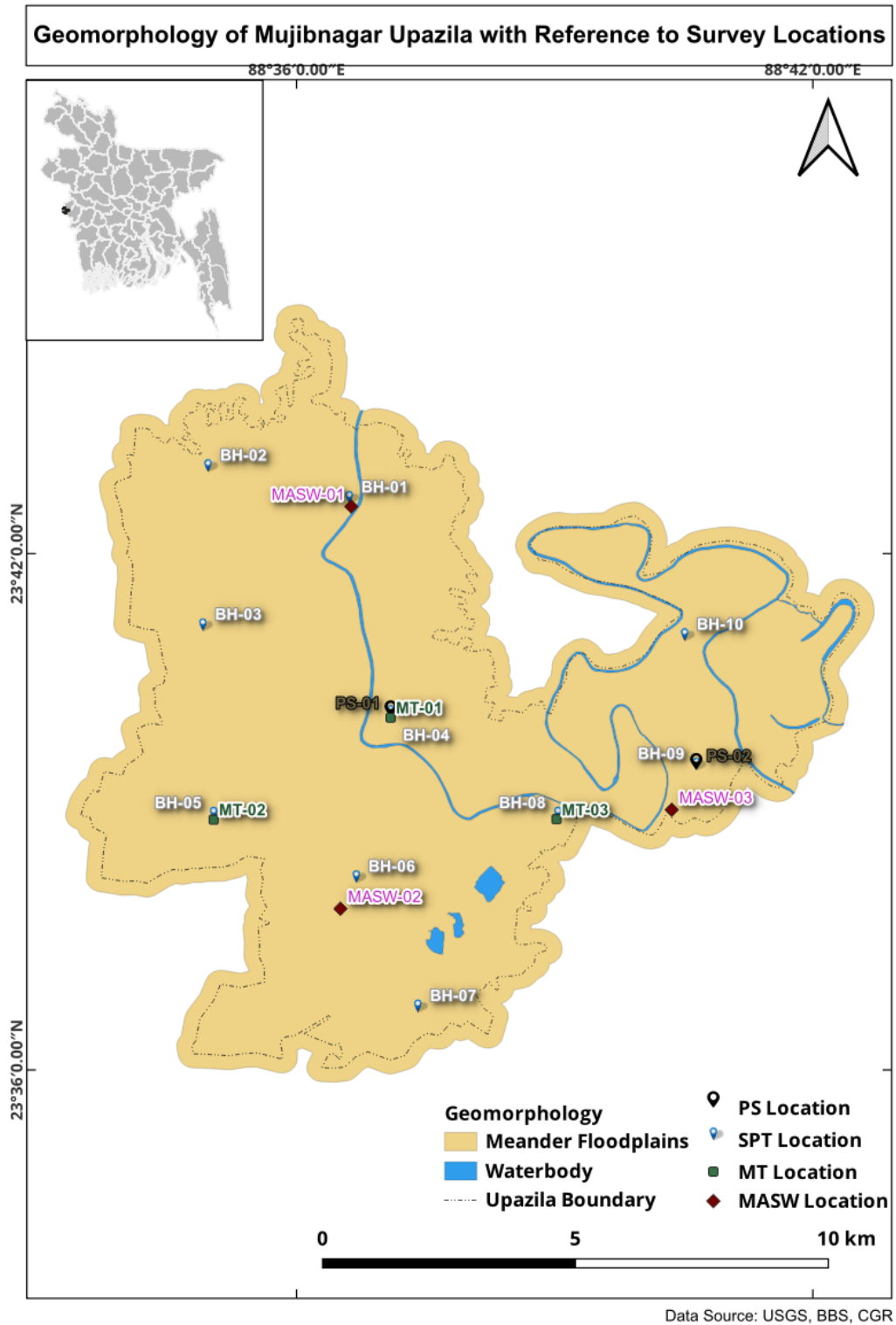


Figure 5 Test Location Map of Mujibnagar Upazila, Meherpur with Geomorphological units

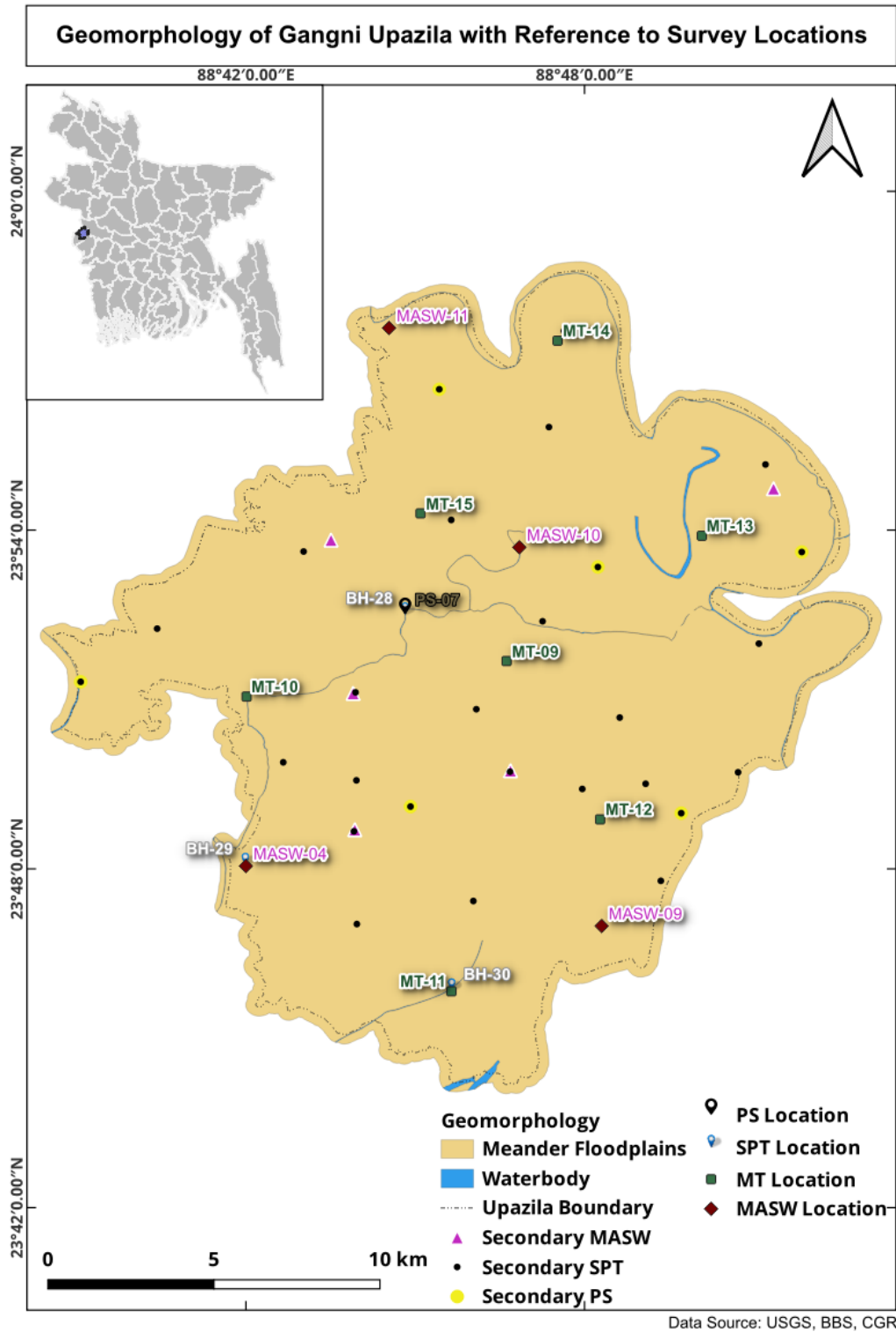


Figure 6 Test Location Map of Gangni Upazila, Meherpur with Geomorphological units


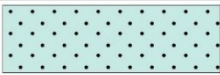




### 3. SUB-SURFACE GEOLOGY OF THE STUDY AREA

#### 3.1. Subsurface 3D Model of Different Layers through Geotechnical Investigation

According to 250m × 250m grid pattern, Standard penetration test locations are selected and drilling for identifying the geological characteristics of sub-surface soft sedimentary rocks. Description of different layers of the soil, its sedimentary characteristics, structure, and lithology are reflected in 3D model. 3D model for subsurface information of different layers of the area can be done by using GIS.

Lithological succession encounter in the boreholes reveal that geologically the study area is very common type for its sand and silt alteration almost throughout the whole area. Based on distinct lithological characteristics, Standard Penetration Test blow counts (SPT-N) the borelogs encompasses eight distinct lithofacies, denoted as layers 1 to layer 6 as described in Figure 7 A.

A.

Stratigraphy		
	<b>Layer-1</b>	<b>Brownish Gray Stiff SILT with Little Very Fine Sand</b>
	<b>Layer-2</b>	<b>Brownish Gray to Gray very Loose to loose Very Fine SAND</b>
	<b>Layer-3</b>	<b>Gray Soft to medium stiff Clayey SILT</b>
	<b>Layer-4</b>	<b>Gray Medium Dense very Fine to Fine SAND</b>
	<b>Layer-5</b>	<b>Gray Medium Stiff Clayey SILT</b>
	<b>Layer-6</b>	<b>Gray Dense to very Dense fine to very Fine SAND with Little Silt</b>

B.

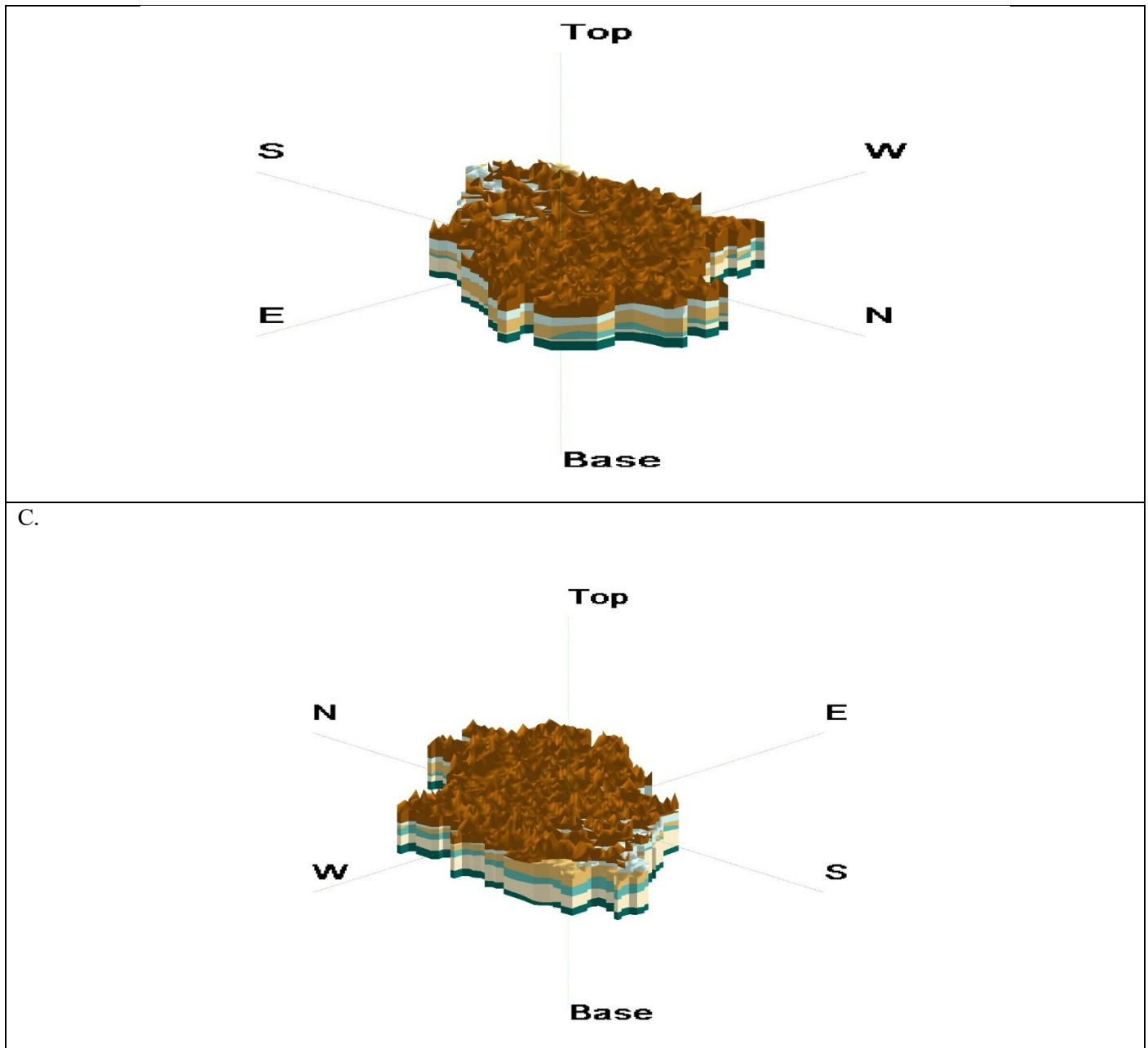


Figure 7 (A) Legend and Lithologic Characteristic of Subsurface of Study Area; (B) Subsurface 3-D Model Showing NE Part; (C) Subsurface 3-D Model in SW Part.

Subsurface 3D model has been prepared showing Northeastern part and along Southwestern direction using ArcGIS to elucidate the subsurface geological conditions of the study area; as shown in Figure 7 B & C respectively. All 62 (Primary 32 and Secondary 30) boreholes of 30m depth carefully have been examined to delineate the spatial distribution of the subsurface lithological units of the area.

### 3.2. Subsurface Cross-section

Two cross sections have been illustrated here, all of them roughly in North Northwestern to South Southeastern direction. Each section covers multiple boreholes having many nearby (Figure 8).

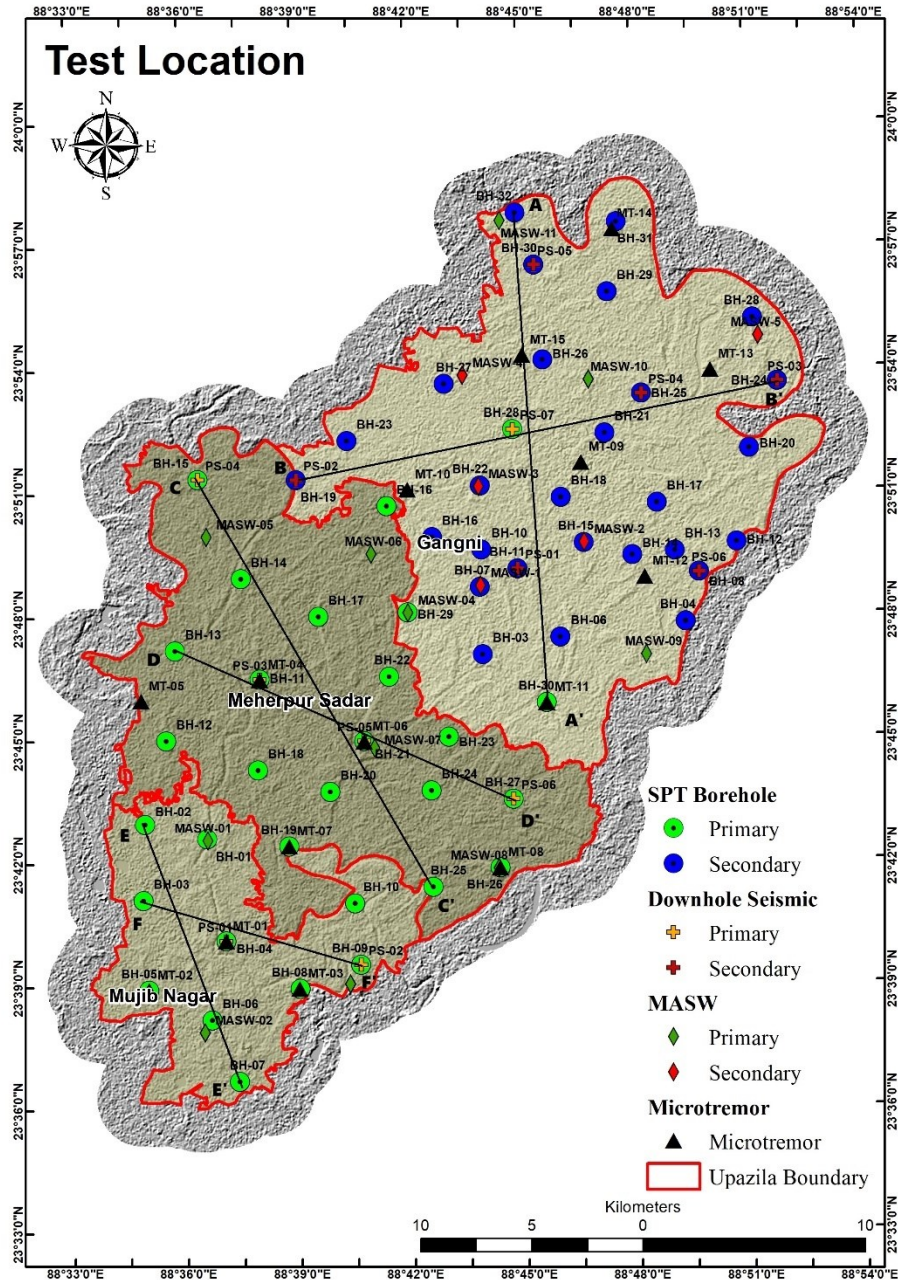


Figure 8 Cross-section Line Map of Meherpur.

### Cross section A-A'

The cross-section AA' (NNW- SSW) (Figure 9) extends approximately 22.00 km from BH-06 to BH-32, connecting BH-11, BH-18, BH-26, BH-28 and BH-30 along the way; this area is located in Gangi upazila. Layer 1 is undulated throughout the section, with its maximum thickness found in the western region and thickness ranges from 2 to 20 meters. Layer 2 reaches its maximum thickness in the east and thickness ranges from 0.5 to 15 meters. Layer 6, the deepest layer, is thickest at the western part, with a thickness that varies between 5 and 20 meters. In contrast, Layers 3, 4, and 5 have inconsistent thicknesses, ranging from 0.5 to 10 meters.



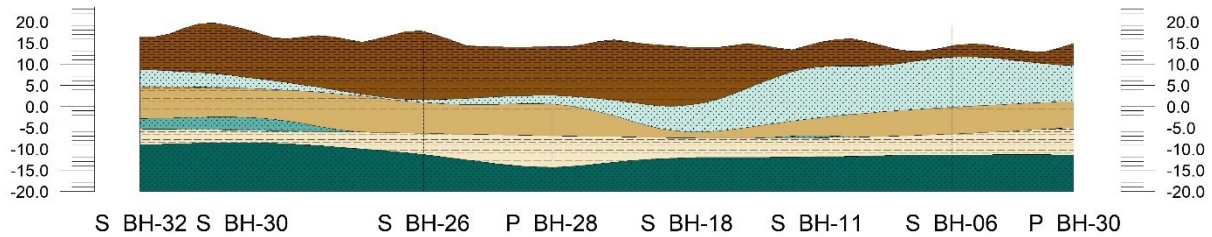


Figure 9 Cross-section A-A'.

### Cross-section B-B'

The cross-section BB' (NE-SW) (Figure 10) extends approximately 20.00 km from BH-19 to BH-28, connecting BH-23, BH-24, BH-25 and BH-26 along the way. This section is also located in Gangi upazila. Layer 1, along with Layers 6, exhibits undulation throughout the section. Layer 1, which is the uppermost layer, has a thickness ranging from 7 to 20 meters. Layer 6 is not much undulated and is the deepest section, with thicknesses varying between 5 to 20 meters. In contrast, Layers 2, 3, 4 and 5 have inconsistent thicknesses, ranging from 0.5 to 10 meters.

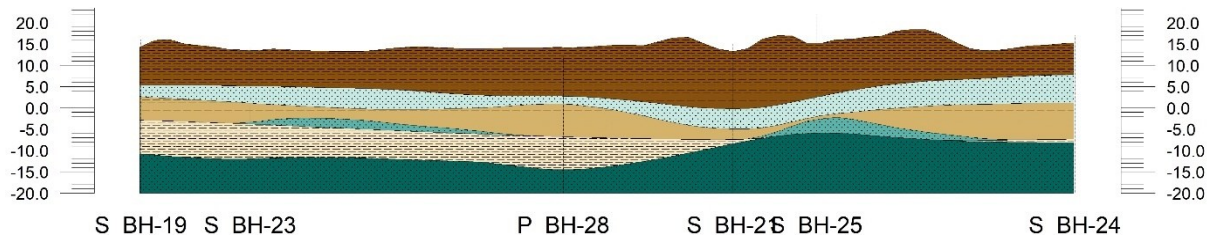


Figure 10 Cross-section B-B'.

### Cross-section C-C'

The cross-section CC' (WNW-ESE) (figure 11) extends approximately 20.00 km from BH-14 to BH-25, connecting BH-15 and BH-21 along the way. This section is located in Meherpur Sadar Upazila. Layer 1, which is the uppermost layer, has a thickness ranging from 2 to 20 meters. Layers 5 and 6 are the deeper layers with uniform thickness ranging from 15 to 20 meters. In contrast, Layers 2, 3, and 4 have inconsistent thicknesses, ranging from 2 to 20 meters.

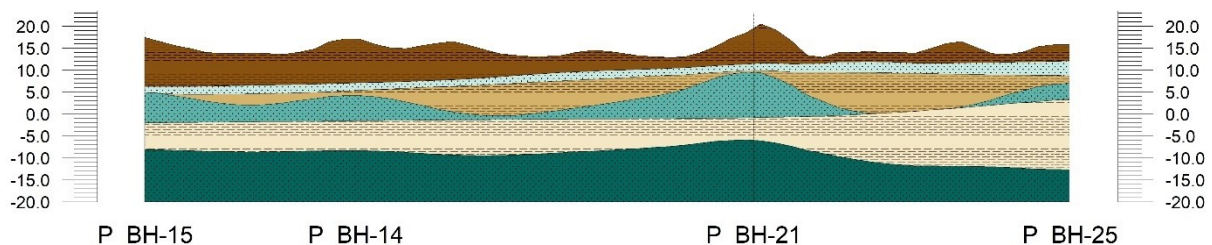


Figure 11 Cross-section C-C'.

### Cross-section D-D'

The cross-section DD' (W-E) (Figure 12) extends approximately 20.00 km from BH-13 to BH-27, connecting BH-11, and BH-21 along the way. This section is located in Meherpur Sadar Upazila. Layer 6, exhibits uniform thickness throughout the section ranging from 15.00 to 20.00 meters. In contrast, Layers 1, 2, 3, 4 and 5 have inconsistent thicknesses, ranging from 2 to 20 meters.

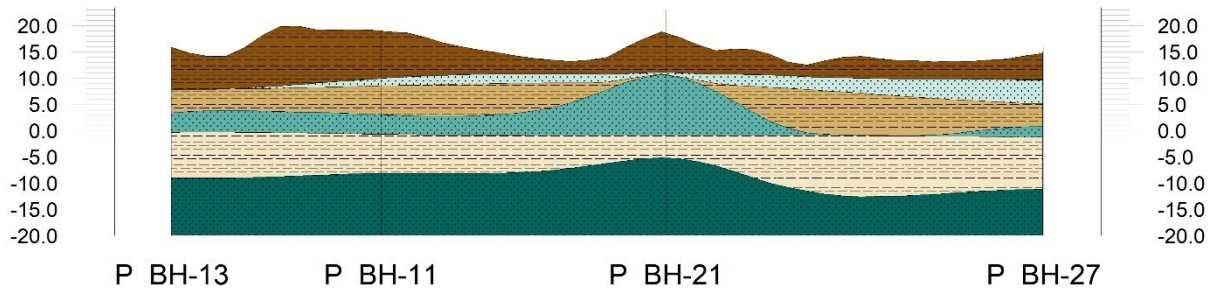


Figure 12 Cross-section D-D'.

### Cross-section E-E'

The cross-section EE' (NW-SSE) (Figure 13) extends approximately 18.00 km from BH-02 to BH-07, connecting BH-03, BH-04, and BH-06 along the way. This section is located in Mujib Nagar Upazila. Layers 3, 4, 5 and 6 exhibit uniform thickness throughout the section ranging from 15.00 to 25.00 meters. In contrast, Layers 1 and 2 have inconsistent thicknesses, ranging from 1 to 10 meters.

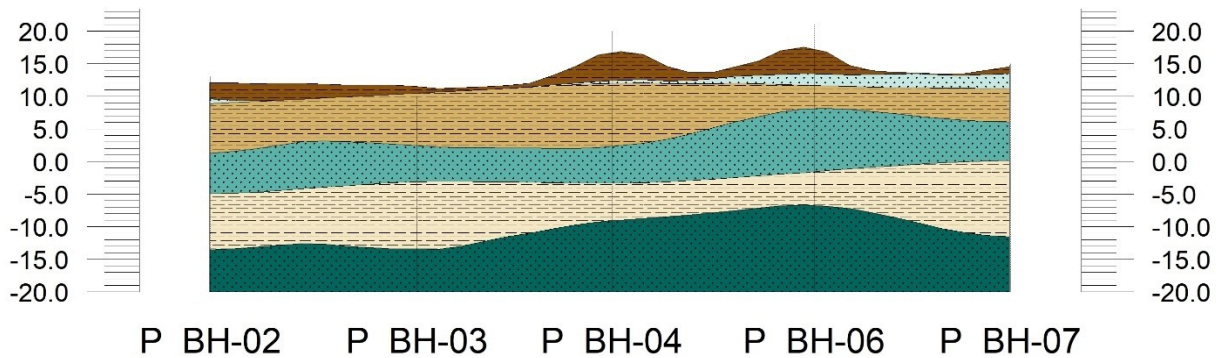


Figure 13 Cross-section E-E'.

### Cross-section F-F'

The cross-section FF' (W-E) (Figure 14) extends approximately 15.00 km from BH-03 to BH-09, connecting BH-04, and BH-08 along the way. This section is located in Mujib Nagar Upazila. Layer 3, has a thickness ranging from 2 to 20 meters. Thickness of layers 5 and 6 are varying between 5 to 25 meters. In contrast, Layers 1, 2 and 4 have inconsistent thicknesses, ranging from 0.5 to 10 meters.

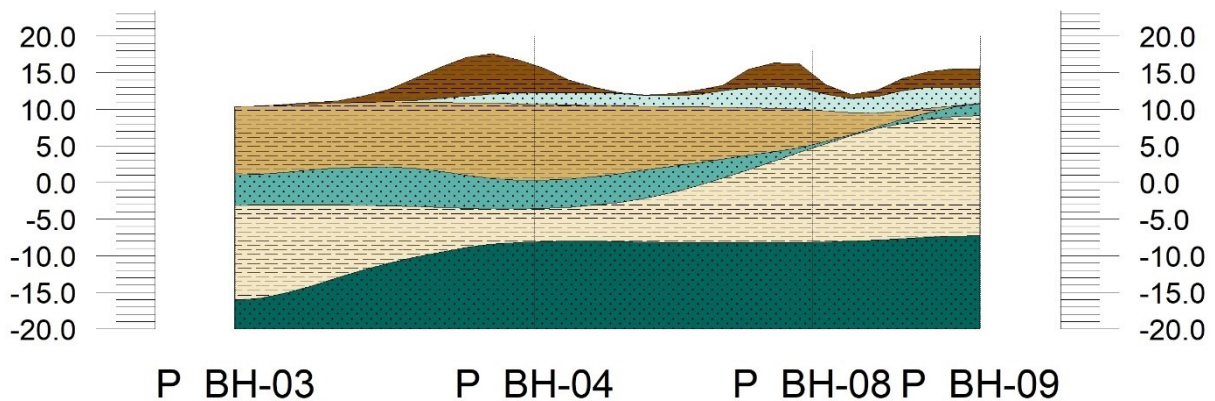


Figure 14 Cross-section F-F'.

### 3.3. Bearing Capacity for Shallow Foundation

#### SPT N-Value Correction

The Bearing capacities of the shallow foundation have been evaluated for the existing subsoil condition. In doing so, the overall field SPT values have been corrected at the different layers of investigation in the case of each borehole. In the project area a lot of the boreholes exhibits SPT N-value more than 50 which represent very dense and stiff type of soil. When the advancement through a 150 mm (6 in) interval is not possible with 50 blows, the penetration level is documented at 50 blows. In these cases, the actual SPT-value exceeds 50. However, for the purpose of analysis, the value was assumed to be 50. This indicates that the given value is the minimum, and the true value is greater than this.

On the basis of field observations, it appears reasonable to standardize the field SPT number as a function of the input driving energy and its dissipation around the sampler around the surrounding soil. The variations in testing procedures may be at least partially compensated by converting the measured SPT values as follows (Skempton 1986)-

$$N_{60} = \frac{E_H C_B C_S C_R N}{0.60}$$

Where:

$N_{60}$  = Corrected SPT N-value for field procedures

$E_H$  = Hammer efficiency

$C_B$  = Borehole diameter correction

$C_S$  = Sampler correction

$C_R$  = Rod length correction

$N$  = Measured SPT N-value in field

The correction due to overburden pressure has been performed according to Peck et al. (1991) and BNBC (2015). During the correction of over N-values of SPT, the correction is not performed as it does not reflect the actual value. And in most of the cases the SPT N-values exceeds 50.

$$(N_1)_{60} = C_N * N_{60} \leq 2N_{60}$$

Where:

$(N_1)_{60}$  = Corrected SPT N-value due to overburden pressure

$C_N$  = Overburden pressure correction factor

Suggested the following equation for  $C_N$ .

$$C_N = 0.77 \log \left( \frac{2000}{\sigma'_0} \right)$$



Where:

$\sigma'_0$  is the effective overburden pressure in  $\text{kN/m}^2$  or  $\text{kPa}$ , which is calculated from the unit weight of soil or  $\text{kPa}$ .

### **Bearing Capacity for Shallow Foundation**

Bearing capacity refers to the maximum load or weight that a foundation, soil, or supporting material can withstand without experiencing excessive settlement, deformation, or failure. It is a critical consideration in civil engineering and construction, as it ensures the stability and safety of structures such as buildings, bridges, roads, and retaining walls. Allowable bearing capacity is the maximum allowable net loading intensity on the soil at which the soil neither fails in shear nor undergoes excessive or intolerable settlement detrimental to the structure. This is the minimum of safe bearing capacity and safe bearing pressure. The allowable bearing capacity of cohesive soil is calculated according to Terzaghi (1947) and Terzaghi & Peck (1948). The safety factor was considered to be 3 for normal control according to Coduto (1994) and BNBC (2020). The value of effective cohesion is measured from the SPT-value and soil type using an empirical equation and the vertical effective stress is calculated using the depth and unit weight. And the width or the diameter of the foundation is considered to be 1 meter.

$$Q_a = \frac{1}{F} (1.3 c' N_c + \sigma'_{zD} N_q + 0.4 \gamma B N_\gamma)$$

Where:

$Q_a$  is the allowable bearing load in  $\text{kPa}$ .

$c'$  is the effective cohesion.

$\sigma'_{zD}$  is the vertical effective stress at the depth the foundation is laid.

$F$  is the safety factor.

$\gamma'$  is the effective unit weight when saturated or the total unit weight when not fully saturated.

$B$  is the width or the diameter of the foundation.

$N_c$ ,  $N_q$  and  $N_\gamma$  are the bearing capacity factor which are constant for different friction.

For cohesionless soil the bearing capacity is calculated using the following equation by Meyerhoff (1956). Width of the footing was considered as 1 m and the tolerable settlement is considered to be 25 mm.

$$Q_a (\text{kPa}) = 12 N F_d \left( \frac{s}{25.4} \right) \text{ for } B \leq 1.2 \text{ m}$$

Where:

$$F_d = \text{Depth factor} = 1 + \frac{D_f}{3B}$$

$s$  = tolerable settlement (mm)

$B$  = width of the footing (m)

$D_f$  = depth of footing (m)

$N$  = Average  $N$ -value from depth of footing to  $D_f+B$ .

The bearing capacity (Table 2) has been calculated for the available borehole data.

*Table 2 Allowable Bearing Capacity for Shallow Foundation of Meherpur District*

Borehole (Primary)	Depth (m)	Soil Type	Average Corrected SPT N-Value	Footing Width (m)	Depth Factor	Tolerable Settlement (mm)	Allowable Bearing Capacity (kPa)	Allowable Bearing Capacity (ksf)
BH-01	1.5	Cohesive	8.25	1	1.495	25	147.13	3.07
	3	Cohesive	7.22	1	1.99	25	165.46	3.46
	4.5	Cohesive	6.65	1	2.485	25	187.06	3.91
	6	Non-cohesive	8.94	1	2.98	25	314.57	6.57
BH-02	1.5	Cohesive	2.06	1	1.495	25	42.41	0.89
	3	Cohesive	2.41	1	1.99	25	65.19	1.36
	4.5	Cohesive	2.29	1	2.485	25	79.26	1.66
	6	Cohesive	2.23	1	2.98	25	94.11	1.97
BH-03	1.5	Non-cohesive	4.81	1	1.495	25	84.98	1.77
	3	Cohesive	3.78	1	1.99	25	93.79	1.96
	4.5	Cohesive	3.21	1	2.485	25	101.90	2.13
	6	Cohesive	3.27	1	2.98	25	123.74	2.58
BH-04	1.5	Non-cohesive	4.13	1	1.495	25	72.84	1.52
	3	Cohesive	7.22	1	1.99	25	165.67	3.46
	4.5	Cohesive	8.02	1	2.485	25	221.34	4.62
	6	Non-cohesive	8.25	1	2.98	25	290.37	6.06
BH-05	1.5	Non-cohesive	2.75	1	1.495	25	48.56	1.01
	3	Non-cohesive	3.78	1	1.99	25	88.87	1.86
	4.5	Cohesive	3.21	1	2.485	25	101.90	2.13
	6	Cohesive	4.47	1	2.98	25	158.63	3.31
BH-06	1.5	Cohesive	2.75	1	1.495	25	54.04	1.13
	3	Cohesive	6.53	1	1.99	25	151.37	3.16
	4.5	Cohesive	5.96	1	2.485	25	170.03	3.55
	6	Cohesive	5.50	1	2.98	25	187.71	3.92
BH-07	1.5	Cohesive	6.19	1	1.495	25	112.22	2.34
	3	Cohesive	4.47	1	1.99	25	108.09	2.26
	4.5	Cohesive	3.44	1	2.485	25	107.51	2.25
	6	Cohesive	3.95	1	2.98	25	143.61	3.00
BH-08	1.5	Non-cohesive	4.13	1	1.495	25	72.84	1.52
	3	Non-cohesive	4.13	1	1.99	25	96.95	2.02
	4.5	Non-cohesive	8.02	1	2.485	25	235.41	4.92
	6	Non-cohesive	7.73	1	2.98	25	272.23	5.69

BH-09	1.5	Cohesive	2.75	1	1.495	25	54.04	1.13
	3	Cohesive	6.53	1	1.99	25	151.37	3.16
	4.5	Cohesive	6.65	1	2.485	25	187.17	3.91
	6	Cohesive	6.19	1	2.98	25	207.44	4.33
BH-10	1.5	Non-cohesive	6.88	1	1.495	25	121.40	2.54
	3	Non-cohesive	8.25	1	1.99	25	193.91	4.05
	4.5	Non-cohesive	14.67	1	2.485	25	430.47	8.99
	6	Non-cohesive	18.56	1	2.98	25	653.34	13.65
BH-11	1.5	Cohesive	1.38	1	1.495	25	30.77	0.64
	3	Cohesive	2.06	1	1.99	25	58.04	1.21
	4.5	Cohesive	2.75	1	2.485	25	90.73	1.89
	6	Cohesive	4.13	1	2.98	25	148.80	3.11
BH-12	1.5	Cohesive	22.00	1	1.495	25	379.85	7.93
	3	Cohesive	20.63	1	1.99	25	444.96	9.29
	4.5	Cohesive	15.13	1	2.485	25	396.40	8.28
	6	Cohesive	12.72	1	2.98	25	394.31	8.24
BH-13	1.5	Non-cohesive	3.44	1	1.495	25	60.70	1.27
	3	Non-cohesive	5.50	1	1.99	25	129.27	2.70
	4.5	Non-cohesive	5.50	1	2.485	25	161.43	3.37
	6	Non-cohesive	6.19	1	2.98	25	217.78	4.55
BH-14	1.5	Cohesive	3.44	1	1.495	25	65.68	1.37
	3	Cohesive	3.09	1	1.99	25	79.49	1.66
	4.5	Non-cohesive	6.65	1	2.485	25	195.06	4.07
	6	Non-cohesive	8.59	1	2.98	25	302.47	6.32
BH-15	1.5	Non-cohesive	6.88	1	1.495	25	121.40	2.54
	3	Non-cohesive	8.25	1	1.99	25	193.91	4.05
	4.5	Non-cohesive	8.94	1	2.485	25	262.32	5.48
	6	Non-cohesive	8.77	1	2.98	25	308.52	6.44
BH-16	1.5	Cohesive	6.19	1	1.495	25	112.22	2.34
	3	Cohesive	4.47	1	1.99	25	108.09	2.26
	4.5	Cohesive	4.13	1	2.485	25	124.65	2.60
	6	Cohesive	4.47	1	2.98	25	158.36	3.31
BH-17	1.5	Non-cohesive	8.94	1	1.495	25	157.81	3.30
	3	Non-cohesive	11.34	1	1.99	25	266.62	5.57
	4.5	Non-cohesive	12.83	1	2.485	25	376.66	7.87
	6	Non-cohesive	11.86	1	2.98	25	417.41	8.72
BH-18	1.5	Cohesive	2.06	1	1.495	25	42.41	0.89
	3	Cohesive	2.41	1	1.99	25	65.19	1.36
	4.5	Cohesive	3.21	1	2.485	25	102.11	2.13
	6	Non-cohesive	4.81	1	2.98	25	169.38	3.54
BH-19	1.5	Cohesive	0.69	1	1.495	25	19.14	0.40
	3	Cohesive	2.06	1	1.99	25	58.07	1.21
	4.5	Non-cohesive	6.42	1	2.485	25	188.33	3.93
	6	Non-cohesive	7.73	1	2.98	25	272.23	5.69
BH-20	1.5	Cohesive	4.13	1	1.495	25	77.32	1.61

	3	Non-cohesive	6.53	1	1.99	25	153.51	3.21
	4.5	Non-cohesive	7.79	1	2.485	25	228.69	4.78
	6	Non-cohesive	7.73	1	2.98	25	272.23	5.69
BH-21	1.5	Cohesive	8.25	1	1.495	25	147.13	3.07
	3	Cohesive	12.38	1	1.99	25	273.23	5.71
	4.5	Non-cohesive	12.83	1	2.485	25	376.66	7.87
	6	Non-cohesive	14.61	1	2.98	25	514.20	10.74
BH-22	1.5	Cohesive	1.38	1	1.495	25	30.77	0.64
	3	Non-cohesive	6.19	1	1.99	25	145.43	3.04
	4.5	Non-cohesive	15.58	1	2.485	25	457.38	9.55
	6	Non-cohesive	18.73	1	2.98	25	659.39	13.77
BH-23	1.5	Cohesive	5.50	1	1.495	25	100.59	2.10
	3	Cohesive	5.84	1	1.99	25	136.86	2.86
	4.5	Non-cohesive	7.79	1	2.485	25	228.69	4.78
	6	Non-cohesive	7.91	1	2.98	25	278.28	5.81
BH-24	1.5	Cohesive	1.38	1	1.495	25	30.77	0.64
	3	Cohesive	1.38	1	1.99	25	43.67	0.91
	4.5	Cohesive	2.29	1	2.485	25	79.41	1.66
	6	Non-cohesive	3.44	1	2.98	25	120.99	2.53
BH-25	1.5	Cohesive	3.44	1	1.495	25	65.68	1.37
	3	Cohesive	5.50	1	1.99	25	129.78	2.71
	4.5	Non-cohesive	6.65	1	2.485	25	195.06	4.07
	6	Non-cohesive	6.70	1	2.98	25	235.93	4.93
BH-26	1.5	Cohesive	13.06	1	1.495	25	228.58	4.77
	3	Non-cohesive	10.31	1	1.99	25	242.38	5.06
	4.5	Non-cohesive	9.17	1	2.485	25	269.05	5.62
	6	Non-cohesive	10.31	1	2.98	25	362.97	7.58
BH-27	1.5	Non-cohesive	10.31	1	1.495	25	182.09	3.80
	3	Non-cohesive	11.69	1	1.99	25	274.70	5.74
	4.5	Non-cohesive	12.83	1	2.485	25	376.66	7.87
	6	Non-cohesive	16.33	1	2.98	25	574.70	12.00
BH-28	1.5	Cohesive	3.44	1	1.495	25	65.68	1.37
	3	Cohesive	4.81	1	1.99	25	115.41	2.41
	4.5	Cohesive	3.44	1	2.485	25	107.46	2.24
	6	Cohesive	2.92	1	2.98	25	113.70	2.37
BH-29	1.5	Cohesive	3.44	1	1.495	25	65.68	1.37
	3	Non-cohesive	2.75	1	1.99	25	64.64	1.35
	4.5	Non-cohesive	8.71	1	2.485	25	255.59	5.34
	6	Non-cohesive	15.13	1	2.98	25	532.35	11.12
BH-30	1.5	Cohesive	8.25	1	1.495	25	147.13	3.07
	3	Cohesive	16.84	1	1.99	25	366.62	7.66
	4.5	Non-cohesive	14.90	1	2.485	25	437.20	9.13
	6	Non-cohesive	14.78	1	2.98	25	520.25	10.87

Borehole (Secondary)	Depth (m)	Soil Type	Average Corrected SPT N-Value	Footing Width (m)	Depth Factor	Tolerable Settlement (mm)	Allowable Bearing Capacity (kPa)	Allowable Bearing Capacity (ksf)
BH-03	1.5	Non-cohesive	6.19	1	1.495	25	109.26	2.28
	3	Non-cohesive	6.19	1	1.99	25	145.43	3.04
	4.5	Non-cohesive	7.33	1	2.485	25	215.24	4.50
	6	Non-cohesive	10.83	1	2.98	25	381.12	7.96
BH-04	1.5	Non-cohesive	4.13	1	1.495	25	72.84	1.52
	3	Non-cohesive	4.81	1	1.99	25	113.11	2.36
	4.5	Non-cohesive	5.04	1	2.485	25	147.97	3.09
	6	Non-cohesive	4.98	1	2.98	25	175.43	3.66
BH-06	1.5	Cohesive	4.81	1	1.495	25	88.95	1.86
	3	Cohesive	3.09	1	1.99	25	79.42	1.66
	4.5	Non-cohesive	2.98	1	2.485	25	87.44	1.83
	6	Non-cohesive	4.47	1	2.98	25	157.29	3.28
BH-07	1.5	Non-cohesive	7.56	1	1.495	25	133.53	2.79
	3	Non-cohesive	6.53	1	1.99	25	153.51	3.21
	4.5	Non-cohesive	5.96	1	2.485	25	174.88	3.65
	6	Non-cohesive	7.05	1	2.98	25	248.03	5.18
BH-10	1.5	Cohesive	1.38	1	1.495	25	30.77	0.64
	3	Cohesive	1.72	1	1.99	25	50.85	1.06
	4.5	Cohesive	1.60	1	2.485	25	62.23	1.30
	6	Cohesive	1.55	1	2.98	25	74.38	1.55
BH-11	1.5	Non-cohesive	6.88	1	1.495	25	121.40	2.54
	3	Non-cohesive	7.56	1	1.99	25	177.75	3.71
	4.5	Non-cohesive	8.25	1	2.485	25	242.14	5.06
	6	Non-cohesive	6.88	1	2.98	25	241.98	5.05
BH-12	1.5	Cohesive	2.75	1	1.495	25	54.04	1.13
	3	Non-cohesive	2.06	1	1.99	25	48.48	1.01
	4.5	Non-cohesive	2.06	1	2.485	25	60.54	1.26
	6	Non-cohesive	2.92	1	2.98	25	102.84	2.15
BH-13	1.5	Cohesive	2.06	1	1.495	25	42.41	0.89
	3	Cohesive	2.41	1	1.99	25	65.19	1.36
	4.5	Cohesive	2.06	1	2.485	25	73.55	1.54
	6	Cohesive	2.06	1	2.98	25	89.19	1.86
BH-14	1.5	Cohesive	1.38	1	1.495	25	30.77	0.64
	3	Cohesive	1.38	1	1.99	25	43.67	0.91
	4.5	Cohesive	1.60	1	2.485	25	62.28	1.30
	6	Cohesive	2.06	1	2.98	25	89.33	1.87
BH-15	1.5	Cohesive	1.38	1	1.495	25	30.77	0.64
	3	Non-cohesive	3.09	1	1.99	25	72.72	1.52
	4.5	Non-cohesive	4.81	1	2.485	25	141.25	2.95
	6	Non-cohesive	5.84	1	2.98	25	205.68	4.30
BH-16	1.5	Non-cohesive	4.13	1	1.495	25	72.84	1.52
	3	Non-cohesive	4.81	1	1.99	25	113.11	2.36

	4.5	Non-cohesive	5.50	1	2.485	25	161.43	3.37
	6	Non-cohesive	7.56	1	2.98	25	266.18	5.56
BH-17	1.5	Non-cohesive	3.44	1	1.495	25	60.70	1.27
	3	Non-cohesive	4.13	1	1.99	25	96.95	2.02
	4.5	Non-cohesive	4.58	1	2.485	25	134.52	2.81
	6	Cohesive	4.47	1	2.98	25	158.22	3.30
BH-18	1.5	Non-cohesive	2.75	1	1.495	25	48.56	1.01
	3	Non-cohesive	3.44	1	1.99	25	80.79	1.69
	4.5	Non-cohesive	3.90	1	2.485	25	114.34	2.39
	6	Non-cohesive	3.78	1	2.98	25	133.09	2.78
BH-19	1.5	Cohesive	2.75	1	1.495	25	54.04	1.13
	3	Cohesive	2.75	1	1.99	25	72.34	1.51
	4.5	Cohesive	2.75	1	2.485	25	90.63	1.89
	6	Cohesive	3.44	1	2.98	25	128.86	2.69
BH-20	1.5	Cohesive	3.44	1	1.495	25	65.68	1.37
	3	Cohesive	4.13	1	1.99	25	101.04	2.11
	4.5	Cohesive	4.58	1	2.485	25	136.12	2.84
	6	Non-cohesive	5.16	1	2.98	25	181.48	3.79
BH-21	1.5	Cohesive	1.38	1	1.495	25	30.77	0.64
	3	Cohesive	1.38	1	1.99	25	43.67	0.91
	4.5	Cohesive	1.15	1	2.485	25	50.85	1.06
	6	Non-cohesive	2.75	1	2.98	25	96.79	2.02
BH-22	1.5	Cohesive	2.06	1	1.495	25	42.41	0.89
	3	Cohesive	1.72	1	1.99	25	50.82	1.06
	4.5	Cohesive	1.60	1	2.485	25	62.23	1.30
	6	Cohesive	1.72	1	2.98	25	79.36	1.66
BH-23	1.5	Cohesive	4.81	1	1.495	25	88.95	1.86
	3	Cohesive	3.78	1	1.99	25	93.79	1.96
	4.5	Cohesive	3.67	1	2.485	25	113.32	2.37
	6	Cohesive	3.95	1	2.98	25	143.54	3.00
BH-24	1.5	Cohesive	3.44	1	1.495	25	65.68	1.37
	3	Cohesive	3.78	1	1.99	25	93.86	1.96
	4.5	Cohesive	4.35	1	2.485	25	130.46	2.72
	6	Non-cohesive	4.81	1	2.98	25	169.38	3.54
BH-25	1.5	Cohesive	0.69	1	1.495	25	19.14	0.40
	3	Cohesive	1.72	1	1.99	25	50.89	1.06
	4.5	Cohesive	2.52	1	2.485	25	85.07	1.78
	6	Cohesive	3.27	1	2.98	25	123.95	2.59
BH-26	1.5	Cohesive	1.38	1	1.495	25	30.77	0.64
	3	Cohesive	1.72	1	1.99	25	50.85	1.06
	4.5	Cohesive	1.60	1	2.485	25	62.23	1.30
	6	Non-cohesive	2.58	1	2.98	25	90.74	1.90
BH-27	1.5	Cohesive	1.38	1	1.495	25	30.77	0.64
	3	Cohesive	3.09	1	1.99	25	79.59	1.66
	4.5	Cohesive	3.90	1	2.485	25	119.14	2.49

	6	Non-cohesive	6.19	1	2.98	25	217.78	4.55
BH-28	1.5	Cohesive	2.75	1	1.495	25	54.04	1.13
	3	Cohesive	3.44	1	1.99	25	86.71	1.81
	4.5	Cohesive	3.21	1	2.485	25	101.95	2.13
	6	Non-cohesive	3.95	1	2.98	25	139.14	2.91
BH-29	1.5	Cohesive	2.75	1	1.495	25	54.04	1.13
	3	Cohesive	5.50	1	1.99	25	129.81	2.71
	4.5	Non-cohesive	6.42	1	2.485	25	188.33	3.93
	6	Non-cohesive	7.05	1	2.98	25	248.03	5.18
BH-30	1.5	Cohesive	1.38	1	1.495	25	30.77	0.64
	3	Cohesive	1.38	1	1.99	25	43.67	0.91
	4.5	Cohesive	1.83	1	2.485	25	67.99	1.42
	6	Cohesive	2.23	1	2.98	25	94.25	1.97
BH-31	1.5	Non-cohesive	4.13	1	1.495	25	72.84	1.52
	3	Cohesive	2.75	1	1.99	25	72.27	1.51
	4.5	Cohesive	2.52	1	2.485	25	84.92	1.77
	6	Cohesive	4.30	1	2.98	25	153.85	3.21
BH-32	1.5	Cohesive	2.06	1	1.495	25	42.41	0.89
	3	Cohesive	1.72	1	1.99	25	50.82	1.06
	4.5	Cohesive	1.83	1	2.485	25	67.94	1.42
	6	Cohesive	2.23	1	2.98	25	94.25	1.97

### Allowable Bearing Capacity for Shallow Foundations of Meherpur:

The allowable bearing capacity is the maximum pressure that can be exerted on the soil by the foundation without causing shear failure or excessive settlement. In this case, allowable bearing capacities for depths of 1.5 meters, 3 meters, 4.5 meters, and 6 meters were calculated using SPT data. These values indicate how much load the soil at each respective depth can safely support. The Bangladesh National Building Code (BNBC) provides specific guidelines regarding the safe bearing capacity for different soil types and building types. These guidelines are particularly significant for low-rise buildings to prevent issues related to foundation failure and structural instability. The safe bearing capacity in the BNBC is essentially a benchmark that ensures a conservative and standardized approach to foundation design.

*Table 3 Presumptive Values of Bearing Capacity for Lightly Loaded Structures (BNBC 2020)*

Sl.	Soil Description	Safe Bearing Capacity, kPa
1	Soft Rock or Shale	440
2	Gravel, sandy gravel, silty sandy gravel; very dense and offer high resistance to penetration during excavation (soil shall include the groups GW, GP, GM, GC)	400**
3	Sand (other than fine sand), gravelly sand, silty sand; dry (soil shall include the groups SW, SP, SM, SC)	200**
4	Fine sand; loose & dry (soil shall include the groups SW, SP)	100**
5	Silt, clayey silt, clayey sand; dry lumps which can be easily crushed by finger (soil shall include the groups ML, SC, & MH)	150
6	Clay, sandy clay; can be indented with strong thumb pressure (soil shall include the groups CL, & CH)	150

7	Soft clay; can be indented with modest thumb pressure (soil shall include the groups CL, & CH)	100
8	Very soft clay; can be penetrated several centimeters with thumb pressure (soil shall include the groups CL & CH)	50
9	Organic clay & Peat (soil shall include the groups OH, OL, Pt)	To be determined after investigation
** 50% of these values shall be used where water table is above the base, or below it within a distance equal to the least dimension of foundation.		

The borehole data indicates that the predominant shallow soil types are sand, silt, silty sand, clay, silty clay, clayey silt, clayey sand, and silty sand. For this type of soil, the safe bearing capacity ranges from 100 to 150 kPa. When the calculated allowable bearing capacity (which considers safety factors to prevent soil failure and control settlement) is greater than or equal to the safe bearing capacity as per the BNBC guidelines, it indicates that the soil is capable of supporting the load from the building. This makes the use of shallow foundations feasible and safe for construction. If the calculated allowable bearing capacity is less than the safe bearing capacity, this implies that the soil may not provide sufficient support for the intended load. In this case, the potential risks include shear failure and excessive settlement.

The assessment reveals that most areas of Meherpur District are suitable for shallow foundations supporting lightly loaded structures at an allowable bearing capacity up to a depth of 4.5 meters. However, a small portion of Gangi Upazila, particularly in the northwestern region, has been identified as unsuitable for shallow foundations at this depth due to lower soil bearing capacity. Furthermore, when considering an increased depth of up to 6.0 meters, the vast majority of Meherpur District remains suitable for shallow foundations for lightly loaded structures. Only a negligible portion of land, again primarily within Gangi Upazila, is considered unsuitable even at this depth.



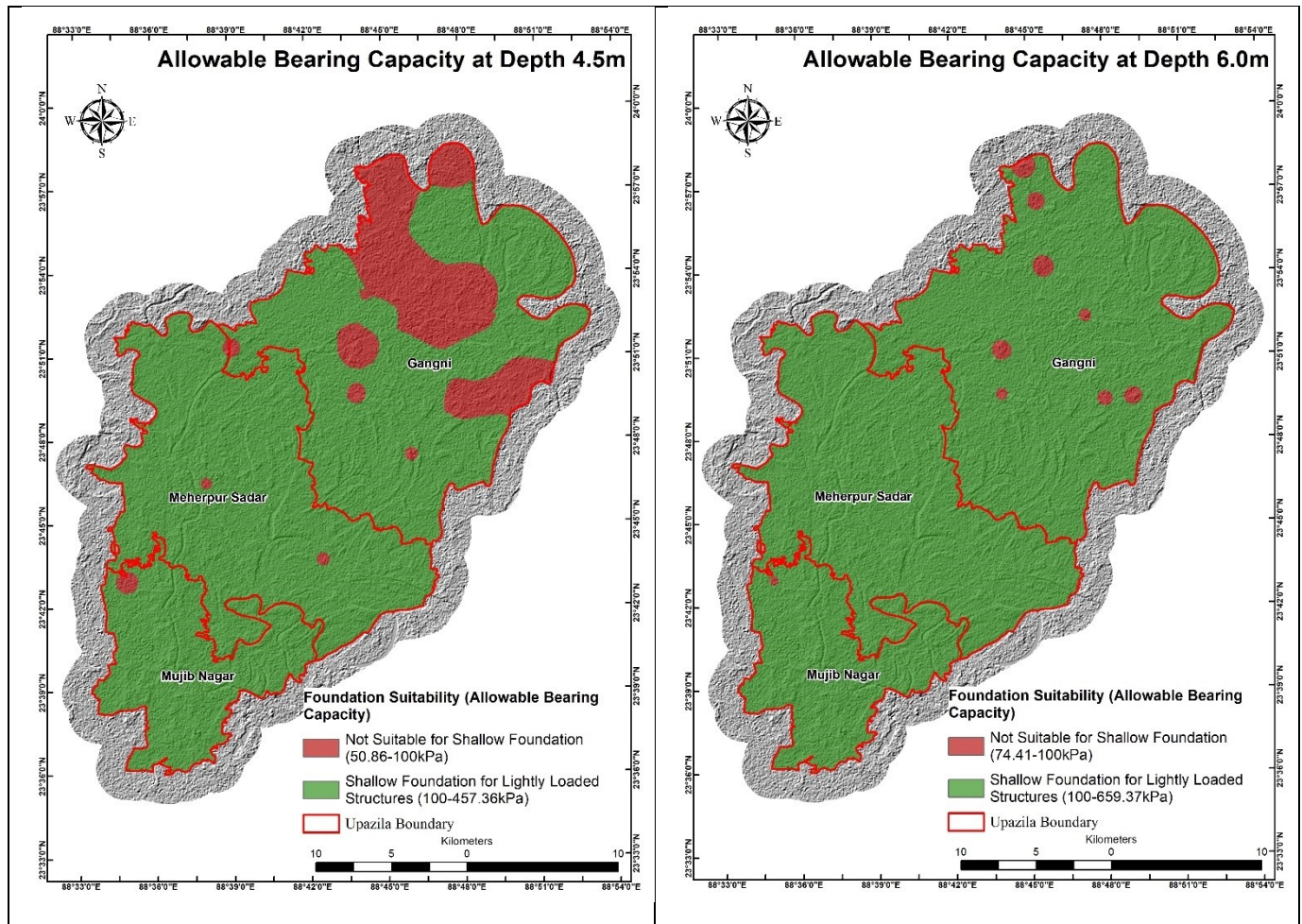


Figure 15 Foundation Layer Depth of Meherpur District.

In addition, the allowable bearing capacities for foundation depths of 4.5 meters and 6.0 meters have been estimated based on preliminary Standard Penetration Test (SPT) data. These values provide a general understanding of the soil's load-bearing capacity at those depths and can guide initial planning considerations. However, for the construction of individual structures, a detailed geotechnical investigation is essential to obtain accurate, site-specific soil properties.

## 4. SEISMIC HAZARD ASSESSMENT

Earthquakes are impact-based events. In most cases, the impacts are catastrophic with numerous injuries, severe damage, and destruction to the infrastructure. With the sudden elastic energy released from accumulated strain in the rocks, earthquake cause shaking to the ground during the transmission of elastic energy outwards through rocks as seismic waves. These seismic waves are responsible for ground failure, structural damage, landslides or slope failure, and liquefaction, which are termed the primary effects of earthquake hazards. Moreover, tsunamis, fire outbreaks, and subsidence are seen as by-products of earthquakes. These catastrophic impacts are amplified by human-induced activities, such as poor construction practices due to the infringement of the existing building code, and urbanization-related malpractices. Recent earthquakes that occurred in 2001, 2005, 2008, 2010, and 2011 in India, Pakistan, China, Haiti, and Japan respectively are the vivid illustration of these malpractices and their consequences (Kamal, 2013). To reduce these dreadful impacts, seismic risk assessment of an earthquake-prone area is crucial. Seismic hazard analysis is the fundamental step for assessing existing seismic risk in an area which provides the quantitative measure of ground motion parameters, like the peak ground acceleration and the spectral acceleration of individual spectral periods. Considering these parameters, the seismic design of infrastructures aiming to withstand a certain level of shaking can potentially reduce seismic risk. For several years, different researchers have conducted substantial studies on Bangladesh since 1979. GSB authority first released its seismic zonation map of Bangladesh in 1979. National Building Code of Bangladesh further revised this map to institutionalize the National Building Code of Bangladesh, represented in 3 different zones, each containing a unique hazard range.

### 4.1. Seismic Hazard Analysis in Bangladesh

Later in 2020, during the revision of the code, the notion of Maximum Credible Earthquake (MCE) motion with a 2% exceedance probability in a 50-year timeframe was applied to produce different zonation (4 zones) than the previous code. Therefore, seismic hazard analysis utilizing updated data, science, and technology is essential for reducing seismic risk in tectonically active areas. Ansary Sharifuddin (2002) modified the seismic zones neglecting the required justification about their assumed magnitude and frequency recurrence correlation. Islam et al. in 2010, used the software CRISIS (Ordaz & Salgado-Gálvez, 2017) to conduct PSHA based on seven different seismogenic source zone for this country. In 2019, Haque et al. tried to dispel some of the limitations in the former studies by incorporating updated sources obtained from Wang et al. (2014) and particular GMPEs dedicated to these zones. However, they considered only one type of source zonation based on Wang et al. (2014). Recently, Rahman et al, (2020) has regarded the potential sources and seismicity models more extensively than the previous works, computed hazard parameters through EZ-Frisk software.

#### **Seismotectonic of Bangladesh**

The collision between Indian Plate and Eurasian Plate created the Himalayan Ranges and Bengal Basin (Curry et al., 1982; Steckler et al., 2008), which includes Bangladesh and parts of West Bengal, Tripura, and Assam of Indian states (Figure 5.1). The Bengal Basin is unique because of its colossal sediment thickness (approximately 22 km). It is considered one of the world's largest basins (M. Alam, 1989), bounded by the Precambrian Shilling Massif in the

north, the Bay of Bengal in the south, the Indo-Burman Folded Belt in the east, and the Indian Platform in the west. Bangladesh covers almost three-fourths of the Bengal Basin (Steckler et al., 2008). The Himalayan system in the north and the Arakan subduction-collision system are the two major tectonic systems that can produce large earthquakes in the Bengal Basin area (Steckler et al., 2016). The frequent occurrence of large-magnitude earthquakes and the rate of plate movement suggest that the Bengal Basin is quite seismically active (Rahman & Siddiqua, 2017).

Several historical earthquakes occurred in the northeastern parts of India, Nepal, Myanmar, and Bangladesh along these tectonic belts in the last 256 years (Rahman et al., 2015, 2018). Among them, the 1762 Bengal–Arakan, 1885 Bengal, 1897 Great Assam, and 1918 Srimangal earthquakes caused severe damage in northern, northeastern, southeastern, and central parts of Bangladesh (Ambraseys & Douglas, 2004; Middlemiss, 1885; Oldham, 1899; Stuart, 1920; Szeliga et al., 2010). The Himalayan thrust belts and Arakan megathrust beneath the Indo-Burman Ranges are responsible for the occurrence of large-magnitude ( $M_w > 7.0$ ) earthquakes in northern and northeastern parts of India, Nepal, Bhutan, and Myanmar (Kayal et al., 2012; Steckler et al., 2016; Wang et al., 2014). Steckler et al., (2016) anticipated that a potential earthquake of  $M_w$  8.2–9.0 might occur along the Arakan megathrust. Bilham (2004) also identified the seismic gaps along two-thirds of the Himalayan Ranges that might generate one or more  $M_w = 8.0$  earthquakes. If a large magnitude ( $M_w > 8.0$ ) occurs along these megathrusts, it may cause unprecedented damage to the life and properties of the urban areas in these regions (Bilham, 2009; Steckler et al., 2016).

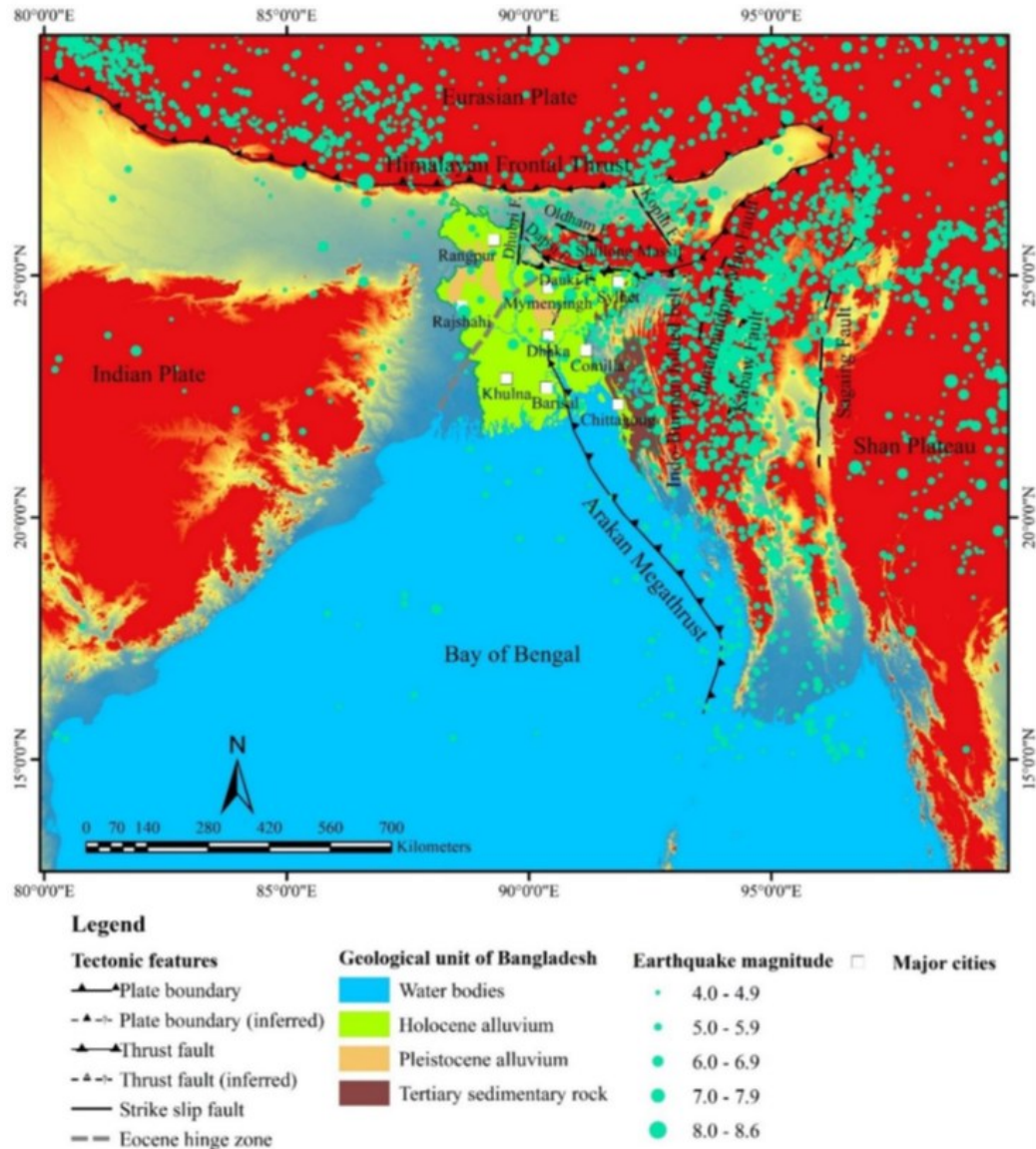


Figure 16 Seismotectonic Map of Bangladesh and Surrounding Regions Showing Epicenters of Earthquakes (Declustered Catalog) from 1762 To 2016 ((Rahman Et Al., 2020).

## 4.2. Methodology

### Overview of Probabilistic Seismic Hazard Analysis (PSHA)

Baker (2013) has summarized the activities associated with PSHA in 5 generalized steps based on the procedure of Cornell (1968) who is considered as the pioneer of PSHA. These steps are as follows:

Step-1: Identification of Possible Earthquake Sources

Step-2: Identification of Magnitude

Step-3: Source to Site Distance Identification

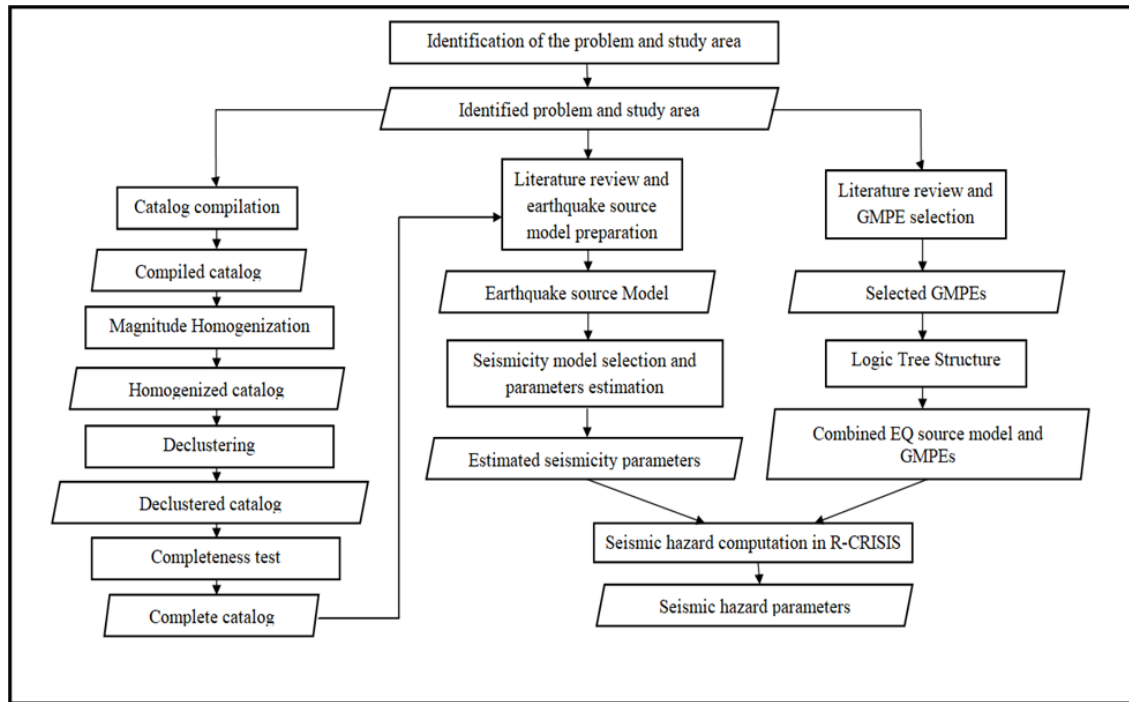
Step-4: Employment of Appropriate Ground Motion Prediction Equation (GMPE)

Step-5: Combination of All Information



## Methodological Framework

Probabilistic Seismic Hazard Analysis (PSHA) considers all potential sources, respective seismicity parameters, uncertainties associated with them and computes parameters for ground motion such as peak ground acceleration, and spectral acceleration at different spectral periods. This particular hazard assessment has considered all the steps described above applicable for PSHA and combined those according to the flexibility of the study. The steps are re-arranged in this study and summarized in the methodological framework:



## Source Model

While considering the seismogenic sources applicable to Bangladesh, special attention has been given to geodesy, active tectonic structures, and geodynamic characteristic of the study regions through a literature review combined with internationally accessible catalogs from renowned authorities in this field. Seismic sources taken for this research contain

- Gridded Seismicity or Background Seismicity Source,
- Linear Source,
- Areal Source.

## Earthquake Catalog

Earthquake catalog plays the role of basic information to quantify risk regardless of the approach as recurrence relation is derived from the catalog. Unfortunately, Bangladesh does not possess regular documentation of earthquakes in Bangladesh and its adjoining tectonic region. As compensation, information is collected from different international sources and published literature to compile an earthquake catalog. Instrumental earthquake records are taken from USGS online catalog, GCMT-Global Centroid Moment Tensor, ISC-GEM, and NEIC catalog. For historical earthquakes, the published literature of Alam & Dominey-Howes (2016), Ambraseys and Douglas (2004) and Szeliga et al. (2010) were followed. These records had a geographical limit of 16.1080N -31.1340N latitude in decimal degrees and 83.66°-96.92°

E longitude in decimal degrees. The earthquake events from these catalogs were compiled, sorted in chronological order, and inspected to remove any redundancy. While examining the redundancy, priority was assigned to GCMT, USGS, ISC, and NEIC catalog, respectively.

### Magnitude Conversion and Declustering

The catalog contains earthquake events in various magnitude scales like Body wave magnitude (Mb), Surface wave magnitude (Ms), and Moment magnitude (Mw). For further computation, the catalog must be in homogeneous form. In this study, the catalog is standardized in a single unit of measurement, Moment magnitude (Mw), as there lies a direct proportionate relation between Mw and the logarithm value of the seismic moment, remaining unsaturated at a larger magnitude.

The catalog contains events with moment magnitude, Surface wave magnitude (4.5- 6.2 Ms magnitude) and body wave magnitude (4 - 6.1 Mb magnitude). In order to remove this heterogeneity, all the events in the catalog were converted into moment magnitude using the globally accepted conversion equation of Scordilis (2006).

$$M_W = 0.8m_b + 1.03, 3.5 \leq m_b \leq 6.2 \dots \dots \dots (1)$$

$$M_W = 0.67 M_s + 2.07; 3.0 \leq M_s \leq 6.10,$$

$$R^2 = 0.77 \text{ (Scordilis, 2006) } \dots \dots \dots (2)$$

The seismicity model assumes the events of the earthquake catalog to be independent, inferred in the Poisson assumption. Therefore, Dependent events (aftershocks, foreshocks) are not kept in the catalog during further computation. Gardner and Knopoff, GK (1974) declustering algorithms are used to remove dependent events (58% of mainshock)

### Completeness

It is generally believed that earthquake catalogs for larger magnitudes are complete for extended periods. The scenario with smaller magnitudes is quite the opposite owing to socioeconomic and historical circumstances, variations in demography, and recording station location. With an unaddressed incompleteness issue in the catalog, the recurrence rate for a smaller and larger earthquake may be overestimated and underestimated. This study has evaluated various magnitude class completeness periods approaching the method of Stepp.

*Table 4 Completeness of Different Catalogs Estimated with the Method of Stepp (1972)*

Magnitude Range	Catalog declustered by GK (1974) algorithm	
	Completeness period	Interval (years)
4.5 and greater	1991-2023	33
5.0 and greater	1961-2023	63
5.5 and greater	1951-2023	73
6.0 and greater	1931-2023	93
6.5 and greater	1901-2023	123
7.5 and greater	1821-2023	203

## Areal Source

Delineation of the areal seismic source demands unvarying and homogeneous seismicity within the unit zone. Baker (2013) assumes that each point of the areal source has equal potential to create a future earthquake. Based on the changes of seismicity in the case of magnitude and focal depth distributed along the study area, and consideration of events in the comprehensive declustered catalog around geological structures, published literature dealing with similar concepts to this study, 10 areal source zones are delineated for this study. Parameters of truncated Gutenberg-Richter model for declustered catalog is estimated considering the lower extreme magnitude value at 4.5 Mw and respective completeness period for each zone assessed by the method of Tinti & Mulargia (1985). The regional maximum magnitude of all areal sources has been estimated from Kijko and Singh's (2011) Mmax program in MATLAB 2018a. This package comes with facilities to compute the maximum magnitude even for those catalogs which are independent of the assumed frequency-magnitude distribution. This algorithm can also be used for the worst scenario where there is no information available for the nature of earthquake distribution. The upper and lower bound of the maximum magnitude has also been assigned in the form of  $M_c + 0.2$  and  $M_c - 0.2$ . R-CRISIS software attributes by default weightings for these magnitudes.

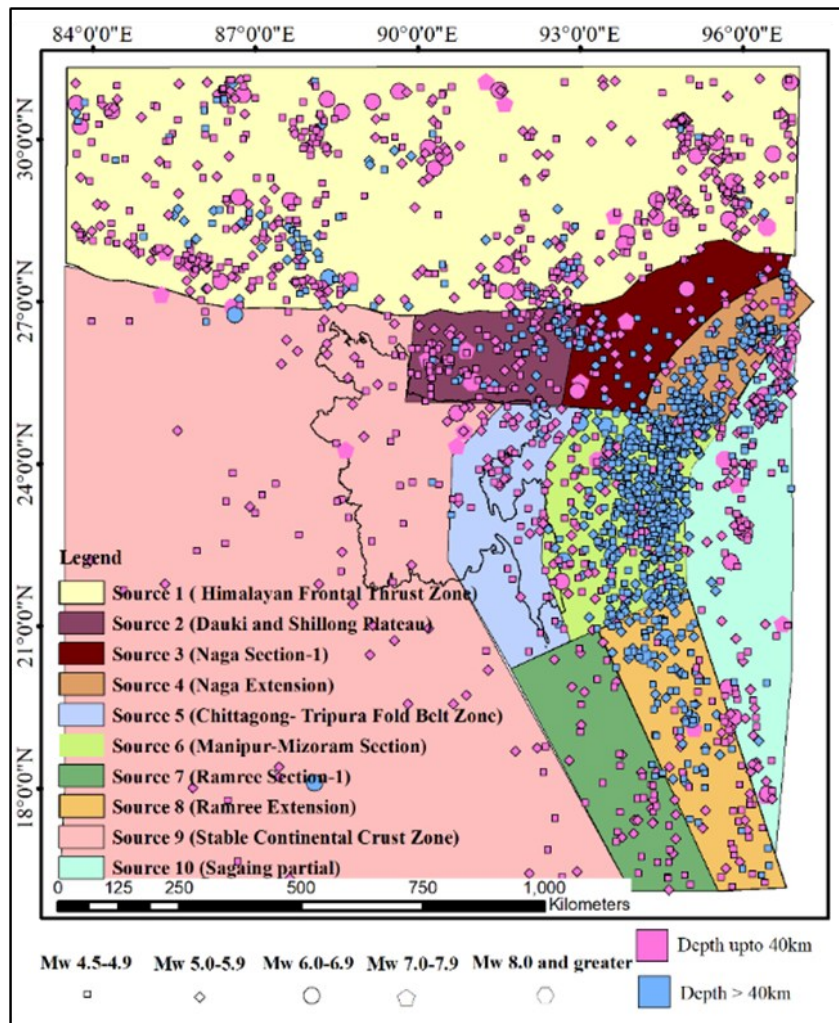


Figure 17 Seismotectonic Areal Sources for the Study Area.

*Table 5 Seismicity Parameters for the Areal Sources.*

Source Name	A-Value	B-Value	A	Mu	Uncertainty In Mu	Computed Slip Rate	Shallow EQ (%)	GMPE (Shallow Crustal, Subduction)
Himalayan Frontal Thrust	4.21	0.76	14.13	9.00	0.5	10.7	85	(85,15)
Dauki	4.37	0.95	3.55	8.98	1.0	6.37	74	(74,26)
Naga Section	3.46	0.79	1.95	7.95	0.6	1.85	58	(58,42)
Naga Extension	3.96	0.82	4.50	7.21	0.3	1.71	20	(20,80)
Chittagong-Tripura Section	3.71	0.86	1.94	7.08	0.3	0.28	90	(90,10)
Mizoram-Manipur Section	4.55	0.87	11.82	8.85	0.2	17.2	17	(17,83)
Ramree Section 1	4.30	1.02	1.55	9.30*	0.7	1.57	93	(93,07)
Ramree-Extension	4.37	0.92	4.72	8.18	0.6	2.14	33	(33,67)
Sagaing	3.49	0.72	4.00	8.45	0.5	6.85	78	(78,22)
Stable Continental Crust	3.05	0.65	2.75	8.49	0.5	1.14	95	(95,05)

### Ground Motion Prediction Equation (GMPE)

2 sets of Ground Motion Prediction Equations (GMPEs) are applied for this study. The first set contains a combination of 5 established GMPEs for shallow crustal earthquakes formulated in 2008 utilizing five global data sets of ground motions under the NGA-west program of PEER. PEER (Pacific Earthquake Engineering Research Center) serves as a web-based repository for collection and dissemination of ground motion data. These equations belong to 5 different teams of researchers who later updated the equations using more extensive and newest strong motion data in 2014. The first set has been assigned for shallow crustal earthquake sources (Linear sources). Logic tree weights for this set are assigned, conserving the similarity of weight assignment to this first set with Petersen et al. (2014) and Rahman et al. (2020). These groups of GMPE constructors for the first set of GMPEs are:

1. Abrahamson, Silva and Kamai (2014) [ASK 14]
2. Idriss (2014) [I 14]
3. Campbell and Bozorgnia (2014) [CB 14]
4. Boore, Stewart, Seyhan and Atkinson (2014) [BSSA 14]
5. Chiou and Youngs (2014) [CY 14]

The second set of GMPEs is the combination equations formulated by Atkinson and Boore (2003) who used globally extensive ground motion information set of interfaces and intra-slab sections of subduction zone, Abrahamson et al. (2016) who employed similar dataset as Atkinson and Boore (2003) and the third equation is of Zhao et al. (2006). They also considered earthquakes with similar tectonic setting but for Japanese dataset instead of global data set.

Apart from the linear sources, the other two sources are assigned GMPEs using combination of these two sets. Background seismicity has been assigned with 50-50 weighting for each set to avoid bias. Areal sources (subduction and shallow crustal zone) are given combined weighting with these two sets based on the depth distribution of the catalog. Each source is given weight according to the statistical distribution of shallow and deep earthquake.



### Seismic Hazard Calculation

To estimate seismic hazard on basis of computed seismicity parameters, final computation procedure has been carried out in the seismic hazard module R-CRISIS version 18.4.2 (Ordaz et al., 2017) due to its lucrative features. The module at a time allows combination of different source models, seismicity models, and attenuation models through logic tree structure and computation at large number of sites according to user's demand. The study area has been divided into small grids with sizes  $0.025^\circ \times 0.025^\circ$ . Peak ground acceleration (PGA) and SA (spectral acceleration) values at each grid are calculated for a referenced bedrock condition ( $V_{s30} = 760$  m/s). The maximum integration distance was preserved at 300 km, maintaining balance with the attenuation intensity models. The hazard value had been assessed finally.

### 4.3. Results and Discussion

After computation in the R-CRISIS version 18.4.2 (Ordaz & Salgado-Gálvez, 2017), two different PGA (g) maps were developed for 2% and 10% probability of exceedance in 50 years. A uniform hazard spectrum has been developed utilizing the PGA and SA values at 0.2s, and 1.0s for one central point of study area at 2%, and 10% exceedance probability in 50 years timeframe at 0.05 critical damping factor. UHS of the sites shows the highest SA values in 0.2s spectral period and lowest value in longer spectral period (2s) which implies that structures with 0.2s natural frequency are at greater risk. The estimated PGA for different return periods is cross referenced with the PGA estimated in former investigation. PGA value of the current study has been compared with results of former studies in figure 4.7. For the Meherpur Zila area, the maximum PGA is up to 0.146174 g and 0.372132g for 10% and 2% probability of exceedance in 50 years. Current study results don't show too much deviation from a portion of the previous studies. The PGA of the study aligns with the seismic zonation map of BNBC (2020), in which the seismic zonation is carried out based on the PGA exceedance of Maximum Credible Earthquake (MCE). It is generally considered that an MCE has 2% probability of exceeding 50 years. The BNBC (2020) has 0.20g PGA exceedance for Meherpur Zila area exceedance whereas the current study shows around 0.372132g PGA exceedance for Meherpur Zila area. However, the BNBC zonation has been carried out based on the study of Islam et al. (2010), which dates back to 2010. Our current study has used a combination of updated GMPEs and modelled the sources with a more comprehensive earthquake catalog. Therefore, this study is believed to have more accurate results than the BNBC (2020) values. Moreover, the recent studies of Rahman (2020) and Haque (2019) show quite similar results compared to our study. The slightly different values of our current study may be attributed to the consideration of a comprehensive catalog up to 2023, characterization of the source model based on the extensive literature review of recent works and the combination of updated GMPEs. Thus, the results of this study claim to be more accurate than the previous ones.

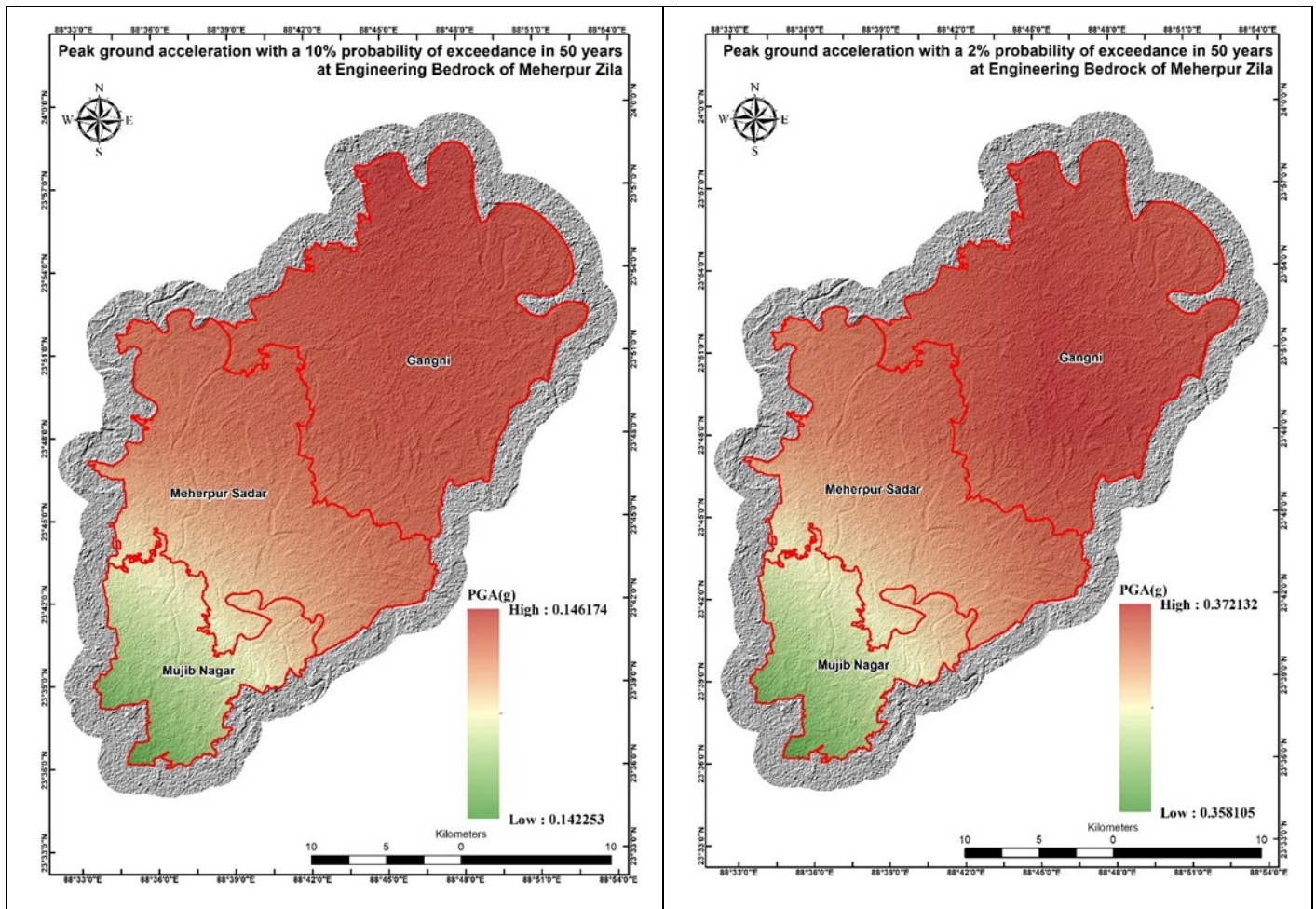


Figure 18 PGA Maps of Meherpur District at 10% Probability of Exceedance in 50 Years and at 2% Probability of Exceedance in 50 Years.

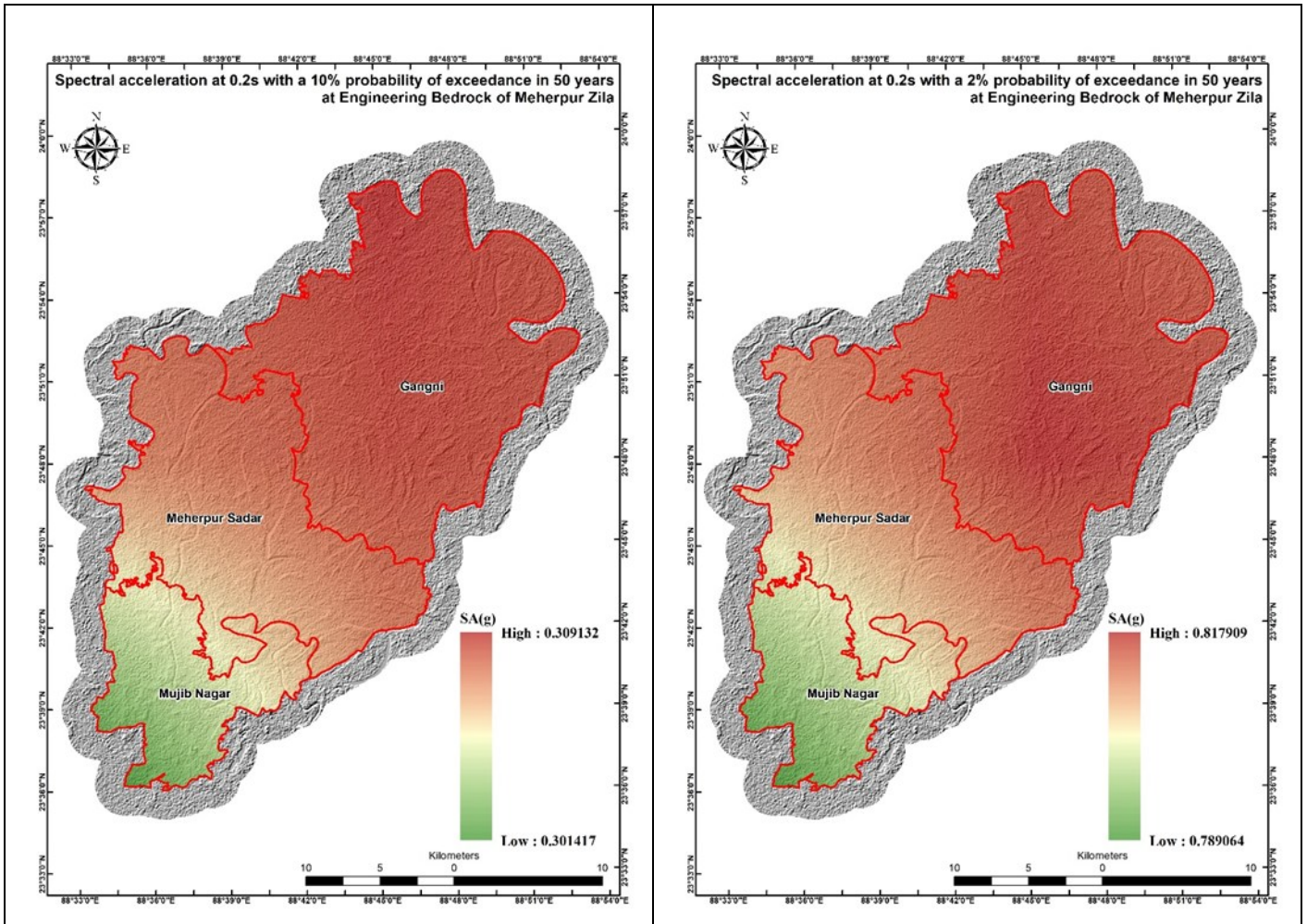


Figure 19 SA Maps of Short Period of Meherpur District at 10% Probability of Exceedance in 50 Years and at 2% Probability of Exceedance in 50 Years.



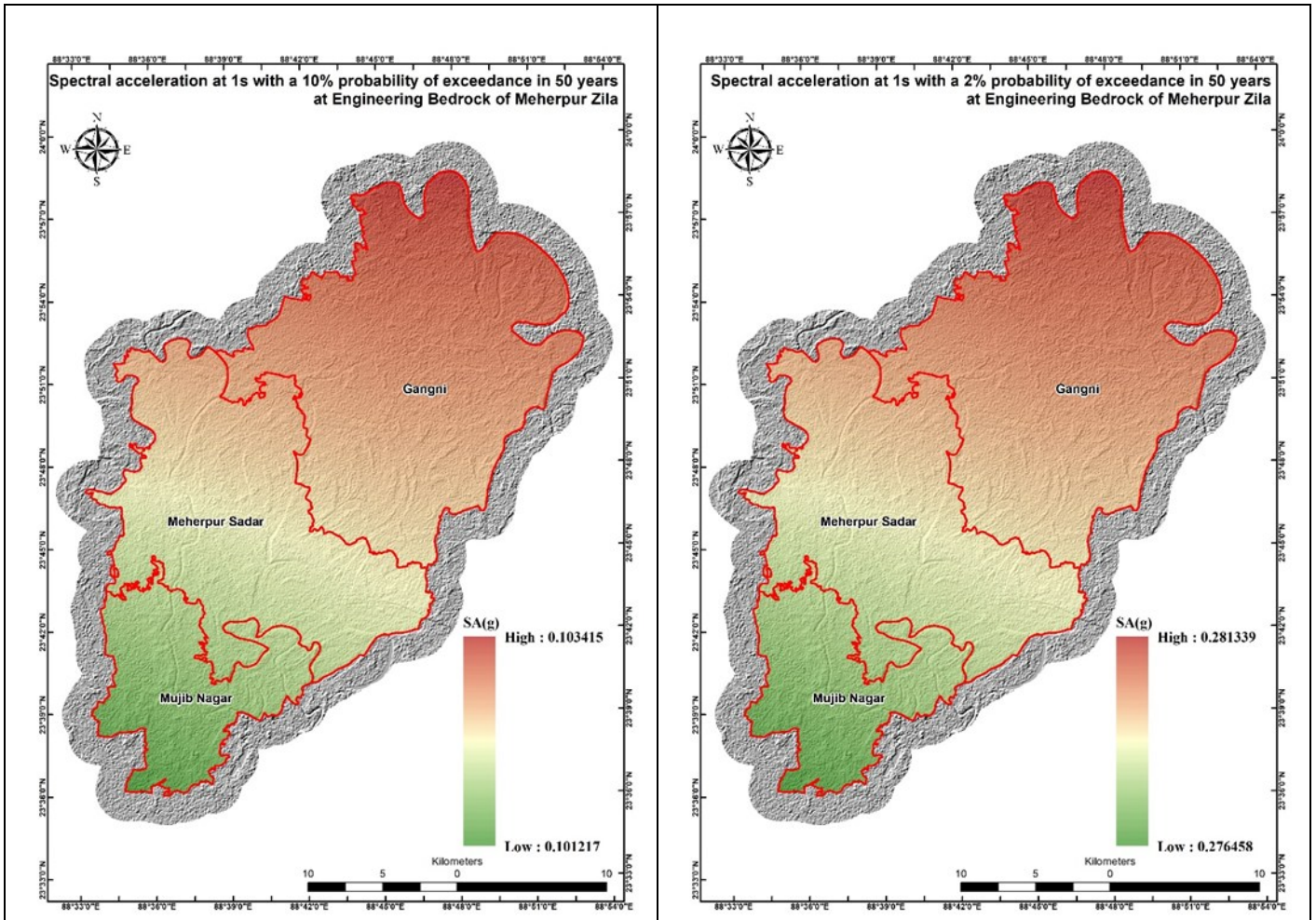


Figure 20 SA Maps of Long Period of Meherpur District at 10% Probability of Exceedance in 50 Years and at 2% Probability of Exceedance in 50 Years.

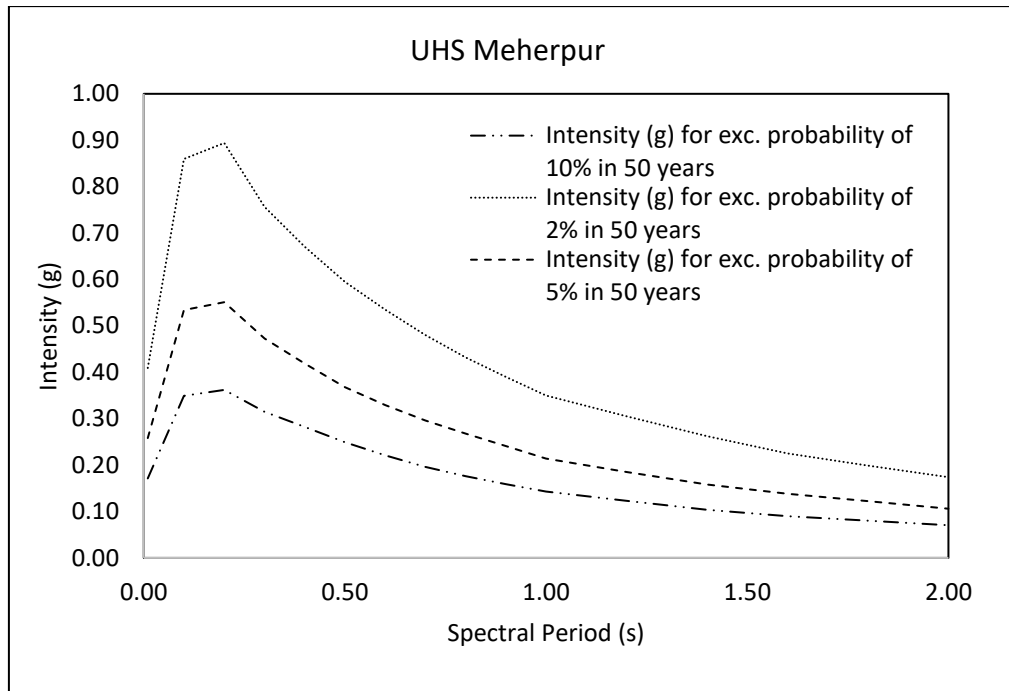


Figure 21 Uniform Hazard Spectra for the Study Area.

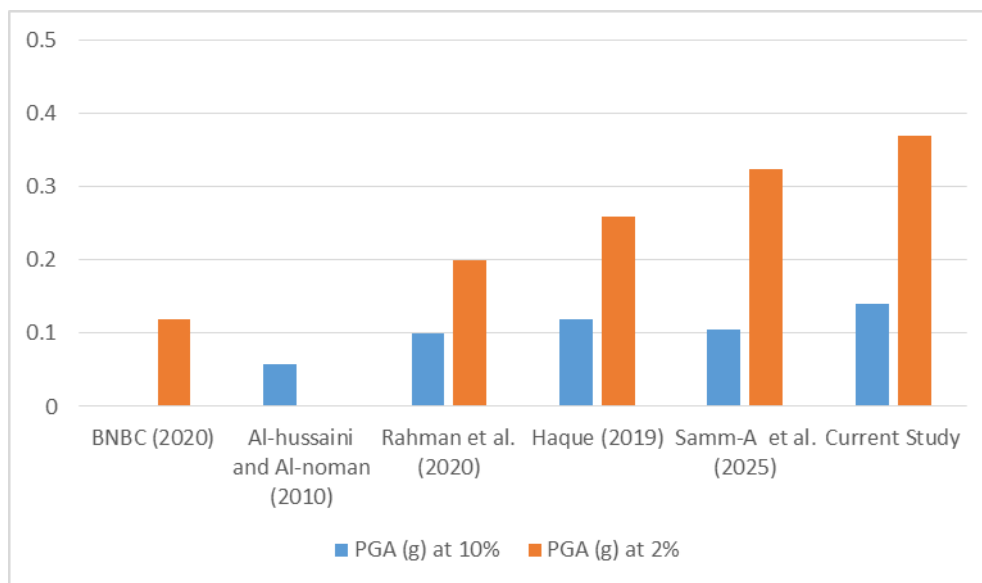


Figure 22 Comparison between PGA Values of Study Area at 10% and 2% Probability of Exceedance in 50 Years.

#### 4.4. Engineering Geological Mapping

There are various types of "Engineering Geological Maps", each designed for a specific purpose. For example, if the goal is to identify suitable foundation soil layers for a planned building, the engineering geology map should include properties related to geotechnical strength. Conversely, if the aim is to assess groundwater potential for water resource development, the map would be based on soil permeability.

In this study, the focus is on estimating and evaluating earthquake phenomena. Therefore, we require seismic and engineering characteristics of soil to create an engineering geology map

that can analyze seismic hazards. A key piece of information necessary for seismic hazard assessment is the ground motion at the surface, which is typically calculated using the S-wave velocity. As a result, our engineering geological map will be developed based on S-wave velocity data.

It is important to note that in the analysis of seismic ground motion, particularly in calculating soil amplification, an empirical method is used that employs the average S-wave velocity of the ground to a depth of 30 meters (referred to as  $V_s30$ ). This approach is necessary because point data from boreholes or P-S logging must be extrapolated to cover the entire study area for an accurate ground model.

Therefore, in this study, the "Soil Type Map based on  $AVS30$ " is defined as the "Engineering Geological Map".

#### 4.4.1 Shear Wave Velocity Estimation

Estimation of shear wave velocity ( $V_s$ ) and mapping is a way to characterize varying site conditions, and it can also be used to model earthquake-related ground shaking. Estimation of  $V_s$  aims to generate a map of estimated average shear wave velocities for the upper 30m of the subsurface,  $AVs30$ . Field measurement of  $V_s$  of near surface layers implying near surface seismic surveys alike Downhole seismic test (PS Logging) and multi-channel analysis of surface wave (MASW) can serve the purpose.  $V_s$  of subterranean layers can be obtained by another mean— determination of shear wave velocity from SPT N value from empirical relation between  $V_s$  and N value. Because of near surface seismic tests are expensive and so conducted in limited number while SPT tests could be done more extensively, a probabilistic correlation between  $V_s$  obtained from near surface seismic and SPT's are used for to depict extrapolated gestalt picture of  $AVs30$  distribution throughout the study area from point data ( $AVs30$  at each borehole). The resulting velocities can be more confidently used for  $AVs30$  mapping. Further this map can be used for seismic site response analysis i.e., to determine peak ground acceleration (PGA) and spectral acceleration (SA) values of both bedrock and ground surface.

As a part of engineering geological or  $AVs30$  mapping, as mentioned earlier, of the study area, shear wave velocity ( $V_s$ ) of the local near surface geological units were obtained by PS Logging, Multi-channel analysis of surface wave (MASW) and SPT test. The shear wave velocity is a fundamental parameter required to define the dynamic properties of soils. A viable formula for velocity determination at the project area was adopted by probabilistic correlation between  $V_s$  yielded from PS-logging and SPT. Then the  $AVs30$  categories assigned to the generalized geologic units were used to generate an  $AVs30$  map. Finally, the hybridized  $AVs30$  map has been used for seismic site response analysis — PGA and SA mapping, which is hopefully believed to pave the way to the structural engineers and planners to sustainable infrastructure development for Meherpur District (Gangni, Meherpur Sadar and Muzibnagar Upazila) Area.

#### N Value and $V_s$ Correlation

Correlations between SPT resistance and shear wave velocity have been proposed for a number of different soil types (Ohba and Toriumi, 1970; Imai and Yoshimura, 1970; Fujiwara, 1972; Ohsaki and Iwasaki, 1973; Imai, 1977; Ohta and Goto, 1978; Seed and Idriss, 1981; Imai and CGR and CSI (JV)

Tonouchi, 1982; Sykora and Stokoe, 1983; Jinan, 1987; Lee, 1990; Sisman, 1995; Iyisan, 1996; Kayabali, 1996; Jafari et al., 1997; Pitilakis et al., 1999; Kiku et al., 2001; Jafari et al., 2002; Andrus et al., 2006; Hasançebi and Ulusay, 2007; Hanumantharao and Ramana, 2008; Dikmen, 2009). A summary of empirical relationships between SPT resistance and Vs in the literature is presented in for different soil types. In these relationships, SPT-N60 blow count is mostly considered and use a power-law relationship between Vs and SPT N-value. In these relationships, the values of the exponent, which control the curvature of the relationship, are more consistent than the constant that controls the amplitude. This accounts for the generally similar shapes of the curves.

The shear wave velocity of the study area soil has been determined from downhole seismic (PS-logging) method at 13 (7 primary data and 6 secondary data) locations and MASW at 16 (11 primary data and 5 secondary data) locations. The shear wave velocity (Vs30) determines from SPT blow counts (N) and down-hole seismic tests have been considered during the development of empirical relationships. The following power-law expression based on regression has been obtained to derive Vs from N (red dashed line in Figure 23).

$$V_s = 82.155x^{0.3487} \dots\dots\dots (4.1)$$

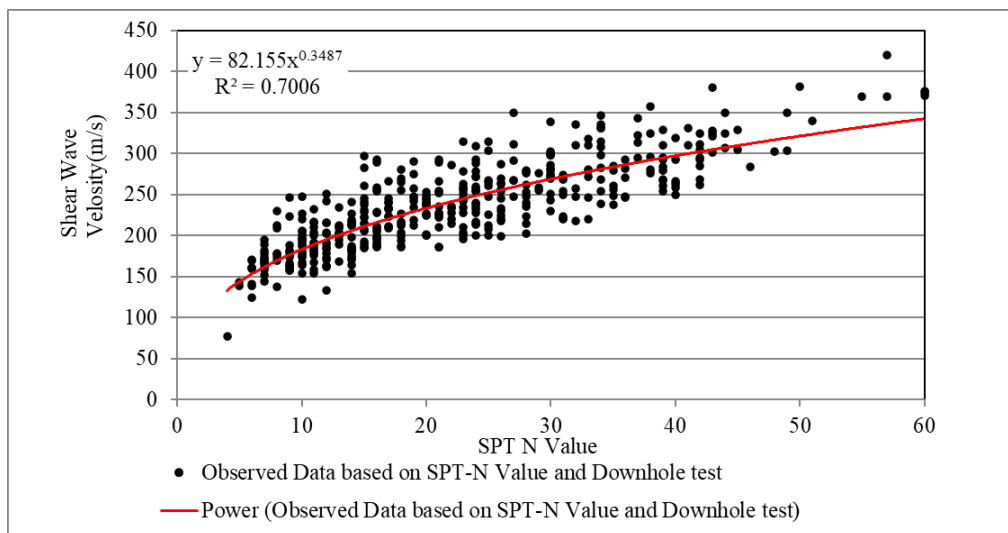


Figure 23 Regression Analysis Between Measured SPT-N Value and Shear Wave Velocity (Vs) Obtained from Down-Hole Seismic Test (PS-logging).

The shear wave velocity has been measured by down-hole tests compared with those estimated using empirical models for different soil types. The relationship proposed for project area soil in this study (red dash line in Figure 4.8) is quite compatible with the following equation (Equation – 4.2), which has similar trend, introduced by Ohta and Goto (1978) (Green dashed line in Figure 24).

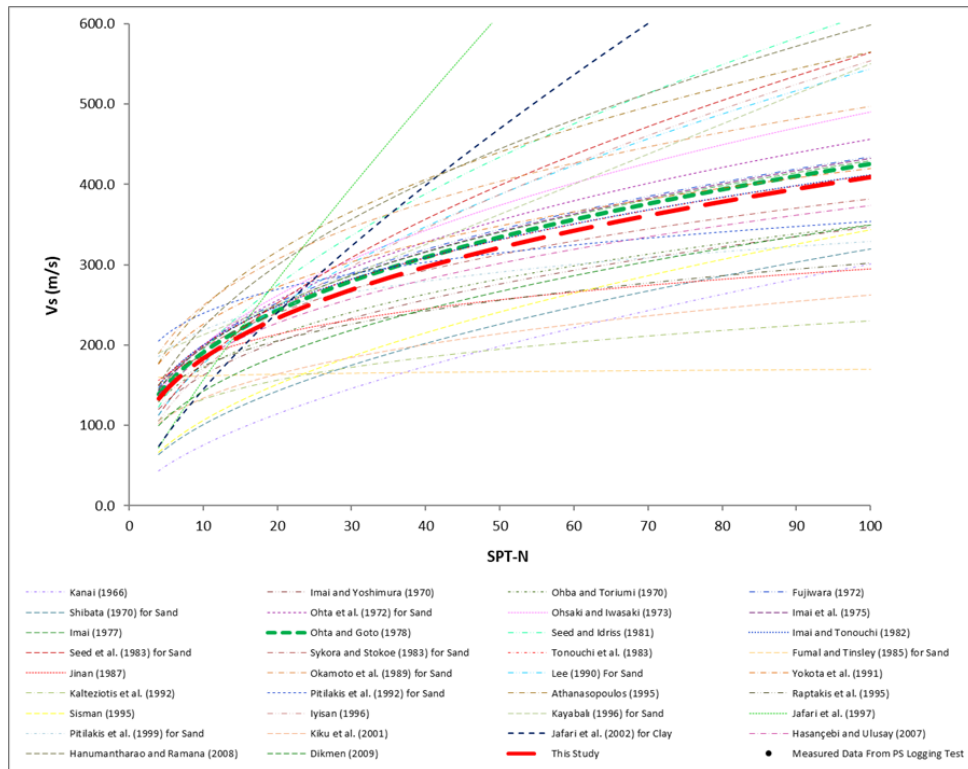


Figure 24 SPT-N Value and Vs Empirical Relations for All Soils in the Study Area.

The distribution of the shear wave velocity data with respect to SPT-N value at the same depth with SPT application and SPT-based geophysical test is considered in the interpretations.

$$V_s = 85.35N^{0.349} \dots\dots\dots (4.2)$$

Based on this equation 4.2, shear wave velocity (Vs) at every 1.5 m interval has been calculated at every borehole drilled in the project area.

### Vs 30 Calculation

Near surface shear wave velocity is crucial for earthquake-hazard assessment studies (Wald & Mori 2000; Kanli et al. 2006). The average shear wave velocity of the upper 30 m ( $AV_{s30}$ ) can be computed in accordance with the following expression:

$$V_s^{30} = \frac{30}{\sum_{i=1}^N (h_i / v_i)} \dots\dots\dots (4.3)$$

where  $h_i$  and  $v_i$  denote the thickness (in meters) and shear-wave velocity of the  $i^{th}$  formation or layer respectively in a total of  $N$  existing in the top 30 m.  $V_{s30}$  was accepted for site classification in the USA (NEHRP) by the UBC (Uniform Building Code) in 1997 (Dobry et al, 2000). Using the aforementioned equation 4.3,  $AV_{s30}$  at every borehole was calculated. Figure 254.10 represents the  $AV_{s30}$  map of the project area.



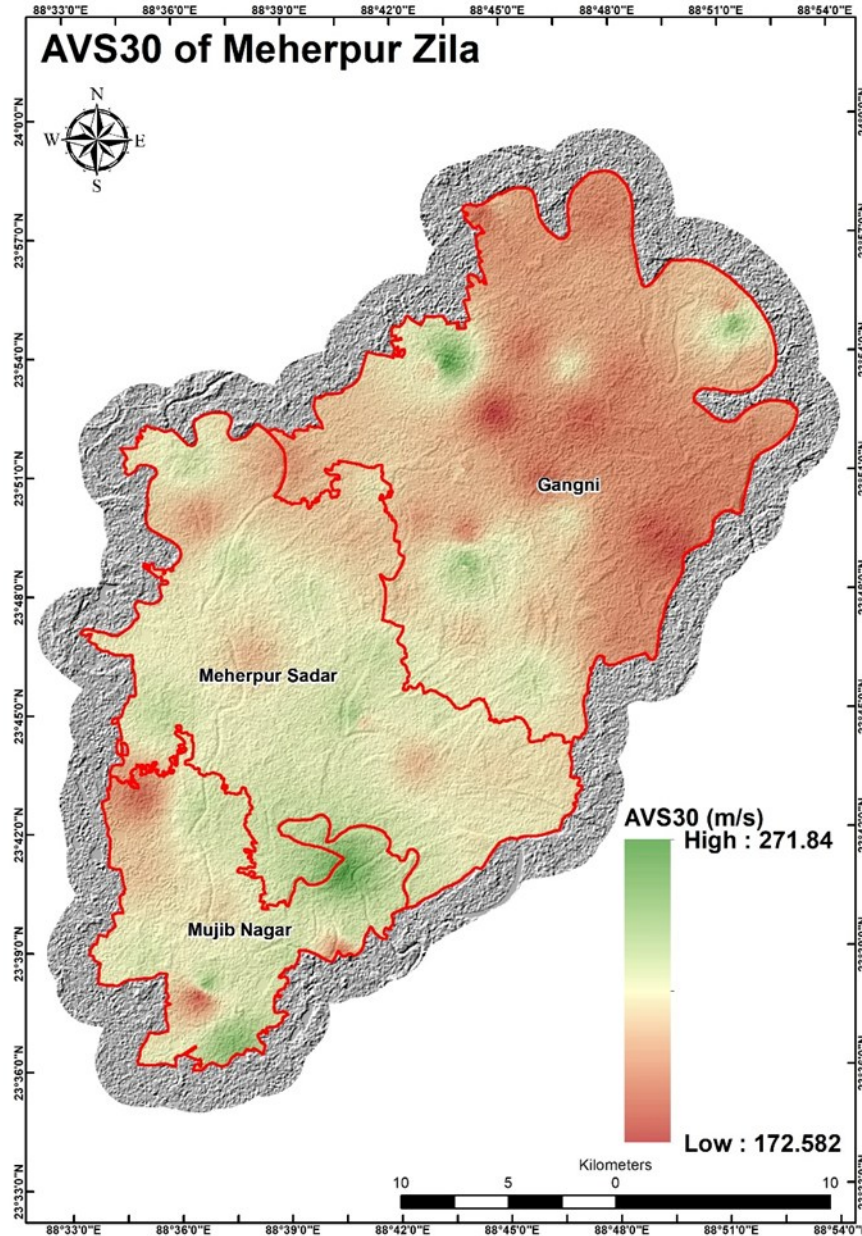


Figure 25 Engineering Geological Map of Meherpur District.

From the figure it can be clearly visualize that the red hue area of northern Meherpur zila Area represents the Very Low shear wave velocity zone ranging from 172.582 to 180.0 m/s; Most of the area is comprising with the white to Light Green color areas represents shear wave velocity ranging from 180 to 271.84 m/s. Vs30 of soil is a very use full tool for soil type classification.

#### 4.4.2. Soil Type Determination Based on AVS30

An important part of this study is the soil classification of the project area. The area has been investigated and classified according to a method provided by NEHRP (National Earthquake Hazard Reduction Program, USA) Provisions. NEHRP Provisions describe; first to define the site class based on  $AV_{S30}$  as shown in Table 6.

*Table 6 Definition of Site Class Based on AVS30 — According to NEHRP (National Earthquake Hazard Reduction Program, USA) Provisions*

Site Class	Site class description	Shear wave velocity (m/sec)	
		Minimum	Maximum
A	HARD ROCK Eastern United States only	1500	
B	ROCK	760	1500
C	VERY DENSE SOIL AND SOFT ROCK Unstrained shear strength $u_s > 2000\text{psf}$ ( $u_s \geq 100\text{kPa}$ ) or $N \geq 50$ blows/ft	360	760
D	STIFF SOILS Stiff soil with undrained shear strength $1000\text{psf} \leq u_s \leq 2000\text{psf}$ ( $50\text{KPa} < u_s < 100\text{KPa}$ ) or $15 \leq N \leq 50$ blows/ft	180	360
E	SOFT SOILS Profile with more than 10 ft (3m) of soft clay defined as soil with plasticity index $PI > 20$ , moisture content $w > 40\%$ and undrained shear strength $u_s < 1000\text{psf}$ (50kpa) ( $N \leq 15$ blows/ft)	100	180
F	SOILS REQUIRING SITE SPECIFIC EVALUATIONS 1. Soils vulnerable potential failures or collapse under seismic loading: e.g., liquefiable soils, quick and highly sensitive clays, collapse weakly connected soils. 2. Peats and/or highly organic clays: (10ft (3m) or thicker layer) 3. Very high plasticity clays: (25ft (8m) or thicker layer with plasticity index $> 75$ ) 4. Very thick soft/medium stiff clays: (120ft (36m) or thicker layer)	<100	

*Table 7 Site Classification Based on Soil Properties (BNBC, 2020)*

Site Class	Description of Soil Profile Up To 30 Meters Depth	Shear Wave Velocity (M/Sec)	
		Minimum	Maximum
SA	Rock or other rock-like geological formation, including at most 5 m of weaker material at the surface.	> 800	
SB	Deposits of very dense sand, gravel, or very stiff clay, at least several tens of meters in thickness, characterized by a gradual increase of mechanical properties with depth.	360	800
SC	Deep deposits of dense or medium dense sand, gravel or stiff clay with thickness from several tens to many hundreds of meters.	180	360
SD	Deposits of loose-to-medium cohesion less soil (with or without some soft cohesive layers), or of predominantly soft-to-firm cohesive soil.	<180	
SE	A soil profile consisting of a surface alluvium layer with Vs values of type SC or SD and thickness varying between about 5 m and 20 m, underlain by stiffer material with Vs > 800 m/s.	-	-
S <sub>1</sub>	Deposits consisting, or containing a layer at least 10 m thick, of soft clays/silts with a high plasticity index ( $PI > 40$ ) and high-water content	<100 (indicative)	
S <sub>2</sub>	Deposits of liquefiable soils, of sensitive clays, or any other soil profile not included in types SA to SE or S <sub>1</sub>	-	-

In this study, the ground of each grid was classified based on the NEHRP (National Earthquake Reduction Program) Provisions in USA. NEHRP Provisions classify the ground to five classes from A to E based on Vs30. According to NEHRP, our study area shows E and D type soil and according to Bangladesh National Building code, our study area shows SC and SD type soil. Both D type and SC type soil represent 180 to 360 m/sec Shear wave velocity. Velocity range

of the soils of the project area is 172.582 to 271.84 m/s i.e., they belong to the class D and E according to the provision.

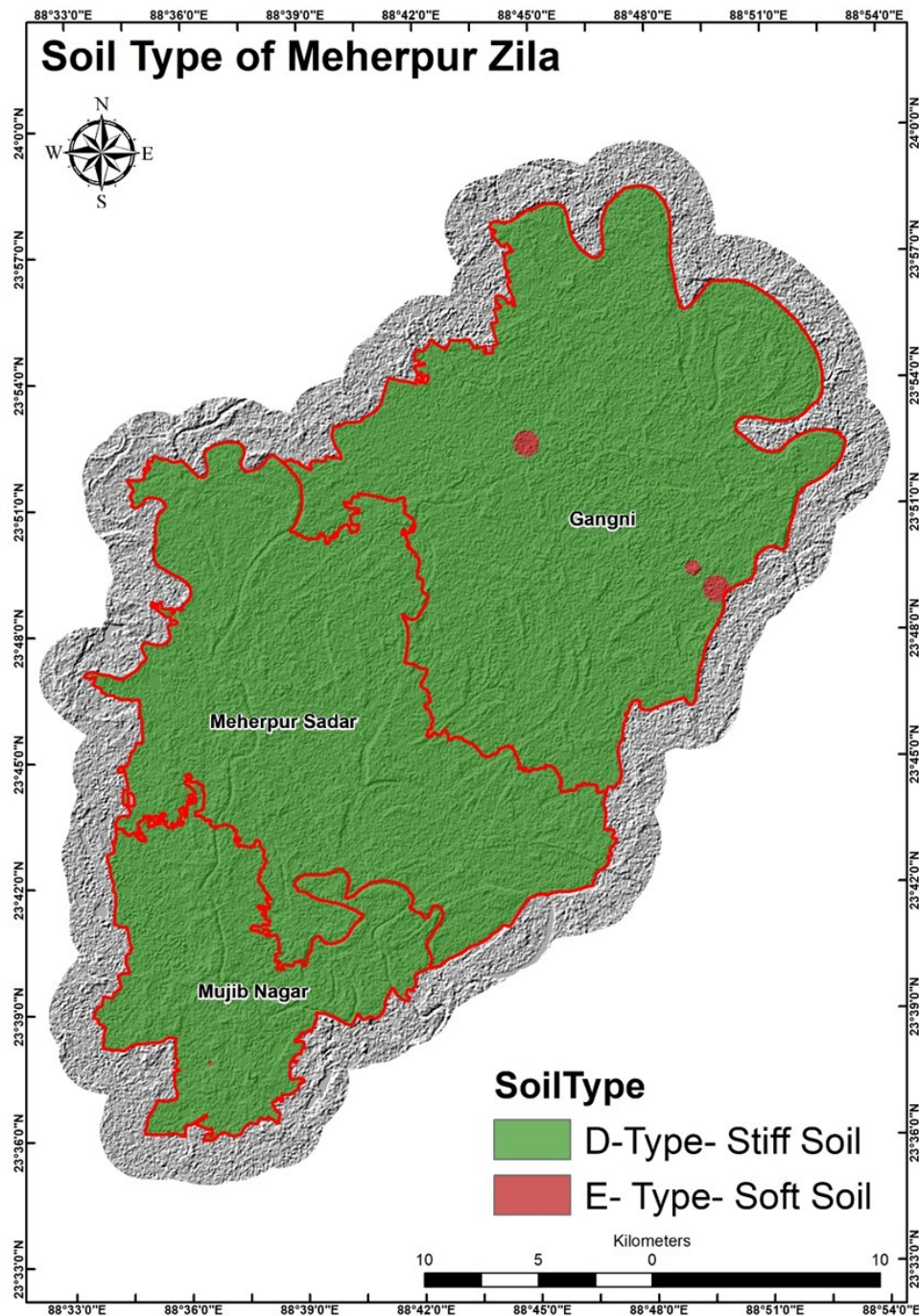


Figure 26 Soil Classification Map of Meherpur District- According to NEHRP Provisions Based on the Average Shear Wave Velocity Distribution Down to 30 m.

## 4.5. Site Response

### Amplification Analysis

The intensity of ground motion during an earthquake is significantly altered as seismic waves propagate from bedrock to near-surface soft sediments. Bedrock, where shear wave velocity ( $V_s$ ) exceeds 760 m/s, is often used as a reference. Over the past three decades, surface ground



motion at soil sites has been estimated by multiplying bedrock motion with an empirically derived site coefficient based on the time-averaged shear wave velocity in the top 30 m ( $V_{s30}$ ).

The BNBC 2020 (Bangladesh National Building Code 2020) includes essential seismic provisions for designing buildings and infrastructure to resist earthquake forces. It offers guidelines for estimating ground motion parameters, such as Peak Ground Acceleration (PGA) and spectral acceleration, which are critical for characterizing the intensity and nature of earthquake shaking at the ground surface. BNBC 2020 provides specific design spectra and recommendations for selecting ground motion parameters based on seismic hazard maps, regional geology, and site-specific conditions. These provisions are designed to reduce earthquake risks by accounting for anticipated seismic activity and its potential impact on structures.

Similarly, the National Earthquake Hazard Reduction Program (NEHRP) in the United States plays a significant role in advancing earthquake risk reduction strategies, particularly in defining ground motion parameters. NEHRP provisions, often referenced in ASCE 7 standards (Minimum Design Loads for Buildings and Other Structures), outline comprehensive methodologies for determining parameters such as PGA, spectral acceleration across various periods, and site class effects. NEHRP emphasizes the use of accurate, site-specific data to estimate ground motion, accounting for factors like soil amplification and the characteristics of seismic sources. These factors influence the intensity and duration of ground shaking. The program's guidelines aim to enhance earthquake resilience by ensuring that buildings are designed with a detailed understanding of the seismic hazards specific to their location.

In this study, ground classification was conducted following the NEHRP (National Earthquake Hazard Reduction Program) provisions. NEHRP divides the ground into five classes (A to E) based, in part, on the average shear wave velocity ( $V_{s30}$ ) values (Table 5.5). Class E corresponds to a  $V_{s30}$  of less than 180 m/sec, while Class D covers the range of 180 to 360 m/sec, which encompasses the entire study area. The short-period amplification factors for weak motion are 1.3, 1.6, and 2.4 for Classes C, D, and E, respectively (Table 5.7). The soil amplification factors for PGA, short-period (0.2 sec), and 1.0-second spectral acceleration (SA), as per BSSC 2015 provisions, are detailed in Tables 8 to 11 for Classes A to E.

*Table 8 Site Soil Classification According to NEHRP (BSSC, 2015) and BNBC, 2020*

Site Class NHREP (Shear wave velocity (m/s))	Site Class BNBC 2020 (Shear wave velocity (m/s))	Description of soil profile up to 30m depth	SPT Value (blows/30cm)
A (>1500)		Hard Rock	-
B (750-1500)	SA (>800)	Rock	-
C (360-800)	SB (360-800)	Very dense soil/soft rock	>50
D (180-360)	SC (180-360)	Stiff soil	15-50
E (<180)	SD (<180)	Soft soil	<15
F	SE	Special soils requiring site-specific evaluation	-

Table 9 Peak Ground Acceleration Site Coefficients ( $F_{PGA}$ ) (BSSC, 2015)

Site Class	PGA≤0.1	PGA=0.2	PGA=0.3	PGA=0.4	PGA=0.5	PGA≥0.6
A	0.8	0.8	0.8	0.8	0.8	0.8
B	0.9	0.9	0.9	0.9	0.9	0.9
C	1.3	1.2	1.2	1.2	1.2	1.2
D	1.6	1.4	1.3	1.2	1.1	1.1
E	2.4	1.9	1.6	1.4	1.2	1.1
F	section 11.4.8					

Note: Use straight-line interpolation for intermediate values of PGA

Table 10 Short-Period Site Coefficients  $F_a$  (BSSC, 2015)

Site Class	Ss≤0.25	Ss=0.5	Ss=0.75	Ss=1.0	Ss=1.25	Ss≥1.5
A	0.8	0.8	0.8	0.8	0.8	0.8
B	0.9	0.9	0.9	0.9	0.9	0.9
C	1.3	1.3	1.2	1.2	1.2	1.2
D	1.6	1.4	1.2	1.1	1.0	1.0
E	2.4	1.7	1.3	1*	1*	1*
F	*	*	*	*	*	*

Note: Use straight-line interpolation for intermediate values of  $S_1$ .

Note: \* See BSSC (2015); section 11.4.7

Table 11 Long-Period Site Coefficients  $F_v$  (BSSC, 2015)

Site Class	$S_1$ ≤0.1	$S_1$ =0.2	$S_1$ =0.3	$S_1$ =0.4	$S_1$ =0.5	$S_1$ ≥0.6
A	0.8	0.8	0.8	0.8	0.8	0.8
B	0.8	0.8	0.8	0.8	0.8	0.8
C	1.5	1.5	1.5	1.5	1.5	1.4
D	2.4	2.2 <sup>1</sup>	2.0 <sup>1</sup>	1.9 <sup>1</sup>	1.8 <sup>1</sup>	1.7 <sup>1</sup>
E	4.2	3.3 <sup>1</sup>	2.8 <sup>1</sup>	2.4 <sup>1</sup>	2.2 <sup>1</sup>	2.0 <sup>1</sup>
F	*	*	*	*	*	*

Note: <sup>1</sup>Also, see requirements for site-specific ground motions in section 11.4.7

Note: Use straight-line interpolation for intermediate values of  $S_1$ .

Note: \* See BSSC (2015); section 11.4.7

#### 4.5.1 Site Response of Meherpur District

##### Ground Motion Parameters at Ground Surface

From the above amplification analysis, PGA, SA 0.2s and SA 1.0s at ground surface have been calculated and prepared maps of the study area (Figure 27 to Figure 29).

## PGA at Ground Surface

The project area comprises soil layers of PGA value ranging from 0.195318 to 0.21265g for 10% probability of exceedance and from 0.494938 to 0.541582g for 2% probability of exceedance.

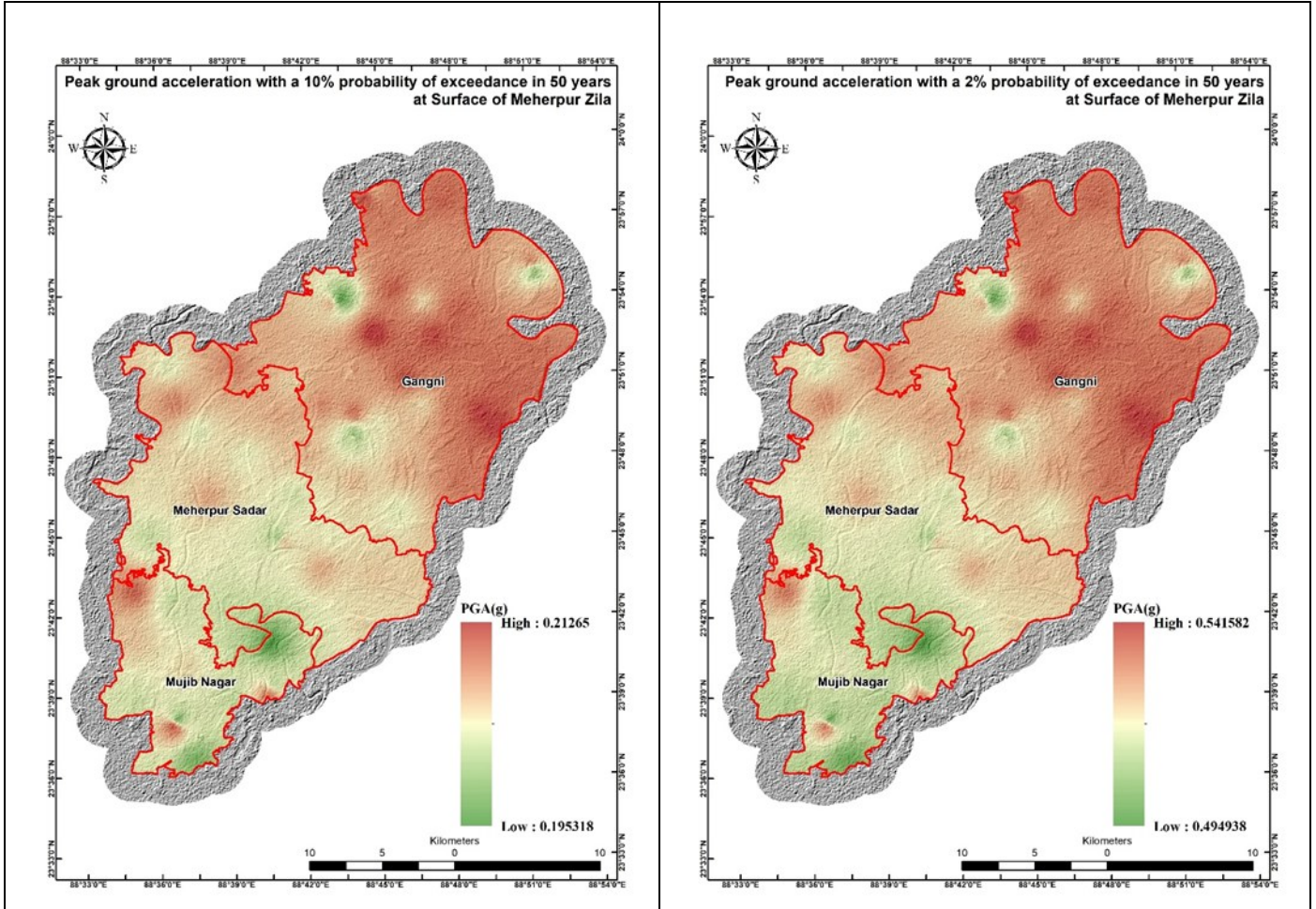


Figure 27 PGA Maps at Ground Surface of Meherpur District at 10% Probability of Exceedance in 50 Years and at 2% Probability of Exceedance in 50 Years.

## SA of Short Period at Ground Surface

The project area comprises soil layers of SA of Short Period values ranging from 0.581549 to 0.690433g for 10% probability of exceedance and from 0.969643 to 0.996486g for 2% probability of exceedance.

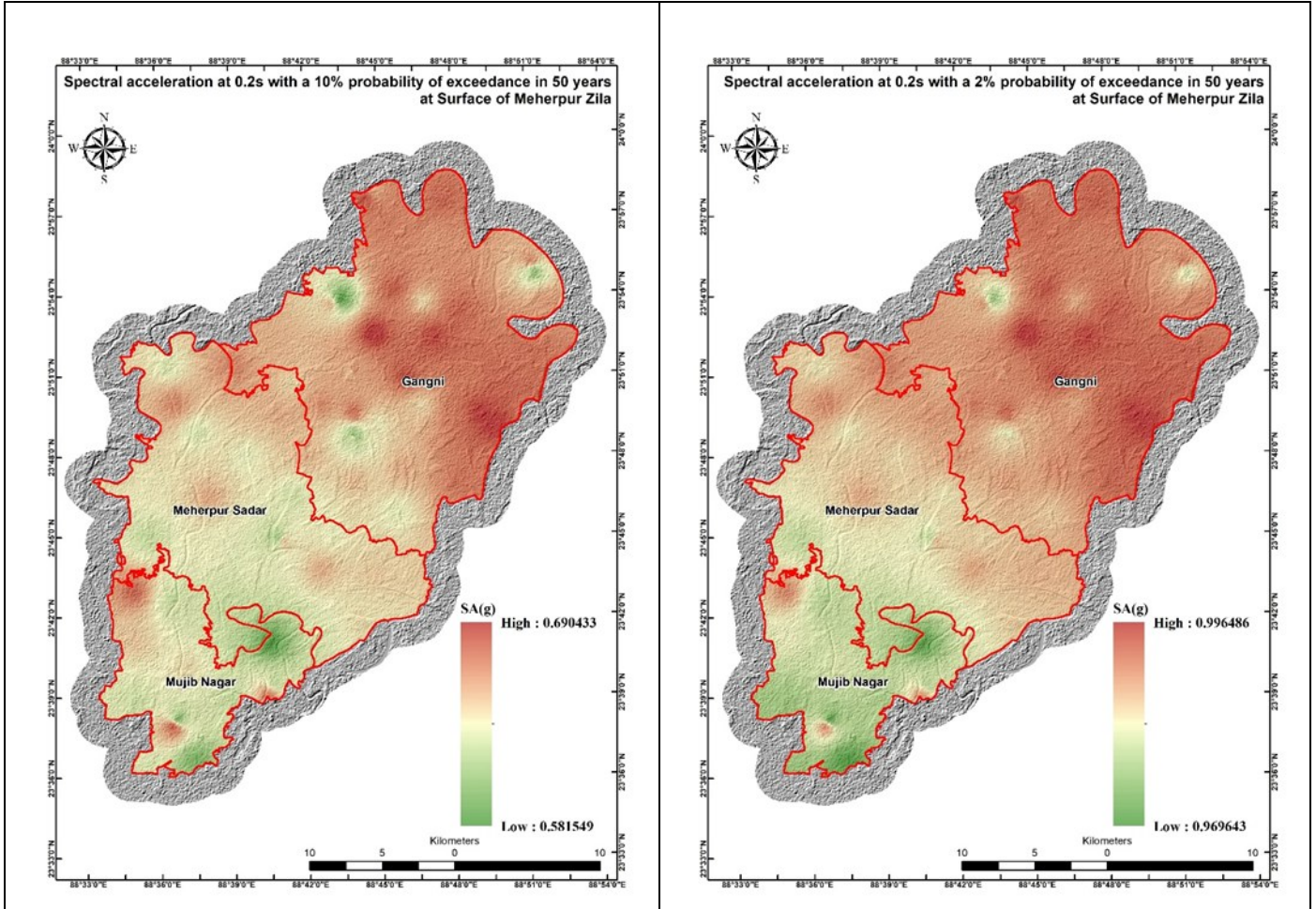


Figure 28 SA Maps of Short Period at Ground Surface of Meherpur District at 10% Probability of Exceedance in 50 Years and at 2% Probability of Exceedance in 50 Years.



## SA of Long Period at Ground Surface

The project area comprises soil layers of SA of Long Period value ranging from 0.335315 to 0.429694g for 10% probability of exceedance and from 0.688524 to 0.812497g for 2% probability of exceedance.

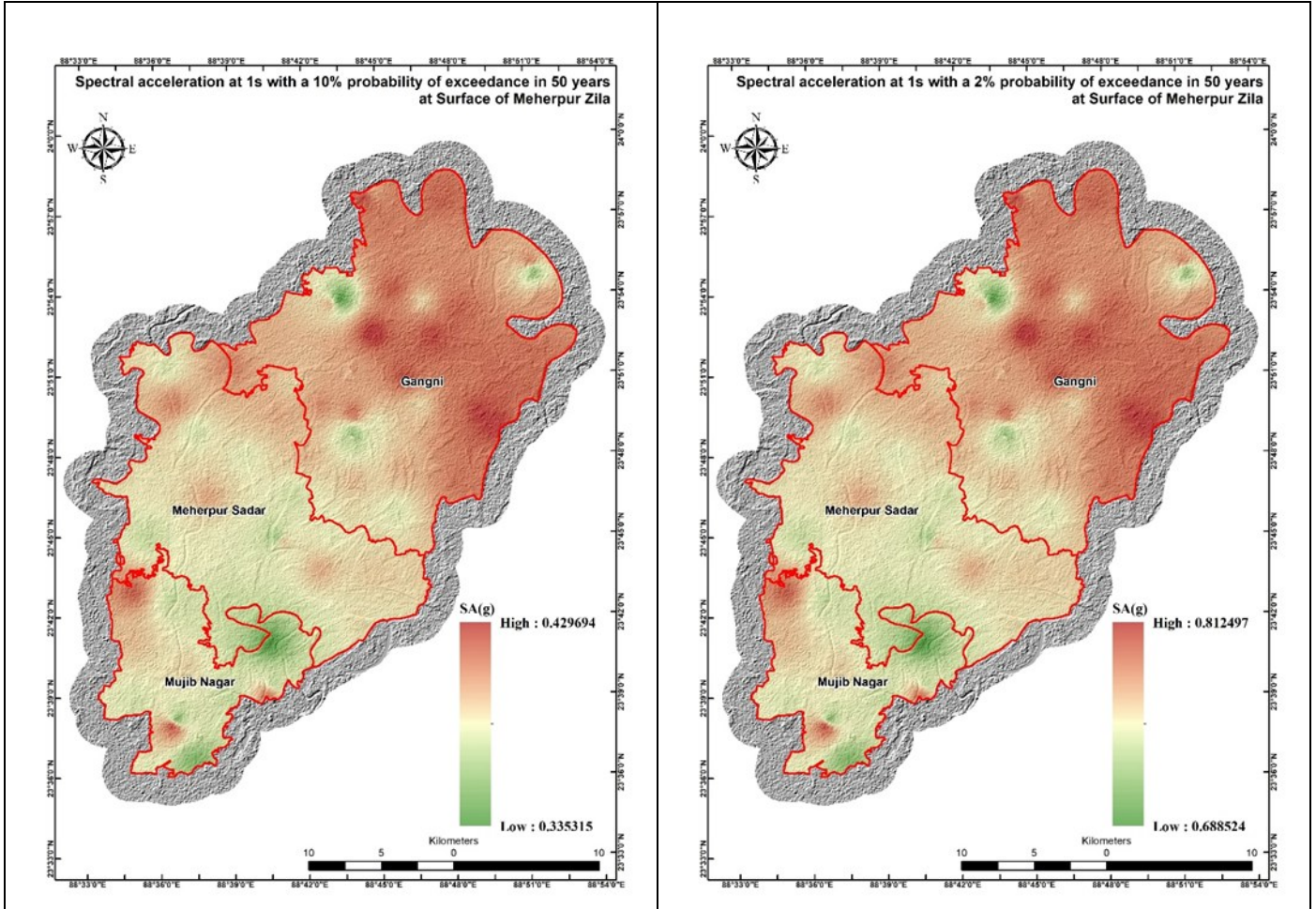


Figure 29 SA Maps of Long Period at Ground Surface of Meherpur District at 10% Probability of Exceedance in 50 Years and at 2% Probability of Exceedance in 50 Years.



## 5. LIQUEFACTION POTENTIAL INDEX (LPI) ASSESSMENT

Liquefaction is a secondary seismic hazard that provides an unsupportive environment for the built structures by altering previously solid ground into a liquefied softened condition (Palacios et al., 2012). It can cause extensive damages to the buildings and infrastructures due to sand boils and lateral spreading (Shafi & Tabassum, 2017) and has become a major concern for civil engineers for over forty years (Sadek et al., 2014). Notably, these damages increase during earthquakes (Zillur Rahman et al., 2015).

Rather than occurring randomly, the liquefaction phenomenon abides by some geological and hydrological conditions of subterranean soil deposits (Youd. et al. 2001). Generally, potentially liquefiable areas are within 20 m of the ground surface, where soils there are dominantly cohesionless and granular, and simultaneously saturated by water. Another factor instrumental for this phenomenon to take place is the intensity of ground shaking, which needs to be substantially strong for liquefying susceptible soils. Preferably, moderate to great earthquakes effectively trigger liquefaction, which commonly induces ground failure and deformation (Palacios et al. 2014).

Water-saturated loose gravelly, sandy, and silty soils of the Holocene age are susceptible to liquefaction during an earthquake (M.Z. Rahman & Siddiqua, 2017; YoudI. et al., 2001). Holzer et al., (2006), Lee et al., (2004)). Rahman et al., (2015) has predicted that earthquake of moment magnitude,  $M_w \geq 7$  and having a peak horizontal ground acceleration (PGA) of  $\geq 0.15g$  can cause severe liquefaction in the Quaternary (Pleistocene and Holocene) sandy and silty sediments. Most of Bangladesh consists of the fluvial-deltaic alluvial sediments that have been deposited in the floodplains of the major rivers: the Padma (in the upstream called the Ganges), Jamuna (in the upstream called the Brahmaputra), Meghna, and their numerous tributaries (Alam et al., 1990; Morgan & McIntire, 1959). Therefore, the water-saturated loose sandy and silty sediments of the floodplains have the high potentiality to liquefy during an earthquake. Historical earthquakes, such as the 1885 Bengal Earthquake, the 1897 Great Assam Earthquake, and the 1918 Srimangal Earthquake, witnessed that severe liquefaction occurred in the alluvial sediments of Bangladesh and surroundings (Middlemiss, 1885; Oldham, 1899; Stuart, 1920).

The present study attempts to estimate the factor of safety of liquefaction from the in-situ test data, i.e., the SPT using the simplified procedure (H. B. Seed & Idriss, 1971) and to calculate the liquefaction potential index (LPI) for assessing the severity of liquefaction using the procedure proposed by Iwasaki et al. (1978, 1982). The SPT-N data up to a depth of 20 m at each location of the study area were used to evaluate the liquefaction potential of the project area. These findings are crucial for master planning and designing earthquake-resilient infrastructure to mitigate earthquake and liquefaction-induced damage.

### 5.1. Methodology

In this study, we used the most widely accepted and simplified procedure proposed by Iwasaki et al., (1978, 1982) to evaluate the study area liquefaction potential index (LPI) using SPT data. Further details of each component are explained in the subsequent sub-sections.

### Simplified Procedure for Estimating Factor of Safety of Liquefaction ( $F_s$ )

The simplified procedure is originally developed by Seed and Idriss (1971), later updated and validated to evaluate liquefaction potential (Seed et al., 1985, 1983; Youd et al., 2001). In this method, the factor of safety of liquefaction ( $F_s$ ) was calculated by comparing the cyclic stress ratio (CSR) with the liquefaction resistance of the soils, represented by the cyclic resistance ratio (CRR) (Seed and Idriss, 1971):

$$F_s = (CRR_{7.5}/CSR) * MSF \quad (1)$$

where,  $F_s$ : factor of safety of liquefaction,  $CRR_{7.5}$ : cyclic resistance ratio for earthquake magnitude,  $M_w = 7.5$ , CSR: cyclic stress ratio, and MSF: magnitude scaling factor to adjust the  $CRR_{7.5}$  for other earthquake magnitudes.

### Calculation of Cyclic Stress Ratio (CSR)

The cyclic stress ratio (CSR) measures the seismic loading on a soil layer of level ground. Seed and Idriss (1971) formulated the following equation to calculate the CSR:

$$CSR = \frac{\tau_{av}}{\sigma'_v} = 0.65 \left( \frac{a_{max}}{g} \right) \left( \frac{\sigma'_v}{\sigma'_v} \right) r_d \quad (2)$$

where,  $\tau_{av}$  = average equivalent uniform cyclic stress by an earthquake.  $\sigma'_v$  = total vertical overburden stress. To represent the most significant cycles over the full duration of loading, a factor of 0.65 is used for converting the peak cyclic shear stress ratio to a cyclic stress ratio (CSR) (Idriss and Boulanger, 2004);  $a_{max}$  = peak horizontal ground acceleration and  $g$  = gravitational acceleration;  $r_d$  = stress reduction co-efficient that works for the elasticity of the soil column. The value of  $r_d$  depends on the depth ( $z$ ) of soil. Seed and Idriss (1971) produced a chart for the values of  $r_d$  analyzing various earthquake motion and soil condition. The average values given in that chart can be estimated using the following equation (Liao et al., 1988; Robertson & Wride, 2000; Juang et al., 2017):

$$r_d = \begin{cases} 1.000 - 0.00765z, & z \leq 9.15 \text{ m} \\ 1.174 - 0.00267z, & 9.15 < z \leq 23 \text{ m} \\ 0.744 - 0.008z, & 23 < z \leq 30 \text{ m} \\ \text{and } 0.5, & z \geq 30 \text{ m} \end{cases} \quad (2a)$$

For ease of computation, Youd *et al.* (2001) used the following equation for the calculation of  $r_d$ :

$$r_d = \frac{1.000 - 0.4113z^{0.5} + 0.04052z + 0.0017532z^{1.5}}{1.000 - 0.4177z^{0.5} + 0.05729z - 0.006205z^{1.5} + 0.001210z^2} \quad (2b)$$

### Calculation of Cyclic Resistance Ratio (CRR)

The cyclic resistance ratio (CRR) is the resistance of the soil against cyclic loading or stress that is applied by seismic shaking to change the state of the soil. The CSR can be measured from data of several in-situ tests, such as standard penetration test (SPT), cone penetration test (CPT), shear wave velocity ( $V_s$ ), Becker penetration test (BPT) data (Youd et al., 2001).

The following equation has been used to calculate the CRR from the standard penetration test blow count (SPT-N):

$$CRR = \frac{1}{34 - N_{1,60CS}} + \frac{N_{1,60CS}}{135} + \frac{50}{(N_{1,60CS} + 45)^2} - \frac{1}{200} \quad (3)$$

$$\text{where, } N_{1,60CS} = a + bN_{1,60} \quad (4)$$

a and b are the line fitting parameters that depend on the fine content (FC) of soils can be calculated by the following functions:

$$a = \begin{cases} 0, & FC \leq 5\% \\ e^{[1.76 - (190/FC^2)]}, & 5\% < FC < 35\% \\ \text{and } 5, & FC \geq 35\% \end{cases} \quad (4a)$$

$$b = \begin{cases} 1, & FC \leq 5\% \\ [0.99 + (FC^2/1000)], & 5\% < FC < 35\% \\ \text{and } 1.2, & FC \geq 35\% \end{cases} \quad (4b)$$

$N_{1,60}$  is the corrected SPT-N that is normalized to the effective overburden stress of 100kPa. It is calculated from the following equation:

$$N_{1,60} = N_m C_N C_B C_R C_E C_S \quad (4c)$$

where,  $N_m$  denotes SPT-N for each depth,  $C_N$  is effective overburden pressure,  $(100/\sigma'_v)^{0.5}$ ,  $C_B$  = correction factor for borehole diameter,  $C_R$  = correction factor for rod length,  $C_E$  = correction of hammer energy ratio (ER),  $C_S$  = sampler correction.

### Seismic Factors

The magnitude and peak horizontal ground acceleration of earthquakes are necessary parameters to evaluate the liquefaction potential of soils (Seed and Idriss, 1971). This study has taken a scenario of the magnitude of  $M_w$  7.5 and peak maximum horizontal ground acceleration (PGA) of 0.145g to evaluate the liquefaction potential of soils. Except for earthquake magnitude  $M_w$  7.5, the magnitude scaling factor (MSF) is required to calculate the factor of safety. Youd *et al.* (2001) proposed the following equation to calculate the MSF:

$$MSF = \frac{10^{2.24}}{M_w^{2.56}} \quad (5)$$

For moment magnitude,  $M_w$  7.5, the MSF is 1, and except  $M_w$  7.5, the MSF is derived using Equation (5). This gives reduced liquefaction potential for magnitudes  $< M_w$  7.5 and increased potential for magnitudes  $> M_w$  7.5 (Youd et al., 2001).

### Liquefaction Potential Index (LPI)

The severity of liquefaction hazard cannot be estimated by using only the factor of safety, as it indicates whether a layer of a soil column will liquefy or not. Therefore, Iwasaki et al. (1978, 1982) introduced the liquefaction potential index (LPI) in order to estimate the severity of liquefaction. The thickness and depth of liquefiable layers are the two parameters already included in the equation of the factor of safety, where LPI is calculated for each soil profile at each borehole location by following the equations below (Iwasaki et al., 1982):

$$LPI = \int_0^{20} F(z)W(z) dz \quad (6)$$

$$F(z) = \begin{cases} 1 - Fs, & Fs < 1.0 \\ 0, & Fs \geq 1.0 \end{cases} \quad (7a)$$

$$W(z) = \begin{cases} 10 - 0.5z, & z < 20m \\ 0 & , z > 20m \end{cases} \quad (7b)$$

where  $z$  is the depth (generally from 0 to 20 m) from the ground surface in meters,  $dz$  means the depth increment.  $F(z)$  is a function of the  $F_s$  which characterizes the severity of liquefaction, and  $W(z)$  is the weighting factor as defined in Equations 7(a) and 7(b) respectively.

*Table 12 Classification of Liquefaction Potential Index Used in Different Studies*

LPI	Iwasaki <i>et al.</i> (1982)	Luna and Frost (1998)	Chung and Rogers (2011)	Present Study
0	Not likely	Little to none	None	-
$0 < LPI \leq 5$	-	Minor	Little to none	Low
$5 < LPI \leq 15$	-	Moderate	Moderate	Moderate
$LPI > 15$	Severe	Major	Severe	High

## 5.2. Discussions of Liquefaction Hazard Map

This study adopts a quantitative approach to evaluate the seismic liquefaction potential index for Meherpur district. Liquefaction potential was assessed to a depth of 20 m using SPT blow count data as per Youd et al. (2001). The Standard Penetration Test (SPT) was conducted at 30 locations, with SPT-N values recorded at 1.5-m intervals. These are primary data, there are also 28 locations with some secondary data. Analysis was based on a maximum considered earthquake (MCE) of 7.5 magnitude and PGA 0.146g, as specified for the study. Results are presented in Figure 30.

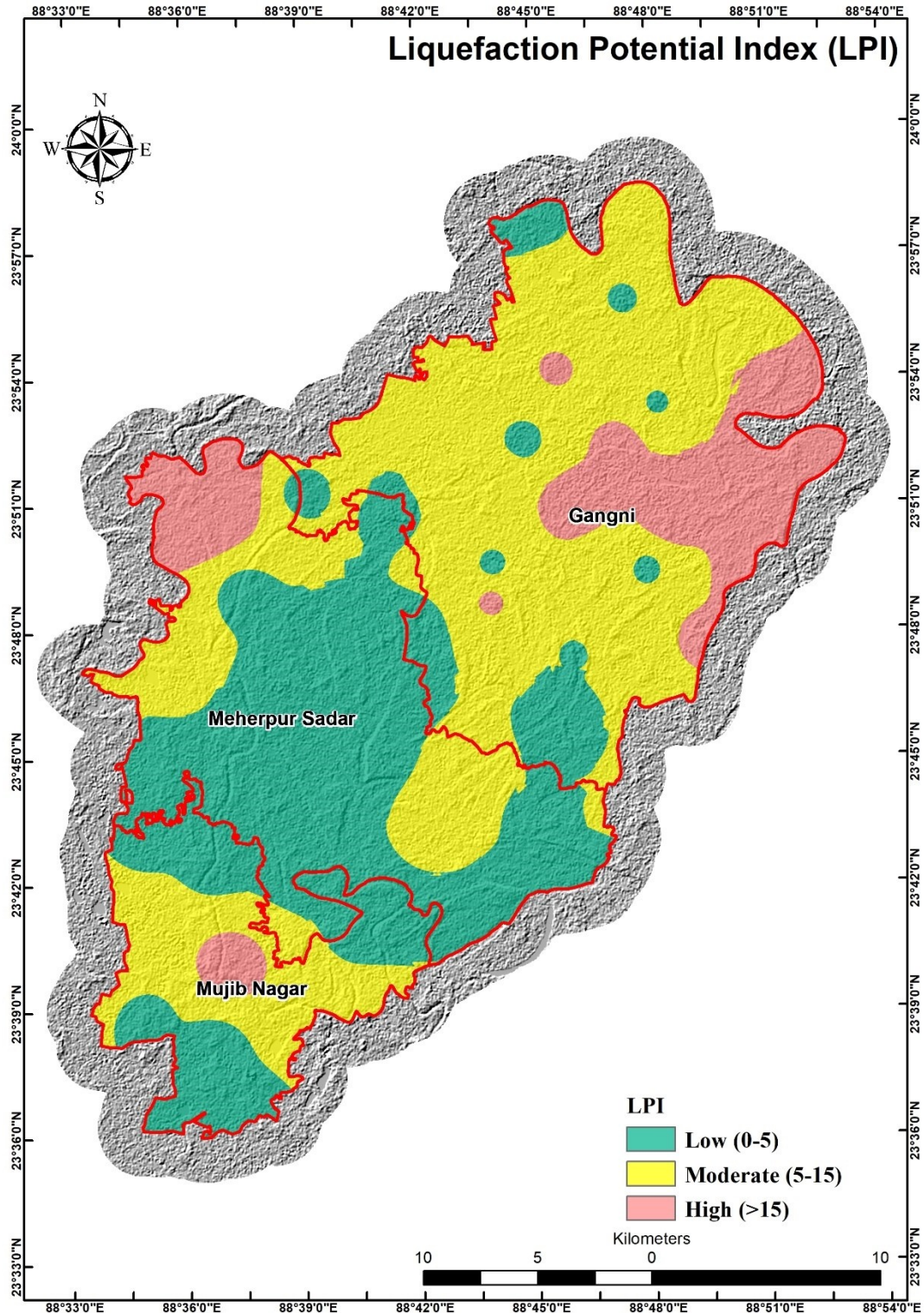


Figure 30 Showing the Liquefaction Hazard Scenario of Pirojpur Sadar Upazila Area Considering Magnitude =7.5 Mw and PGA 0.145g.

Key criteria for defining liquefiable layers included: clay content <10%, plasticity index <12%, SPT <30, and factor of safety <1. Groundwater levels, ranging from 0.3-9.8 m, were a critical factor, as shallow groundwater increases liquefaction susceptibility. The hazard map (Figure 3.1) indicates low to moderate liquefaction risk. From the table 3.1, it can be seen that of the 57 boreholes, 29 show low liquefaction potential, 17 show moderate potential and 11 show high liquefaction potential.



Low liquefaction potential areas are characterized by silt or clay layers with plasticity index  $>12$  and clay content  $>10\%$ , underlying thin sand layers, Moderate liquefaction potential areas feature soft clay or silt layers above sand layers with SPT  $>30$  and finer particles. High liquefaction potential areas are characterized by thick upper sand layers with SPT  $<30$ , and underlying silt or clay layers with plasticity index  $<12$  and clay content  $<10\%$ . Higher SPT values in sand layers result in increased cyclic resistance, increasing the factor of safety and decreasing the liquefaction potential index (LPI). Vice versa, Lower SPT values in sand layers result in reduced cyclic resistance, decreasing the factor of safety and increasing the liquefaction potential index (LPI).

*Table 13 Table Showing the Liquefaction scenario considering magnitude =7.5 Mw and PGA 0.146g for Meherpur District*

BH No.	Data	Upazila	Latitude	Longitude	GWT (m)	LPI
BH-01	Primary	Mujib Nagar	23.7097	88.6102	4.8	0.0
BH-02	Primary	Mujib Nagar	23.7158	88.5828	2.4	3.0
BH-03	Primary	Mujib Nagar	23.6850	88.5818	1.0	14.9
BH-04	Primary	Mujib Nagar	23.6682	88.6182	0.0	26.3
BH-05	Primary	Mujib Nagar	23.6485	88.5839	7.3	3.1
BH-06	Primary	Mujib Nagar	23.6362	88.6115	6.1	0.0
BH-07	Primary	Mujib Nagar	23.6111	88.6235	6.7	0.0
BH-08	Primary	Mujib Nagar	23.6485	88.6506	1.0	14.2
BH-09	Primary	Mujib Nagar	23.6580	88.6774	5.5	6.1
BH-10	Primary	Mujib Nagar	23.6831	88.6752	4.9	0.0
BH-11	Primary	Meherpur Sadar	23.7742	88.6340	5.8	0.0
BH-12	Primary	Meherpur Sadar	23.7496	88.5925	5.1	1.7
BH-13	Primary	Meherpur Sadar	23.7862	88.5969	5.2	12.4
BH-14	Primary	Meherpur Sadar	23.8153	88.6263	0.3	1.4
BH-15	Primary	Meherpur Sadar	23.8555	88.6078	4.6	58.5
BH-16	Primary	Meherpur Sadar	23.8441	88.6911	3.7	1.5
BH-17	Primary	Meherpur Sadar	23.7995	88.6603	7.9	2.7
BH-18	Primary	Meherpur Sadar	23.7375	88.6329	4.2	2.5
BH-19	Primary	Meherpur Sadar	23.7064	88.6463	6.7	0.0
BH-20	Primary	Meherpur Sadar	23.7284	88.6647	4.3	5.0
BH-21	Primary	Meherpur Sadar	23.7488	88.6800	9.8	0.0
BH-22	Primary	Meherpur Sadar	23.7748	88.6912	0.6	0.5
BH-23	Primary	Meherpur Sadar	23.7503	88.7173	4.9	7.9
BH-24	Primary	Meherpur Sadar	23.7285	88.7094	1.5	12.9
BH-25	Primary	Meherpur Sadar	23.6893	88.7098	6.7	4.2
BH-26	Primary	Meherpur Sadar	23.6970	88.7394	6.7	2.4
BH-27	Primary	Meherpur Sadar	23.7247	88.7457	4.0	4.3
BH-28	Primary	Gangni	23.8749	88.7470	0.5	2.1
BH-29	Primary	Gangni	23.8009	88.6998	6.7	0.0
BH-30	Primary	Gangni	23.7639	88.7607	4.9	1.7



GH-03	Secondary	Gangni	23.7837	88.7327	4.6	5.1
GH-04	Secondary	Gangni	23.7964	88.8225	4.0	17.1
GH-06	Secondary	Gangni	23.7905	88.7671	4.0	4.4
GH-07	Secondary	Gangni	23.8111	88.7319	0.6	18.0
GH-10	Secondary	Gangni	23.8261	88.7326	3.1	2.5
GH-11	Secondary	Gangni	23.8184	88.7486	4.3	8.4
GH-12	Secondary	Gangni	23.8285	88.8453	3.1	22.8
GH-13	Secondary	Gangni	23.8251	88.8180	2.7	14.1
GH-14	Secondary	Gangni	23.8236	88.7993	4.3	1.7
GH-15	Secondary	Gangni	23.8286	88.7780	3.4	6.7
GH-16	Secondary	Gangni	23.8314	88.7110	3.7	11.2
GH-17	Secondary	Gangni	23.8446	88.8104	2.4	24.3
GH-18	Secondary	Gangni	23.8471	88.7680	2.4	28.2
GH-19	Secondary	Gangni	23.8552	88.6512	4.6	2.4
GH-20	Secondary	Gangni	23.8665	88.8515	3.7	18.7
GH-21	Secondary	Gangni	23.8731	88.7876	3.1	18.4
GH-22	Secondary	Gangni	23.8521	88.7323	3.1	10.6
GH-23	Secondary	Gangni	23.8709	88.6737	2.1	5.6
GH-24	Secondary	Gangni	23.8935	88.8642	2.4	19.3
GH-25	Secondary	Gangni	23.8891	88.8039	4.3	3.8
GH-26	Secondary	Gangni	23.9030	88.7606	3.7	16.7
GH-27	Secondary	Gangni	23.8937	88.7170	2.1	6.8
GH-28	Secondary	Gangni	23.9193	88.8534	3.4	14.2
GH-29	Secondary	Gangni	23.9304	88.7895	5.8	4.3
GH-30	Secondary	Gangni	23.9416	88.7571	4.0	6.7
GH-31	Secondary	Gangni	23.9588	88.7939	4.3	8.0
GH-32	Secondary	Gangni	23.9628	88.7491	4.9	0.0

Both moderate and high-risk zone there is a potential for surface manifestation if LPI exceeds 5, and lateral spreading may occur where LPI exceeds 12 during liquefaction events.

Liquefaction poses a significant seismic hazard following earthquakes. This study evaluates the liquefaction potential of the target area for a scenario earthquake with a magnitude of 7.5 (Mw) and a peak horizontal ground acceleration (PGA) of 0.146g. The factor of safety for each soil layer in the SPT profiles was calculated using the Simplified Procedure, and LPI values were derived. Results indicate the area has low to moderate susceptible to liquefaction, with many zones exhibiting low to moderate LPI values. Surface manifestations and lateral spreading are likely during liquefaction events where LPI exceeds 5. This information is crucial for urban planners and policymakers to implement soil improvement measures and design appropriate foundations to mitigate potential hazards.

## 6. GEOENGINEERING SUITABILITY

We have used two steps Multi-Criteria Decision Making (MCDM) technique to develop **Geoengineering Suitability Map**. In the first step we have selected major criteria, and to find out the relative weight of these criteria **Analytic Hierarchy Process (AHP)** pairwise comparison have been applied in decision making. The Analytic Hierarchy Process (AHP) (Saaty, 1980 and 1994) decomposes a complex MCDM problem into a system of hierarchies (more on these hierarchies can be found in Saaty, 1980). After getting the weighted value, the weighted sum model has been applied to find the final **Composite Hazard Map**.

### Methodology

The Weighted Sum Model (WSM) is probably the most commonly used approach, especially in single dimensional problems like this. In weighted sum technique, we first convert our criteria raster files to a common numerical system as the WSM needs all data in same unit, a uniform calculation (Figure 6.1). For this, values will be converted into rating based on their impact in scale of 1 to 5; where 1 being less effective and 5 being most effective. If Liquefaction Hazard Zone is 0 or <5 we can say it is safer than >15 one, so <5 value is given 5 where >15 is given 1.

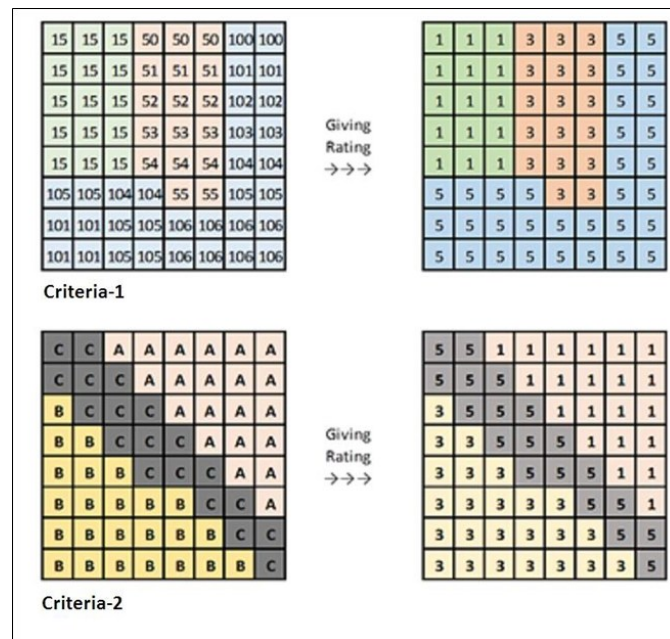


Figure 31 Criteria Raster Files for Composite Hazard Map.

After rating the individual criterion, they have been given a weighted value, which is the impact of each criterion on the decision. This weighted value will be calculated from AHP method. Specialists will be asked to participate in this AHP and give its pairwise rating. Afterward all the rating needs to be calculated in AHP model and the weight value identified. Then rating raster would be multiplied by the weighted value and afterward summed up for the final decision raster which returns value ranging from 100 to 500 (Figure 32). The decision raster will be divided into five Classes *i.e., Very Good, Good, Moderate, Poor, Very Poor* from

equally divided range of 100 to 500. The classes of suitability will relative to this area particularly (Figure 6.3).

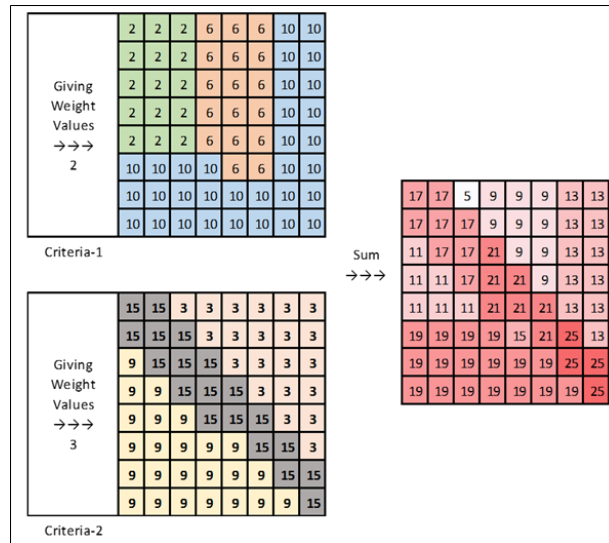


Figure 32 Criteria Raster Files Multiplied by the Weighted and Summed up Value for Composite Hazard Map.

We have used two steps Multi-Criteria Decision Making (MCDM) technique to develop **Geoengineering Suitability Map**. We have selected five (5) major criteria *i.e.* **PGA, SA, AVS30/Soil Type, Foundation depth, Liquefaction Potential Index**. And to find out the relative weight of these criteria Analytic Hierarchy Process (AHP) has been used. Finally, the decision raster will be divided into 5 Classes *i.e.*, **Very High Suitability, High Suitability, Moderate Suitability, Low Suitability and Very Low Suitability** from equally divided range of 0 to 1. Rating and weight value for suitability are shown in the following table.

Table 14 Rating and Weight Value for Geological Suitability

Parameters	Weight	Values/ Values Range	Normalised Value/Range
Earthquake	16.4	0.195318 g to 0.21265g	1 to 0
LPI	13.6	<=5	1
		5-15	<1 to >0
		>=15	0
Foundation Type	25.1	Not Suitable for Shallow Foundation	0.5
		Suitable for Shallow Foundation for Lightly Loded Structures	1
AVS30	26.9	>=360m/s	1
		<360 to >180 m/s	<1 to >0
		<180m/s	0
SA	18	SA of Short Period (0.581549- 0.690433)	1 to 0
		SA of Long Period (0.335315-0.429694)	1 to 0
		Average of Normalised SA of short and Long Period	1 to 0

## 6.1. Geoengineering Suitability of Meherpur District

According to the Geoengineering Suitability Assessment, Meherpur District into five distinct zones: *Very High Suitability Area, High Suitability Area, Moderate Suitability Area, Low Suitability Area and Very Low Suitability Area.*

In Gangi Upazila, most areas fall within the Moderate Suitability, with a significant portion categorized as Low Suitability. Only a negligible area is classified as either Very Low or High Suitability. In contrast, the majority of Meherpur Sadar Upazila lies within the High Suitability, with a smaller portion falling under Moderate Suitability. Mujib Nagar Upazila predominantly features Moderate Suitability areas, along with a notable portion of High Suitability zones.

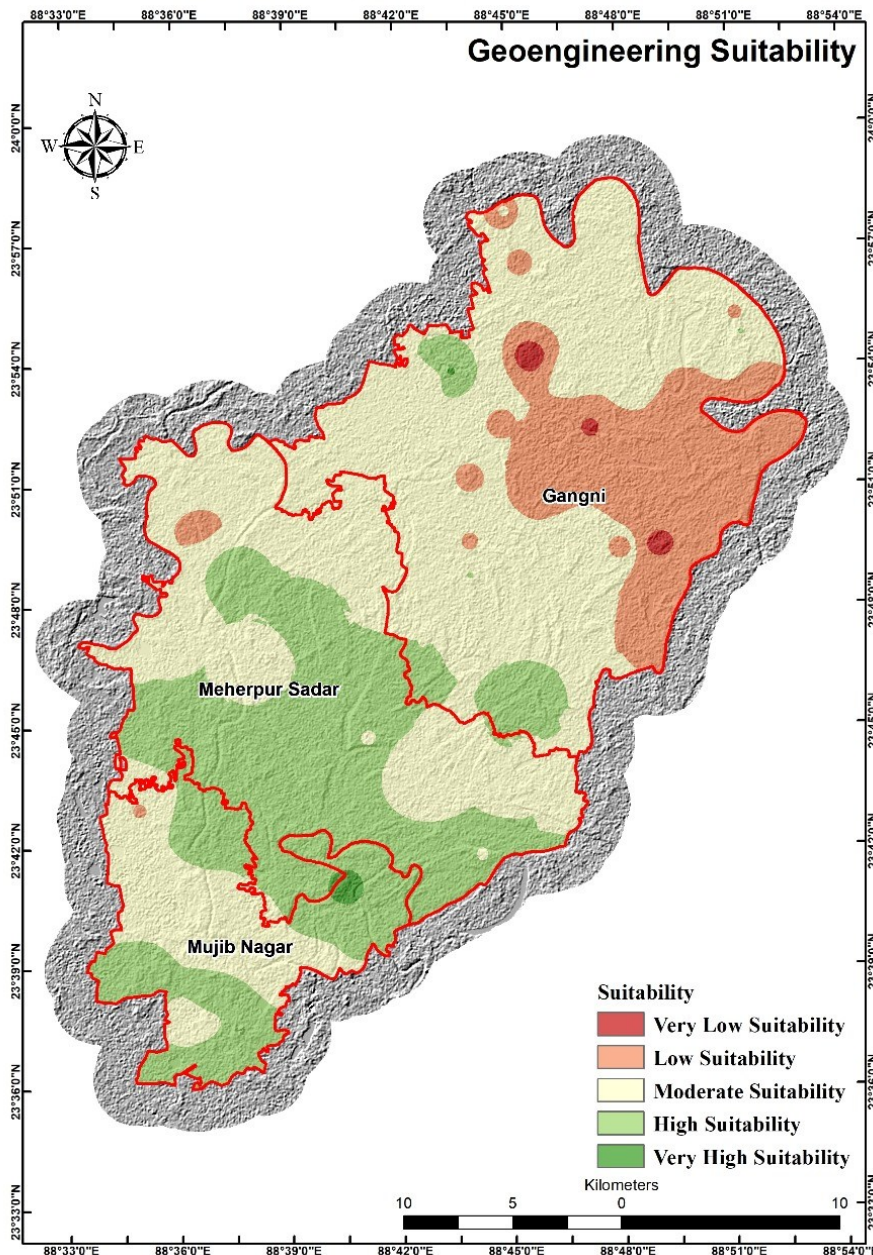


Figure 33 Geoengineering Suitability of Meherpur District.

*Table 15 Land-use Recommendation Based on Geoengineering Suitability*

<b>Geoengineering Suitability</b>	<b>Infrastructure Foundation Suitability</b>	<b>Suggested Land-Use</b>
<b>Very High Suitability</b>	Light infrastructure is suitable with a foundation depth of around 6m. Individual on-site subsoil investigation should be required.	Residential area, Commercial area.
<b>High Suitability</b>	Light infrastructure is suitable with a foundation depth of around 6m. Large and tall infrastructure requires pile foundation placed on proper depth. Individual on-site subsoil investigation should be required.	Commercial area Residential area, Industrial zone
<b>Moderate Suitability</b>	Light infrastructure requires with a proper foundation depth. Large and tall infrastructure requires pile foundation placed on proper depth. Individual on-site subsoil investigation should be required.	Industrial zone, Residential area, Commercial area, Agricultural Zone, Park and Recreation
<b>Low Suitability</b>	Detail subsoil investigation and proper foundation design is required for all types of infrastructure, due to low suitability with hazard potential.	Agricultural zone, Wetland Rural settlement Park and Recreation
<b>Very Low Suitability</b>	Detail subsoil investigation for deep pile foundation is essential, due to very low soil resistance and high hazard potential. Shallow foundation is not preferred.	Agricultural zone, Wetland Rural settlement Park and Recreation



## 7. CONCLUSION

Bangladesh is divided into four seismic zones: Zone IV (high-risk), Zone III (risk), Zone II (moderate risk), and Zone I (low-risk), with Meherpur District located in Zone I (BNBC, 2020). For effective urban planning, it is important to conduct geotechnical and geophysical studies, along with seismic hazard assessments. These studies provide necessary subsurface information, which is crucial for creating durable and sustainable urban environments. The Subsurface Geotechnical and Geophysical Studies module is an important part of the project Preparation of Development Plan for Meherpur District, led by the Urban Development Directorate.

During the project, we carried out both geotechnical and geophysical investigations. The geotechnical survey involved Standard Penetration Test (SPT) boreholes, drilled to depths of up to 30 meters, along with the collection of soil samples for laboratory analysis. The geophysical survey included Downhole Seismic Tests (PS-logging) and Multi-channel Analysis of Surface Waves (MASW). Laboratory testing of both disturbed and undisturbed samples was conducted, including Specific Gravity Analyses, Atterberg Limits, Grain Size Analyses, Direct Shear Tests, Unconfined Compressive Strength Tests, and Triaxial Tests.

This study enhances seismic hazard estimation for district development planning using Probabilistic Seismic Hazard Assessment (PSHA) methods. It incorporates refined seismic source zoning, local site effects, and uncertainty in source parameters and attenuation models. The results, presented through hazard maps and curves, highlight Peak Ground Acceleration (PGA) and Spectral Acceleration (SA) for 10% and 2% probabilities of exceedance. The maximum PGA is up to 0.146 g and 0.372g for 10% and 2% probability of exceedance in 50 years, aligning with the BNBC 2020 zonation (PGA 0.20g). However, the use of updated Ground Motion Prediction Equations (GMPEs) and an expanded earthquake catalogue offers more accurate and site-specific assessments, consistent with recent studies by Rahman (2020) and Haque (2019). This approach supports more reliable seismic risk evaluation and safer urban planning.

An examination of the geological landscape reveals that areas of Meherpur district feature distinct soil types. According to the National Earthquake Reduction Program (NEHRP) of United States, the study area is classified as D-type soil, while the Bangladesh National Building Code (BNBC) classifies it as SD-type soil. Both E-type and SD-type soils have a shear wave velocity of  $\leq 180$  m/s. The recorded shear wave velocities in the project area range from 172.58 to 271.84 m/s, confirming that the soils meet the criteria for class E according to the NEHRP standards.

Most areas of Gangi and Mujib Nagar Upazilas in Meherpur District fall within the Moderate Risk Zone for liquefaction hazards. In contrast, the majority of Meherpur Sadar Upazila lies in the Low-Risk Zone, indicating relatively stable ground conditions. A smaller portion of Gangi Upazila, particularly in the northeastern part, is classified as a High-Risk Zone, where the potential for liquefaction during seismic events is significantly greater.



Most areas of Meherpur District are suitable for shallow foundations for lightly loaded structures at an allowable bearing capacity up to 4.5 meters depth. Only a small part of northwestern Gangi Upazila is not suitable at this depth. At 6.0 meters, almost the entire district remains suitable, with only a negligible area deemed not suitable.

A key outcome of this study is the development of a comprehensive Geoengineering Suitability Assessment, which categorizes Meherpur District into five distinct zones: Very High Suitability, High Suitability, Moderate Suitability, Low Suitability, and Very Low Suitability. In Gangi Upazila, the majority of areas fall within the Moderate Suitability zone, with a significant portion classified as Low Suitability. Only a negligible area is marked as either High or Very Low Suitability. In contrast, Meherpur Sadar Upazila is largely categorized as High Suitability, with smaller areas falling into the Moderate Suitability zone. Mujibnagar Upazila is primarily composed of Moderate Suitability areas, along with a notable portion designated as High Suitability.

This detailed classification offers valuable considerations for urban planning and infrastructure development, aiding in the identification of suitable construction sites and the assessment of potential risks across the region.

### Recommendation

**AVS30 Values:** Engineering geological mapping showed that most of the section of the study area has higher average shear wave velocity (AVS30) values. These locations are relatively stiffer, and in general, stiffer sites are less prone to seismic amplification and liquefaction. It is recommended that new developments, particularly critical and lifeline structures.

**Seismic hazard analysis:** The UHS reveals the highest SA values at a spectral period of 0.2s and the lowest at 2.0s. For Meherpur, the PGA ranges from 0.142g to 0.146g for a 10% probability of exceedance and from 0.358g to 0.372g for a 2% probability of exceedance within a 50-year timeframe.

**Liquefaction analysis:** Based on the liquefaction hazard assessment, Meherpur exhibit moderate liquefaction potential, as indicated by the Liquefaction Potential Index (LPI) values. It is advisable to avoid siting critical facilities—such as hospitals, emergency centers, power stations, and water supply infrastructure—in these zones. If necessary, appropriate ground improvement techniques should be implemented. Preferably, such facilities should be located in areas identified as having low liquefaction risk based on detailed subsurface investigations.

**Risk-Sensitive Land Use Plan:** Integrate the findings of seismic hazard and liquefaction studies into the land-use planning framework for Meherpur. Residential, commercial, and public facilities should be zoned considering seismic risk levels, with denser developments located on stiffer soils (higher AVS30 zones).

## 8. REFERENCES

- i. Abrahamson, N. A., Silva, W. J., & Kamai, R. (2014). Summary of the ASK14 ground motion relation for active crustal regions. *Earthquake Spectra*, 30(3), 1025–1055. <https://doi.org/10.1193/070913EQS198M>
- ii. Abrahamson, N., Gregor, N., & Addo, K. (2016). BC hydro ground motion prediction equations for subduction earthquakes. *Earthquake Spectra*, 32(1), 23–44. <https://doi.org/10.1193/051712EQS188MR>
- iii. Ahmed, B. (2015). Landslide susceptibility mapping using multi-criteria evaluation techniques in Chittagong Metropolitan Area, Bangladesh. *Landslides*, 12(6), 1077–1095. <https://doi.org/10.1007/s10346-014-0521-x>
- iv. Akgün, A., Kincal, C., & Pradhan, B. (2012). Application of remote sensing data and GIS for landslide risk assessment as an environmental threat to Izmir city (west Turkey). *Environmental Monitoring and Assessment*, 184(9), 5453–5470. <https://doi.org/10.1007/s10661-011-2343-7>
- v. Alam, E., & Dominey-Howes, D. (2016). A catalogue of earthquakes between 810BC and 2012 for the Bay of Bengal. *Natural Hazards*, 81(3), 2031–2102. <https://doi.org/10.1007/s11069-016-2174-7>
- vi. Alam, M. (1989). Geology and depositional history of Cenozoic sediments of the Bengal Basin of Bangladesh. *Paleogeography, Palaeoclimatology, Paleoecology*, 69, 125–139.
- vii. Alam, M. K., Hasan, A. K. M. S., Khan, M. R., & Whitney, J. W. (1990). Geological map of Bangladesh.
- viii. Ambraseys, N. N., & Douglas, J. (2004). Magnitude calibration of north Indian earthquakes. *Geophysical Journal International*, 159(1), 165–206. <https://doi.org/10.1111/j.1365-246X.2004.02323.x>
- ix. Anbazhagan P, Sitharam TG. Mapping of average shear wave velocity for Bangalore region: a case study. *Journal of Environmental & Engineering Geophysics* 2008;13(2):69–84.
- x. Anbazhagan P, Sitharam TG. Seismic microzonation of Bangalore. *Journal of Earth System Science* 2008; 117(S2):833–52.
- xi. Anbazhagan P, Sitharam TG. Spatial variability of the weathered and engineering bed rock using multichannel analysis of surface wave survey. *Pure and Applied Geophysics* 2009;166(3):409–28.
- xii. Anika Samm-A, A. S. M. Maksud Kamal, Md. Shakhawat Hossain & Md. Zillur Rahman (2025) Probabilistic seismic hazard mapping for Bangladesh using updated source models, *Geomatics, Natural Hazards and Risk*, 16:1, 2454537, DOI: 0.1080/19475705.2025.2454537
- xiii. Athanasopoulos GA (1995) Empirical correlations  $V_s$ -NSPT for soils of Greece: a comparative study of reliability. In: Cakmak AS (ed) *Proceedings of 7th international conference on soil dynamics and earthquake engineering* (Chania, Crete). *Computational Mechanics*, Southampton, pp 19–36.
- xiv. Atkinson, G. M., & Boore, D. M. (2003). Empirical ground-motion relations for subduction-zone earthquakes and their application to Cascadia and other regions. *Bulletin of the Seismological Society of America*, 93(4), 1703–1729. <https://doi.org/10.1785/0120020156>
- xv. Auld, B., 1977, Cross-Hole and Down-Hole  $V_s$  by Mechanical Impulse, *Journal of Geotechnical Engineering Division, ASCE*, Vol. 103, No. GT12, pp. 1381-1398
- xvi. Ayalew, L., & Yamagishi, H. (2005). The application of GIS-based logistic regression for landslide susceptibility mapping in the Kakuda-Yahiko Mountains, Central Japan. *Geomorphology*, 65(1–2), 15–31. <https://doi.org/10.1016/j.geomorph.2004.06.010>

- xvii. Baker, J. W. (2013). *Introduction To probabilistic seismic hazard analysis*. White paper version 2:1.
- xviii. Banglapedia 2015 - [http://en.banglapedia.org/index.php?title=Dohar\\_Upazila](http://en.banglapedia.org/index.php?title=Dohar_Upazila)
- xix. Bilham, R. (2009). *The seismic future of cities*. *Bulletin of Earthquake Engineering*, 7(4), 839–887. <https://doi.org/10.1007/s10518-009-9147-0>
- xx. Bilham, R., & England, P. (2001). Plateau “pop-up” in the great 1897 Assam earthquake. *Letters to Nature*, 410, 806–809. <https://doi.org/doi:10.4401/ag-3338>
- xxi. BNBC, Bangladesh National Building Code (2020) Housing and Building Research Institute. Dhaka, Bangladesh.
- xxii. BNBC. 2015. Bangladesh National Building Code [Internet]. [place unknown]. [http://hbri.portal.gov.bd/sites/default/files/files/hbri.portal.gov.bd/page/ad124ea6\\_eb26\\_41b7\\_88b9\\_8f7302f3c406/2022-03-21-05-31-7a81770aab61b4341e57d61a28cf98a7.pdf](http://hbri.portal.gov.bd/sites/default/files/files/hbri.portal.gov.bd/page/ad124ea6_eb26_41b7_88b9_8f7302f3c406/2022-03-21-05-31-7a81770aab61b4341e57d61a28cf98a7.pdf)
- xxiii. BNBC. 2020. Bangladesh National Building Code (BNBC) 2020. [place unknown].
- xxiv. Boore, D. M., Stewart, J. P., Seyhan, E., & Atkinson, G. M. (2014). NGA-West2 Equations for predicting PGA, PGV, and 5%-damped PSA from shallow crustal earthquakes. *Earthquake Spectra*, 30, 1057–1085.
- xxv. BSSC. (1997). *NEHRP RECOMMENDED PROVISIONS FOR SEISMIC REGULATIONS FOR NEW BUILDINGS*. Building Seismic Safety Council.
- xxvi. BSSC. (2015). *NEHRP Recommended Seismic Provisions for New Buildings and Other Structures, FEMA Volume II: Part 3 Resource Papers*. Building Seismic Safety Council, II, 174.
- xxvii. Buchanan, C. H., Dougan, P. J., & Kelly, L. M. (2020). Landslide susceptibility mapping: A review of methods and applications. *Natural Hazards Review*, 21(2), 04020017.
- xxviii. Campbell, K. W., & Bozorgnia, Y. (2014). NGA-West2 ground motion model for the average horizontal components of PGA, PGV, and 5% damped linear acceleration response spectra. *Earthquake Spectra*, 30(3), 1087–1114. <https://doi.org/10.1193/062913EQS175M>
- xxix. Chiou, B. S. J., & Youngs, R. R. (2014). Update of the Chiou and Youngs NGA model for the average horizontal component of peak ground motion and response spectra. *Earthquake Spectra*, 30(3), 1117–1153. <https://doi.org/10.1193/072813EQS219M>
- xxx. Chung, J.-W., & Rogers, J. D. (2011). Simplified Method for Spatial Evaluation of Liquefaction Potential in the St. Louis Area. *Journal of Geotechnical and Geoenvironmental Engineering*, 137(5), 505–515. [https://doi.org/10.1061/\(asce\)gt.1943-5606.0000450](https://doi.org/10.1061/(asce)gt.1943-5606.0000450)
- xxxi. Coduto DP. 1994. *Foundation Design; Principles and Practis*. Pract Hall Int New Jersey.
- xxxii. Cornell, C. A. (1968). Engineering seismic risk analysis. *Bulletin of the Seismological Society of America*, 58(5), 1583–1606.
- xxxiii. Curray, J. R., Emmel, F. J., Moore, D. G., & Raitt, R. W. (1982). Structure, tectonics, and geological history of the northeastern Indian Ocean. In *The ocean basins and margins* (pp. 399–450). Springer.
- xxxiv. Dikmen, Ü. (2009). Statistical correlations of shear wave velocity and penetration resistance for soils. *Journal of Geophysics and Engineering*, 6(1), 61-72.
- xxxv. Dixit, J., Dewaikar, D. M., & Jangid, R. S. (2012). Assessment of liquefaction potential index for Mumbai city. *Natural Hazards and Earth System Science*, 12(9), 2759–2768. <https://doi.org/10.5194/nhess-12-2759-2012>
- xxxvi. Frankel, A. (1995). Mapping seismic hazard in the central and eastern United States. *Seismological Research Letters*, 66(4), 8–21. <https://doi.org/10.1785/gssrl.66.4.8>
- xxxvii. Fujiwara, T. (1972, September). Estimation of ground movements in actual destructive earthquakes. In *Proceedings of the fourth European symposium on earthquake engineering*, London (pp. 125-132).

- xxxviii. Fumal, T., Tinsley, J. C., & Ziony, J. I. (1985). Mapping shear-wave velocities of near-surface geologic materials. *US Geological Survey Professional Paper*, 1360, 127-150.
- xxxix. Gardner, J. K., & Knopoff, L. (1974). Is the sequence of earthquake in southern California, with aftershocks removed, Poissonian? *Bulletin of the Seismological Society of America*, 64(5), 1363–1367. <https://doi.org/10.2307/1779766>
- xl. Hanumantharao, C., & Ramana, G. V. (2008). Dynamic soil properties for microzonation of Delhi, India. *Journal of earth system science*, 117, 719-730.
- xli. Haque, D. M. E., Khan, N. W., MD.Selim, & Kamal, A. S. M. M. (2019). Towards Improved Probabilistic Seismic Hazard Assessment for Bangladesh. <https://doi.org/10.1007/s00024-019-02393-z>
- xlii. Hasancebi, N., & Ulusay, R. (2007). Empirical correlations between shear wave velocity and penetration resistance for ground shaking assessments. *Bulletin of Engineering Geology and the Environment*, 66, 203-213.
- xliii. Holzer, T. L., Bennett, M. J., Noce, T. E., Padovani, A. C., & Tinsley III, J. C. (2006). Liquefaction hazard mapping with LPI in the greater Oakland, California, area. *Earthquake Spectra*, 22(3), 693–708.
- xliv. Huang, R.-Q. (2007). Large-scale landslides and their sliding mechanisms in China since the 20th century. *Chinese Journal of Rock Mechanics and Engineering*, 26(3), 433–454.
- xlvi. Idriss, I. M. (2014). An NGA-West2 empirical model for estimating the horizontal spectral values generated by shallow crustal earthquakes. *Earthquake Spectra*, 30, 1155–1177. <https://doi.org/10.1193/070613EQS195M>
- xlv. Imai T, Tonouchi K (1982) Correlation of N-value with S-wave velocity and shear modulus. *Proceedings of the 2nd European symposium of penetration testing, Amsterdam*, pp 57–72.
- xlvii. Imai, T. (1977). P and S wave velocities of the ground in Japan. *Proc. 9th ICSMFE, Tokyo*, 1977, 2, 257-260.
- xlviii. Imai, T., & Yoshimura, Y. (1970). Elastic wave velocity and soil properties in soft soil. *Tsuchito-kiso*, 18(1), 17-22.
- xlix. Imai, T., Fumoto, H., & Yokota, K. (1975, November). The relation of mechanical properties of soil to P-and S-wave velocities in Japan. In *Proceedings of 4th Japan Earthquake Engineering Symposium, Tokyo, Japan* (pp. 89-96).
- i. Islam, M. S., Huda, M. M., Al-noman, M. N., & Al-hussaini. (2010). Attenuation of Earthquake Intensity in Bangladesh. *Proceedings, 3rd International Earthquake Symposium, Bangladesh (IBES-3), Dhaka, March 5-6, 2010*, 481–488.
- li. Iwasaki, T., Tatsuoka, F., Tokida, K. -i., & Yasuda, S. (1978). A practical method for assessing soil liquefaction potential based on case studies at various sites in Japan. *Proc. of 2nd International Conference on Microzonation*, 885–896.
- lii. Iwasaki, T., Tokida, K., Tatsuoka, F., Watanabe, S., Yasuda, S., & Sato, H. (1982). Microzonation for soil liquefaction potential using simplified methods. *Proceedings of 3rd International Earthquake Microzonation Conference*, 1319–1330.
- liii. Iyisan R (1996) Correlations between shear wave velocity and in situ penetration test results. *Chamber of Civil Engineers of Turkey. Teknik Dergi* 7(2), 1187-1199 (in Turkish).
- liv. Jafari, M. K., Asghari, A., & Rahmani, I. (1997, May). Empirical correlation between shear wave velocity ( $V_s$ ) and SPT-N value for south of Tehran soils. In *Proceedings of the 4th international conference on civil engineering, Tehran, Iran*.
- lv. Jafari, M. K., Shafiei, A., & Razmkhah, A. (2002). Dynamic properties of fine-grained soils in south of Tehran.
- lvi. Jinan, Z. (1987). Correlation between seismic wave velocity and the number of blows of SPT and depth. *Selected Papers from the Chinese Journal of Geotechnical Engineering*, 92-100.



- lvii. Kalteziotis, N., Sabatakakis, N., & Vassiliou, J. (1992, October). Evaluation of dynamic characteristics of Greek soil formations. In *Second hellenic conference on geotechnical engineering* (Vol. 2, pp. 239-246).
- lviii. Kamal, A. S. M. M. (2013). *Earthquake Risk and Reduction Approaches in Bangladesh*. In R. Shaw et al. (Ed.), *Disaster Risk Reduction Approaches in Bangladesh* (pp. 103–130). <https://doi.org/10.1007/978-4-431-54252-0>
- lix. Kanai, K. (1966). Improved Empirical Formula for the Characteristic of Strong Earthquake Motions. In *Proc. Japan Earthq. Engng. Symp.*
- lx. Kang, G. C., Chung, J. W., & Rogers, J. D. (2014). Re-calibrating the thresholds for the classification of liquefaction potential index based on the 2004 Niigata-ken Chuetsu earthquake. *Engineering Geology*, 169, 30–40. <https://doi.org/10.1016/j.enggeo.2013.11.012>
- lxi. Kayabali, K. (1996). Soil liquefaction evaluation using shear wave velocity. *Engineering geology*, 44(1-4), 121-127.
- lxii. Kayal, J. R., Arefiev, S. S., Baruah, S., Hazarika, D., Gogoi, N., Gautam, J. L., Baruah, S., Dorbath, C., & Tatevossian, R. (2012). Large and great earthquakes in the Shillong plateau-Assam valley area of Northeast India Region: Pop-up and transverse tectonics. *Tectonophysics*, 532–535, 186–192. <https://doi.org/10.1016/j.tecto.2012.02.007>
- lxiii. Khan, M. H., & Sarkar, S. K. (2019). Landslide Modelling and Risk Assessment: Evidence from Chattogram City of Bangladesh. *Journal of Engineering*, 10(2), 91–101.
- lxiv. Kiku, H. (2001). In-situ penetration tests and soil profiling in Adapazari, Turkey. In *Proc. 15th ICSMGE TC4 Satellite Conference on Lessons Learned from Recent Strong Earthquakes*, August 25, 2001, Istanbul, Turkey (pp. 259-265).
- lxv. Kitsunezaki, C., N. Goto, Y. Kobayashi., T. Ikawa, M. Horike, T. Saito, T. Kurota, K. Yamane, and K. Okuzumi, 1990, Estimation of P- and S- wave velocities in Deep Soil Deposits for Evaluating Ground Vibrations in Earthquake, *SIZEN-SAIGAI-KAGAKU*,9-3,1-17 (in Japanese).
- lxvi. Lee, D. H., Ku, C. S., & Yuan, H. (2004). A study of the liquefaction risk potential at Yuanlin, Taiwan. *Engineering Geology*, 71(1–2), 97–117. [https://doi.org/10.1016/S0013-7952\(03\)00128-5](https://doi.org/10.1016/S0013-7952(03)00128-5)
- lxvii. Lee, S. H. H. (1990). Regression models of shear wave velocities in Taipei basin. *Journal of the Chinese Institute of Engineers*, 13(5), 519-532.
- lxviii. Liu, X., Li, D., & Cheng, H. (2021). A GIS-based landslide susceptibility assessment in a rapidly urbanizing region. *Environmental Monitoring and Assessment*, 193, 35.
- lxix. Ludwig, W.J., Nafe, J.E., and Drake, C.L., 1970, Seismic refraction, in *The Sea*, A.E. Maxwell (Editor), Vol. 4, Wiley-Interscience, New York, pp. 53-84
- lxx. Luna, R., & Frost, D. J. (1998). Spatial liquefaction analysis system. *Journal of Computing in Civil Engineering*, 12(1), 48–56.
- lxxi. Maiti, S. K. (2014). Landslide susceptibility mapping: A review. *Environmental Earth Sciences*, 71(4), 1393-1409.
- lxxii. Malczewski, J. (2000). On the use of weighted linear combination method in GIS: Common and best practice approaches. *Transactions in GIS*, 4(1), 5–22. <https://doi.org/10.1111/1467-9671.00035>
- lxxiii. Meyerhoff GG. 1956. Penetration tests and Bearing Capacity of Cohesive Soils. *ASCE Jr SM FE*. 82:866.
- lxxiv. Middlemiss, C. S. (1885). Report on the Bengal earthquake of July 14, 1885. *Rec. Geol. Surv. India* 18 (4).
- lxxv. Middlemiss, C. S. (1885). Report on the bengal earthquake of July 14, 1885 (Vol. 18, Issue 4).
- lxxvi. Miller RD, Xia J, Park CB, Ivanov J. Multichannel analysis of surface waves to map bedrock. *The Leading Edge* 1999;18(12):1392–6.



- lxxvii. Morgan, J. P., & McIntire, W. G. (1959). Quaternary geology of the Bengal Basin, East Pakistan and India. *Bulletin of the Geological Society of America*, 70(March), 319–342.
- lxxviii. Ohba, S., & Toriumi, I. (1970, December). Dynamic response characteristics of Osaka Plain. In *Proceedings of the annual meeting AIJ (in Japanese) (Vol. 12)*.
- lxxix. Ohsaki, Y., & Iwasaki, R. (1973). On dynamic shear moduli and Poisson's ratios of soil deposits. *Soils and Foundations*, 13(4), 61-73.
- lxxx. Ohta, T., Hara, A., Niwa, M., & Sakano, T. (1972, July). Elastic shear moduli as estimated from N-value. In *Proc. 7th Ann. Convention of Japan Society of Soil Mechanics and Foundation Engineering* (pp. 265-268).
- lxxxi. Ohta, Y., & Goto, N. (1978). Empirical shear wave velocity equations in terms of characteristic soil indexes. *Earthquake engineering & structural dynamics*, 6(2), 167-187.
- lxxxii. Okada, H., 2003, The microtremor survey method, Society of Exploration Geophysicist, Tulsa
- lxxxiii. Okamoto, T., Kokusho, T., Yoshida, Y., & Kusunoki, K. (1989, October). Comparison of surface versus subsurface wave source for P-S logging in sand layer. In *Proc. 44th Ann. Conf. JSCE (Vol. 3, pp. 996-7)*.
- lxxxiv. Oldham, R. D. (1899). Report on the Great Earthquake of 12th June 1897. *Mem. Geol. Surv. India* 29.
- lxxxv. Oldham, R. D. (1899). Report on the great earthquake of 12th June 1897. *Mem Geol Surv India* 29:1379 (Calcutta).
- lxxxvi. Ordaz, M., & Salgado-Gálvez, M. A. (2017). R-CRISIS Validation and Verification Document. Technical Report. Mexico City, Mexico.
- lxxxvii. Park CB, Miller RD, Xia J. Multi-channel analysis of surface waves. *Geophysics* 1999; 64(3):800–8.
- lxxxviii. Peck RB, Hanson WE, Thornburn TH. 1991. *Foundation engineering*. [place unknown]: John Wiley & Sons.
- lxxxix. Petersen, M. D., Moschetti, M. P., Powers, P. M., Mueller, C. S., Haller, K. M., Frankel, A. D., Zeng, Y., Rezaeian, S., Harmsen, S. C., Boyd, O. S., Field, N., Chen, R., Rukstales, K. S., Luco, N., Wheeler, R. L., Williams, R. A., & Olsen, A. H. (2014). Documentation for the 2014 Update of the United States National Seismic Hazard Maps. U.S. Geological Survey Open-File Report, 243 p. <https://doi.org/http://dx.doi.org/10.3133/ofr20141091>
- xc. Pitilakis, K. D., Anastasiadis, A., & Raptakis, D. (1992, July). Field and laboratory determination of dynamic properties of natural soil deposits. In *Proceedings of the 10th world conference on earthquake engineering (Vol. 5, pp. 1275-1280)*.
- xci. Pitilakis, K., Raptakis, D., Lontzetidis, K., Tika-Vassilikou, T., & Jongmans, D. (1999). Geotechnical and geophysical description of EURO-SEISTEST, using field, laboratory tests and moderate strong motion recordings. *Journal of Earthquake Engineering*, 3(03), 381-409.
- xcii. Pradhan, B., & Lee, S. (2010). Delineation of landslide hazard areas using frequency ratio, logistic regression, and artificial neural network models at Penang Island, Malaysia. *Environmental Earth Sciences*, 60(5), 1037–1054. <https://doi.org/10.1007/s12665-009-0245-8>
- xciii. Rahman, M. Z., & Siddiqua, S. (2017). Evaluation of liquefaction-resistance of soils using standard penetration test, cone penetration test, and shear-wave velocity data for Dhaka, Chittagong, and Sylhet cities in Bangladesh. *Environmental Earth Sciences*, 76(5). <https://doi.org/10.1007/s12665-017-6533-9>
- xciv. Rahman, M. Z., Kamal, A. S. M. M., & Siddiqua, S. (2015). Shear wave velocity mapping of Dhaka City for seismic hazard assessment. 11th Canadian Conference on Earthquake Engineering. [https://www.researchgate.net/publication/303821022\\_Shear\\_wave\\_velocity\\_mapping\\_of\\_Dhaka\\_City\\_for\\_seismic\\_hazard\\_assessment](https://www.researchgate.net/publication/303821022_Shear_wave_velocity_mapping_of_Dhaka_City_for_seismic_hazard_assessment)

- xcv. Rahman, M. Z., Kamal, A. S. M. M., & Siddiqua, S. (2018). Near-surface shear wave velocity estimation and  $V_{s30}$  mapping for Dhaka City, Bangladesh. *Natural Hazards*, 92(3), 1687–1715. <https://doi.org/10.1007/s11069-018-3266-3>
- xcvi. Rahman, M. Z., Siddiqua, S., & Kamal, A. S. M. M. (2020). Seismic source modeling and probabilistic seismic hazard analysis for Bangladesh. *Natural Hazards*. <https://doi.org/10.1007/s11069-020-04094-6>
- xcvii. Rahman, M.Z., & Siddiqua, S. (2017). Evaluation of liquefaction-resistance of soils using standard penetration test, cone penetration test, and shear-wave velocity data for Dhaka, Chittagong, and Sylhet cities in Bangladesh. *Environmental Earth Sciences*, 76(5). <https://doi.org/10.1007/s12665-017-6533-9>
- xcviii. Rahman, Md Zillur, Siddiqua, S., & Kamal, A. S. M. M. (2015). Liquefaction hazard mapping by liquefaction potential index for Dhaka City, Bangladesh. *Engineering Geology*, 188, 137–147. <https://doi.org/10.1016/j.enggeo.2015.01.012>
- xcix. Raptakis, D. G., Anastasiadis, S. A. J., Pitilakis, K. D., & Lontzetidis, K. S. (1995, August). Shear wave velocities and damping of Greek natural soils. In *Proc. 10th European Conf. Earthquake Engg., Vienna (Vol. 477482)*.
- c. Scordilis, E. M. (2006). Empirical global relations converting MS and mb to moment magnitude. *Journal of Seismology*, 10(2), 225–236. <https://doi.org/10.1007/s10950-006-9012-4>
- ci. Seed, H Bolton, Tokimatsu, K., Harder, L. F., & Chung, R. M. (1985). Influence of SPT procedures in soil liquefaction resistance evaluations. *Journal of Geotechnical Engineering*, 111, 1425–1445. [https://doi.org/10.1061/\(ASCE\)0733-9410\(1985\)111:12\(1425\)](https://doi.org/10.1061/(ASCE)0733-9410(1985)111:12(1425))
- cii. Seed, H. B., & Idriss, I. M. (1971). Simplified procedure for evaluating soil liquefaction potential. *Journal of Soil Mechanics and Foundations Division*, 97(SM9), 1249–1273.
- ciii. Seed, H. B., & Idriss, I. M. (1981, October). Evaluation of liquefaction potential sand deposits based on observation of performance in previous earthquakes. In *ASCE national convention (MO)* (pp. 481-544).
- civ. Seed, H. B., Idriss, I. M., & Arango, I. (1983). Evaluation of liquefaction potential using field performance data. *Journal of Geotechnical Engineering*, 109, 458–482.
- cv. Seed, H. B., Idriss, I. M., & Arango, I. (1983). Evaluation of liquefaction potential using field performance data. *Journal of geotechnical engineering*, 109(3), 458-482.
- cvi. Seed, H. Bolton, & Idriss, I. M. (1970). A simplified procedure for evaluating soil liquefaction potential. Report No. EERC 70-9 (Issue November).
- cvii. Shafi, S. M., & Tabassum, N. (2017). Study the Significance and Possibilities of Liquefaction in Dhaka City and Proposed Some Remedies to Liquefaction Induced Soil. 07(09), 60–68.
- cviii. Shibata, T. (1970). Analysis of liquefaction of saturated sand during cyclic loading. *Disaster Prevention Res. Inst. Bull*, 13, 563-570.
- cix. Sisman, H. (1995). An investigation on relationships between shear wave velocity, and SPT and pressuremeter test results. Master of Science Thesis, Ankara University, Turkey.
- cx. Skempton AW. 1986. Standard penetration test procedures and the effects in sands of overburden pressure, relative density, particle size, ageing and overconsolidation. *Geotechnique*. 36(3):425–447.
- cxi. Steckler, M. S., Akhter, S. H., & Seeber, L. (2008). Collision of the Ganges-Brahmaputra Delta with the Burma Arc: Implications for earthquake hazard. *Earth and Planetary Science Letters*, 273(3–4), 367–378. <https://doi.org/10.1016/j.epsl.2008.07.009>
- cxii. Steckler, M. S., Mondal, D. R., Akhter, S. H., Seeber, L., Feng, L., Gale, J., Hill, E. M., & Howe, M. (2016). Locked and loading megathrust linked to active subduction beneath the Indo-Burman Ranges. *Nature Geoscience*, 9(8), 615–618. <https://doi.org/10.1038/ngeo2760>

- cxiii. Stepp, J. C. (1972). *Analysis of Completeness of the Earthquake Sample in the Puget Sound Area and Its Effect on Statistical Estimates of Earthquake Hazard*. *Proceedings of the Microzonation Conference*. Seattle, WA, 897–909.
- cxiv. Stuart, M. (1920). *The Srimangal earthquake of 8th July 1918*. *Mem. Geol. Surv. India* 46(1).
- cxv. Stuart, M. (1920). *The Srimangal earthquake of 8th July, 1918*.  
<https://www.worldcat.org/title/srimangal-earthquake-of-8th-july-1918/oclc/27157560>
- cxvi. Sultana, N. (2020). *Analysis of landslide-induced fatalities and injuries in Bangladesh: 2000–2018*. *Cogent Social Sciences*, 6(1), 2000–2018.  
<https://doi.org/10.1080/23311886.2020.1737402>
- cxvii. Sykora, D.W., & Stokoe, K.H. (1983). "Correlations of In Situ Measurements in Sands of Shear Wave Velocity." *Soil Dyn Earthq Eng* 20:125–136.
- cxviii. Szeliga, W., Hough, S., Martin, S., & Bilham, R. (2010). *Intensity, magnitude, location, and attenuation in India for felt earthquakes since 1762*. *Bulletin of the Seismological Society of America*, 100(2), 570–584. <https://doi.org/10.1785/0120080329>
- cxix. Terzaghi K, Peck RB. 1948. *Soil mechanics*. Eng Pract John Wiley Sons, Inc, New York.
- cxx. Tinti, S., & Mulargia, F. (1985). *An improved method for the analysis of the completeness of a seismic catalogue*. *Lettere Al Nuovo Cimento Series 2*, 42(1), 21–27.  
<https://doi.org/10.1007/BF02739471>
- cxxi. Tonouchi K, Sakayama T, Imai T (1983) *S wave velocity in the ground and the damping factor*. *Bull Int Assoc Eng Geol* 26–27:327–333.
- cxvii. Trianni, S. C. T., Lai, C. G., & Pasqualini, E. (2014). *Probabilistic seismic hazard analysis at a strategic site in the Bay of Bengal*. *Natural Hazards*, 74(3), 1683–1705.  
<https://doi.org/10.1007/s11069-014-1268-3>
- cxviii. Valverde-Palacios, I., Valverde-Espinosa, I., Chacón, J., & Irigary, C. (2012). *Spatial variability of liquefaction susceptibility in the Metropolitan area of Granada (Spain)*. *Conference Paper*, 15.
- cxviii. Valverde-Palacios, I., Vidal, F., Valverde-Espinosa, I., & Martín-Morales, M. (2014). *Simplified empirical method for predicting earthquake-induced settlements and its application to a large area in Spain*. *Engineering Geology*, 181(September), 58–70.  
<https://doi.org/10.1016/j.enggeo.2014.08.009>
- cxv. Von Terzaghi K. 1947. *Theoretical soil mechanics*. [place unknown]: Chapman and Hall.
- cxvii. Wang, Y., Sieh, K., Tun, S. T., Lai, K.-Y., & Myint, T. (2014). *Active tectonic and earthquake Myanmar region*. *Journal of Geophysical Research: Solid Earth*, 119, 3576–3822.  
<https://doi.org/10.1002/2013JB010762>.Received
- cxvii. Weichart, D. H. (1980). *Estimation of the Earthquake Recurrence Parameters for Unequal Observation Periods for Different Magnitudes*. *Bulletin of the Seismological Society of America*, 70(4), 1337–1346.
- cxviii. Wells, D. L., & Coppersmith, K. J. (1994). *New empirical relationships among magnitude, rupture length, rupture width, rupture area, and surface displacement*. *Bulletin of The Seismological Society of America*, 84(4), 974–1002.
- cxviii. Woo, G. (1996). *Kernel estimation methods for seismic hazard area source modeling*. *Bulletin of the Seismological Society of America*, 86(2), 353–362.
- cxviii. Yokota, K., Imai, T., & Konno, M. (1981). *Dynamic deformation characteristics of soils determined by laboratory tests*. *OYO Tec. Rep*, 3, 13-37.
- cxviii. Youd I, T. L., Idriss, M., Andrus, R. D., Arango, I., Castro, G., Christian, J. T., Dobry, R., Finn, W. D. L., Harder, L. F., Hynes, M. E., Ishihara, K., Koester, J. P., Liao, S. S. C., Iii, W. F. M., Martin, G. R., Mitchell, J. K., Moriwaki, Y., Power, M. S., Robertson, P. K., ... Ii, K. H. S. (2001). *Liquefaction Resistance of Soils: Summary Report from the 1996 Nceer and 1998*

- Nceer/ Nsf Workshops on Evaluation of Liquefaction Resistance of Soils. Journal of Geotechnical and Geoenvironmental Engineering, 127(April), 297–313.*
- cxix. Youd, T. L., Idriss, I. M., Andrus, R. D., Arango, I., Castro, G., Christian, J. T., Dobry, R., Finn, W. D. L., Harder, L. F., Hynes, M. E., Ishihara, K., Koester, J. P., Liao, S. S. C., Marcuson, W. F., Martin, G. R., Mitchell, J. K., Moriwaki, Y., Power, M. S., Robertson, P. K., ... Stokoe, K. H. (2001). *Liquefaction Resistance of Soils: Summary Report from the 1996 NCEER and 1998 NCEER/NSF Workshops on Evaluation of Liquefaction Resistance of Soils. Journal of Geotechnical and Geoenvironmental Engineering, 127(10), 817–833.*  
[https://doi.org/10.1061/\(ASCE\)1090-0241\(2001\)127:10\(817\)](https://doi.org/10.1061/(ASCE)1090-0241(2001)127:10(817))
- cxixiii. Zhao, J. X., Zhang, J., Asano, A., Ohno, Y., Oouchi, T., Takahashi, T., Ogawa, H., Irikura, K., Thio, H. K., Somerville, P. G., Fukushima, Y., & Fukushima, Y. (2006). *Attenuation relations of strong ground motion in Japan using site classification based on predominant period. Bulletin of the Seismological Society of America, 96(3), 898–913.*  
<https://doi.org/10.1785/0120050122>.
- cxixiv. Zhou, H., Yin, Z., & Wu, D. (2018). *Landslide susceptibility mapping using weighted overlay analysis in a GIS environment: A case study in the Zhejiang Province, China. Geomatics, Natural Hazards and Risk, 9(1), 1-16.*